Aus dem Institut für Pharmakologie

der Universitätsmedizin

der Johannes Gutenberg-Universität

Regulation of Nox4 expression by histone deacetylases in human endothelial cells: involvement of epigenetic mechanisms

Dissertation

Zur Erlangung des Grades

Doktor der Naturwissenschaften

Am Fachbereich Biologie

der Johannes Gutenberg-Universität Mainz

Daniel Siuda

Geboren am 26.01.1982 in Stuttgart

Mainz, 2013

Tag der mündlichen Prüfung: 01.10.2013

I hereby declare that this submission is my own work and that, to the best of my knowledge and belief, it contains no material previously published or written by another person nor material which to a substantial extent has been accepted for the award of any other degree or diploma of the university or another institute of higher learning, except where acknowledgement has been made in the text.

Mainz, October 9, 2013

Daniel Siuda

Index of contents

List of figures

List of tables

List of abbreviations

3

3'UTR ..... *3' untranslated region*

5

5mC ..... *5 methyl cytosine*

6

6mA *N6-methyladenine*

7

7-AAD ..... *7-Amino-actinomycin D*

A

A230 ..... *absorbance at 230 nm wavelength*
A549 ..... *adenocarcinoma human alveolar basal epithelial cells*
ADP ..... *adenosine diphosphat*
ANOVA ..... *analysis of variance*
AP-1 ..... *activator protein 1*
APS ..... *adenosine 5' phosphosulfate*, *ammonium persulfate*
ARE ..... *Adenylate-uridylate-rich element*
ATF ..... *activating transcription factor*
ATP ..... *adenosine triphosphate*
AU ..... *absorbance unit*

B

BCA ..... *bicinchoninic acid*
BCoR ..... *Bcl-6-interacting co-repressor*
Bis-Tris ..... *2-[Bis(2-hydroxyethyl)amino]-2-(hydroxymethyl)propane-1,3-diol*
bp. ..... *base pair*
BRCA1 ..... *breast cancer type 1*
BRCT ..... *BRCA1 C-terminal domain*
BSA ..... *bovine serum albumin*

C

$CaCl_2$ ..... *calcium chloride*
cDNA ..... *complementary DNA*
CenH3 ..... *centromeric histone H3*
ChIP ..... *chrommatin immunoprecipitation*
c-Jun ..... *jun proto-oncogene*
CMV ..... *Cytomegalovirus*
CO_2 ..... *carbon dioxide*
CoA ..... *coenzyme A*
Co-REST ..... *REST co-repressor 1*
CpG ..... *cytosine-phosphate-guanine*
C_t ..... *cycle threshold*
CtBP ..... *c-terminal binding protein*
CTCL ..... *cutaneous T-cell lymphoma*
C-terminal domain ..... *carboxyl-terminal domain*

Cu ..... *copper*
$CuSO_4$ ..... *copper(II) sulfate*

D

dATP·S ..... *deoxyadenosine alfa-thio triphosphate*
DGCR8 ..... *DiGeorge syndrome critical region gene 8*
dH_2O ..... *distilled water*
DMEM ..... *Dulbecco's modified eagle's medium*
DMSO ..... *dimethyl sulfoxide*
DNA ..... *deoxyribonucleic acid*
DNMT ..... *DNA methyltransferase*
Dnmt1 ..... *DNA methyltransferase 1*
Dnmt2 ..... *DNA methyltransferase 2*
Dnmt3a ..... *DNA methyltransferase 3a*
Dnmt3b ..... *DNA methyltranferase 3b*
Dnmt3L ..... *DNA methyltransferase 3-Like*
dNTP ..... *deoxynucleoside triphosphate*
DPBS ..... *Dulbecco's phosphate-buffered saline*
DRB *5,6-Dichloro-1-ß-D-ribofuranosylbenzimidazole*
dsRNA ..... *double-stranded RNA*, *double-stranded RNA*
DTT ..... *dithiothreitol*
Duox1 ..... *dual oxidase 1*
Duox2 ..... *dual oxidase 2*

E

E. coli ..... *Escherichia coli*
EA.hy926 ..... *hybridoma human endothelial cell line*
ECGS/H ..... *endothelial cell growth supplement with heparin*
EDTA ..... *ethylenediaminetetraacetic acid*, *ethylenediaminetetraacetic acid*
EF Kit ..... *endotoxin free kit*
eNOS ..... *endothelial nitric oxide synthase*
Ezh2 ..... *enhancer of zeste homolog 2 (Drosophila)*

F

FBS ..... *fetal bovine serum*
Fc region ..... *fragment crystallizable region*
FDA ..... *United States Food and Drug Administration*

G

GAPDH ..... *glyceraldehyde 3-phosphate dehydrogenase*

H

H1 ..... *histone H1*
H1t ..... *histone H1 testis specific*
H2A ..... *histone H2A*
H2A.Bbd ..... *histone H2A Barr body deficient*
H2A.X ..... *histone H2A.X*
H2A.Z ..... *histone H2A.Z*
H2B ..... *histone H2B*
H_2O ..... *water*

H_2O_2 ..... *hydrogen peroxide*
H_2O-EF ..... *endotoxin free water*
H3 ..... *histone H3*
H3.1 ..... *histone H3.1*
H3.1t ..... *histone H3.1 testis-specific*
H3.2 ..... *histone H3.2*
H3.3 ..... *histone H3.3*
H3K27 ..... *histone H3 lysine 27*
H3K36 ..... *histone H3 lysine 36*
H3K4 ..... *histone H3 lysine 4*
H3K9 ..... *histone H3 lysine 9*
H4 ..... *histone H4*
HAT ..... *histone acetylase*
HAT supplement ..... *sodium hypoxanthine, aminopterin and thymidine*
HBB ..... *hemoglobin beta*
HBS ..... *HEPES buffered saline*
HCl ..... *hydrogen chloride*
HDAC ..... *histone deacetylase*
HDAC1 ..... *histone deacetylase 1*
HDAC10 ..... *histone deacetylase 10*
HDAC11 ..... *histone deacetylase 11*
HDAC2 ..... *histone deacetylase 2*
HDAC3 ..... *histone deacetylase 3*
HDAC4 ..... *histone deacetylase 4*
HDAC7 ..... *histone deacetylase 7*
HDAC8 ..... *histone deacetylase 8*
HDAC9 ..... *histone deacetylase 9*
HEPES ..... *4-(2-hydroxyethyl)-1-piperazineethanesulfonic acid*
HGPRT ..... *hypoxanthine guanine phosphoribosyl transferase*
HIF-1α ..... *hypoxia-inducible transcription factor 1 alpha*
HIRA ..... *histone regulator A*
HKMT ..... *histone lysine methyltransferase*
Hox ..... *homeobox*
HP1 ..... *heterochromatin protein 1*
HRP ..... *horseradish peroxidase*
HT supplement ..... *hypoxathine and thymidine*
HUVEC ..... *human umbilical vein endothelial cells*

I

IC_{50} ..... *half maximal inhibitory concentration*
IFN-γ ..... *interferon-γ*
ISWI ..... *imitation switch*

K

kDa ..... *kilo Dalton*

L

LB medium ..... *lysogeny broth medium*
LB-Agar ..... *lysogeny broth agar*
LDH ..... *lactate dehydrogenase*

LSD1 ..... *lysine specific demethylase 1*
luc reporter ..... *luciferase reporter*

M

MAF ..... *v-maf musculoaponeurotic fibrosarcoma oncogene homolog*
MBD ..... *methyl-CpG-binding domain*
MCS ..... *multiple cloning site*
MEF2 ..... *myocyte enhancer factor-2*, *myocyte enhancer factor-2*
$MgCl_2$ ..... *magnesium chloride*
miRNA ..... *micro RNA*
mRNA ..... *messenger RNA*
MuLV ..... *murine leukemia virus*

N

NaCl ..... *sodium chloride*
NAD^+ ..... *nicotinamide adenine dinucleotide*
NADPH ..... *Nicotinamide adenine dinucleotide phosphate*
NaF ..... *sodium fluoride*
NaPPi ..... *sodium pyrophosphate*
NCBI ..... *National Center for Biotechnology Information*
N-CoR ..... *nuclear receptor co-repressor*
NF-κB ..... *nuclear factor kappa-light-chain-enhancer of activated B cells*
nm ..... *nanometer*
Nox1 ..... *NADPH oxidase 1*
Nox2 ..... *NADPH oxidase 2*
Nox3 ..... *NADPH oxidase 3*
Nox4 ..... *NADPH oxidase 4*
Nox5 ..... *NADPH oxidase 5*
NOXA1 ..... *NADPH activator 1*
NOXO1 ..... *NADPH organizer 1*
Nrf2 ..... *NF-E2-related factor 2*
Nuclease-free H_2O ..... *nuclease-free water*
NuRD ..... *nucleosome remodeling and deacetylating*

O

O_2- ..... *superoxide*
Oct-1 ..... *octamer-binding protein 1*
OD ..... *optical density*
oligo(dT) ..... *oligo deoxythymidine*

P

P38 ..... *proline 38*
PAGE ..... *polyacrylamid gel electrophoresis*
PARG ..... *poly-ADP-ribose glycohydrolase*
PcG ..... *polycomb group*
PCR ..... *polymerase chain reaction*
PEG ..... *polyethylene glycol*
PIC ..... *protease inhibitor complex*
PMSF ..... *phenylmethansulfonylfluorid*
pol II ..... *polymerase II*

poly(A) tail ..... *poly adenosine tail*
PPTase ..... *protein phosphatase*
PRMT ..... *protein arginine methyltransferase*
PTGS ..... *posttranscriptional gene silencing*

Q

qPCR ..... *quantitative real time polymerase chain reaction*

R

Rad6p ..... *radiation sensitivity protein 6*
REST ..... *neuron restrictive silencer factor*
RHO ..... *rhodopsin*
RISC ..... *RNA-induced silencing complex*
RITS ..... *RNA-induced transcriptional silencing complex*
RNA ..... *ribonucleic acid*
RNAi ..... *RNA interference*
ROS ..... *reactive oxigen species*
rpm ..... *revolutions per minute*
RT-PCR ..... *reverse transcription polymerase chain reaction*

S

S.E.M. ..... *standard error of mean*
SAHA ..... *suberoylanilide hydroxamic acid*
SDS ..... sodium dodecyl sulfate
Set1p ..... *SET domain-containing protein 1*
Set2 ..... *SET domain containing 2*
SET-domain ..... *Su(var)3-9, Enhancer of zeste E(z), Trithorax domain*
siRNA ..... *small interfering RNA*
SMC ..... *smooth muscle cell*
SMRT ..... *silencing mediator for retinoic acid and thyroid hormone receptor*
SNP ..... *single nucleotide polymorphism*
SUMO ..... *small ubiquitin-related modifier*
SV40 ..... *Simian virus 40*
SWI2/SNF2 ..... *SWItch/Sucrose NonFermentable*
SWR1 ..... *Swi2/SnF related ATPase 1*

T

T75 cell culture flask ..... *75 cm² cell culture flask*
TAE buffer ..... *Tris base, acetic acid and EDTA buffer*
Taq ..... *Thermus aquaticus*
TBS ..... *Tris-buffered saline*
TBST ..... *Tris-buffered saline + Tween 20*
TE buffer ..... *Tris/EDTA buffer*
TEMED ..... *tetramethylethylenediamine*
TF ..... *transcription factor*
TGF-β1 ..... *transforming growth factor-β1*
TGS ..... *transcriptional gene silencing*
T_m ..... *melting temperature*
TNF-α ..... *tumor necrosis factor-α*
TRDMT1 ..... *tRNA* XE "tRNA" \t "*transfer RNA*" *aspartic acid methyltransferase 1*

tRNA ..... *transfer RNA*, *transfer RNA*
trxG ..... *trithorax group*
TSA ..... *trichostatin A*

U

Ubc9 ..... *ubiquitin-conjugating enzyme E2I*
UCSC ..... *university of California, Santa Cruz*
UV ..... *ultraviolet*

X

x g ..... *times gravity*
Xist ..... *X-inactive specific transcript*, *X-inactive specific transcript*

Y

YY1 ..... *Yin Yang 1*

Z

Zn^{2+} ..... *zinc*

Γ

γH2A.X ..... *phosphorylated histone H2A.X*

E

ε ..... *epsilon*

Abstract

Nox4 is a member of the NADPH oxidase family, which represents a major source of reactive oxygen species (ROS) in the vascular wall. Nox4-mediated ROS production mainly depends on the expression levels of the enzyme. The aim of my study was to investigate the mechanisms of Nox4 transcription regulation by histone deacetylases (HDAC). Treatment of human umbilical vein endothelial cells (HUVEC) and HUVEC-derived EA.hy926 cells with the pan-HDAC inhibitor scriptaid led to a marked decrease in Nox4 mRNA expression. A similar down-regulation of Nox4 mRNA expression was observed by siRNA-mediated knockdown of HDAC3. HDAC inhibition in endothelial cells was associated with enhanced histone acetylation, increased chromatin accessibility in the human Nox4 promoter region, with no significant changes in DNA methylation. In addition, the present study provided evidence that c-Jun played an important role in controlling Nox4 transcription. Knockdown of c-Jun with siRNA led to a down-regulation of Nox4 mRNA expression. In response to scriptaid treatment, the binding of c-Jun to the Nox4 promoter region was reduced despite the open chromatin structure. In parallel, the binding of RNA polymerase IIa to the Nox4 promoter was significantly inhibited as well, which may explain the reduction in Nox4 transcription. In conclusion, HDAC inhibition decreases Nox4 transcription in human endothelial cells by preventing the binding of transcription factor(s) and polymerase(s) to the Nox4 promoter, most likely because of a hyperacetylation-mediated steric inhibition. In addition, HDAC inhibition-induced Nox4 downregulation may also involves microRNA-mediated mRNA destabilization, because the effect of the scriptaid could be partially blocked by DICER1 knockdown or by transcription inhibition.

Zusammenfassung

Nox4 gehört zur Familie der NADPH Oxidasen. Diese Familie ist der Hauptverursacher von ROS in den Wänden von Blutgefäßen. Die Menge von Nox4 produziertem ROS hängt hauptsächlich vom Expressionslevels des Enzyms ab. In der folgenden Studie sollten die Mechanismen der transkriptionellen Regulation der Nox4 durch Histone-Deacetylasen (HDAC) genauer erforscht werden. Die Behandlung, von menschlichen Endothelzellen aus der Nabelschnurvene (HUVEC) und von HUVEC abstammenden EA.hy926 Zellen, mit dem pan-HDAC-Inhibitor Scriptaid führte zu einer deutlichen Abnahme der Nox4 mRNA Expression. Eine ähnliche Runterregulation der Nox4 mRNA Expression konnte mit siRNA vermittelten Knockdown von HDAC3 erzielt werden. Die Inhibition in Endothelzellen ging mit verstärkter Acetylierung von Histonen, erhöhter Zugänglichkeit des Chromatins in der Nox4 Promoterregion einher. Jedoch wurde keine signifikante Veränderung der DNA-Methylierung festgestellt. Zusätzlich zeigt diese Studie, dass c-Jun eine wichtige Rolle in der Kontrolle der Nox4 Transkription spielt. Knockdown von c-Jun mit siRNA resultierte in einer Runterregulation der Nox4 mRNA Expression. Nach der Behandlung mit Scriptaid war die Bindung von c-Jun an den Nox4 Promoter verringert und dies obwohl die Chromatinstruktur weiter geöffnet war. Zusätzlich konnte gezeigt werden, dass die Bindung der RNA-Polymerase II ebenfalls deutlich verringert war, was die reduzierte mRNA Expression von Nox4 erklären könnte. Zusammenfassend kann man sagen, dass die Inhibition von HDAC die Transkription von Nox4 in menschlichen Endothelzellen verringert, indem die Bindung von Transkriptionsfaktoren und der Polymerase an den Nox4 Promoter verringert wird. Diese geringere Bindung lässt sich am besten durch ein Modell erklären indem eine Hyperacetylierung an dem Nox4 Promoter zu einer sterischen Inhibition führt. Des Weiteren scheinen auch microRNAs eine Rolle bei dem durch HDAC-induzierten Abbau der Nox4 mRNA zu spielen, denn eine Blockierung oder ein Knockdown von DICER1 hob den Effekt von Scriptaid auf die Nox4 mRNA teilweise wieder auf.

1 Introduction

1.1 Epigenetics

The term epigenetics was first introduced by Waddington in 1942, describing the interaction between environment and gene expression.[1] It is composed of the Greek prefix “epi” meaning “over” or “on top of” and genetics. Epigenetics describes regulation above genetics or in addition to genetic mechanisms. Epigenetic regulation occurs through DNA methylation and DNA hydroxymethylation, histone modifications, chromatin remodeling and non-coding RNAs. Figure 1 shows the three main epigenetic mechanisms and Figure 2 shows the different mechanisms of genetic and epigenetic changes. All described regulating mechanisms act, more or less, on the level of chromatin. Chromatin consists of DNA and its associated proteins and RNAs.[2]

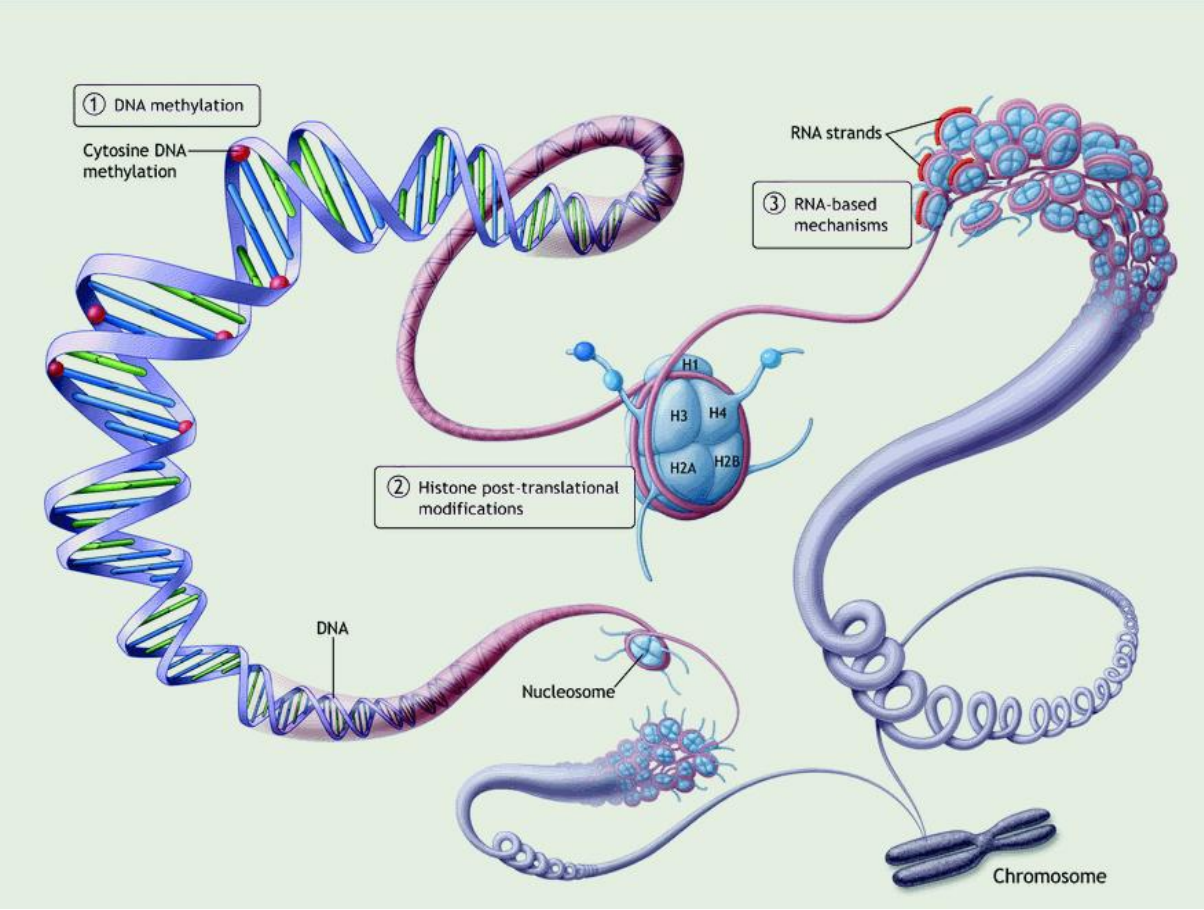

Figure 1: Epigenetic mechanisms.
The main mechanisms of epigenetics are 1) DNA methylation, 2) histone post-translational modifications and 3) RNA-based mechanisms. Addition of methyl groups to cytosines in CpG is associated with closed chromatin structure. Modifications of histones can have positive or negative effects on transcription and RNA-based mechanisms are e.g. Important for imprinting. There is a cross-talk between the different mechanisms. (From Matouk and Marsden 2008)[3]

Histones and DNA can be chemically modified with epigenetic marks (e.g. methylation). These marks can change the electrostatic nature of the chromatin resulting in structure change, and/or alter the binding affinity of chromatin-binding proteins. In mammalian cells most of the chromatin is

heterochromatin, i.e. it is in a condensed, transcriptionally silent state. In heterochromatin, DNA is mostly hypermethylated and the histone tails contain post-translational modifications, which are associated with gene silencing. On the contrary, euchromatin has a more open chromatin structure than heterochromatin. In euchromatin, DNA is hypomethylated in contrast to heterochromatin and the histone tails contain post-translational modifications, which favor a more open chromatin structure resulting in higher transcriptional activity, although not all euchromatic regions are transcriptionally active. Heterochromatin can be further dived into two types: constitutive heterochromatin and facultative heterochromatin. In constitutive heterochromatin, genes are rarely expressed in any cell of the organism, whereas in facultative heterochromatin regions, genes are only repressed in some cells during different cell cycle states or development states.

Other than genetics, which may lead to a diverse phenotype by changes of the DNA sequence (mutations), epigenetics are potentially heritable changes in gene expression, that do not involve changes in the underlying DNA sequence.[4–6] Figure 2 shows how mutations influence the DNA template directly, which may lead to the development of new species, whereas epigenetic changes create a new phenotype and help the cell to adapt to changes in the environment. It becomes more clearer that multisubunit complexes are needed to remodel chromatin by modifying histones and DNA to bring about downstream events.[7] While DNA methylation may state for a more stable epigenetic modification, which may be inherited to the next generation, changes of histones or histone residues may be a more dynamic, short-term modification, reacting on signals from outside the cells.[7] There is an interaction between chromatin structure, DNA methylation and RNA interference (RNAi).[8–13]

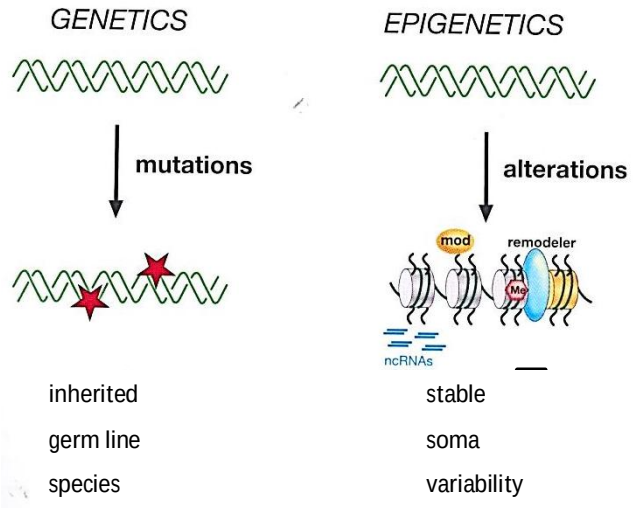

Figure 2: Genetic versus epigenomic alterations.
Genetic changes are caused by mutations (red stars) of the DNA (green helix). The changed DNA sequence is heritable somatically and through the germ line. Mutations of the DNA sequence are responsible for the development of new species. Epigenetic changes do not alter the DNA template. They modulate the use of the genome. Histone modifications (mod), chromatin remodeler (remodeler), histone variants (yellow nucleosome), DNA methylation (red Me) and non-coding RNAs are responsible for the different use of the same DNA template in different cells and under different conditions. These epigenetic changes lead to cell variability (different phenotype) and are heritably transmitted through cell division and can be transgenerational (to a certain degree they are stable). (Modified from Allis at al. 2007)[2]

1.1.1 DNA methylation

DNA methylation was the first epigenetic mechanism found to be correlated with gene repression.[14] DNA methylation can be found in prokaryotes, fungi, plants and mammals. Methyl groups are either added to the C^5 position of cytosines or the N^6 position of adenines resulting in 5-methyl cytosine (5mC) or N^6-methyladenine (6mA), respectively. Figure 3 shows the reaction of C^5 methylation by DNA methyltransferases (DNMT) using S-adenosyl-methionine as methyl-group donor.

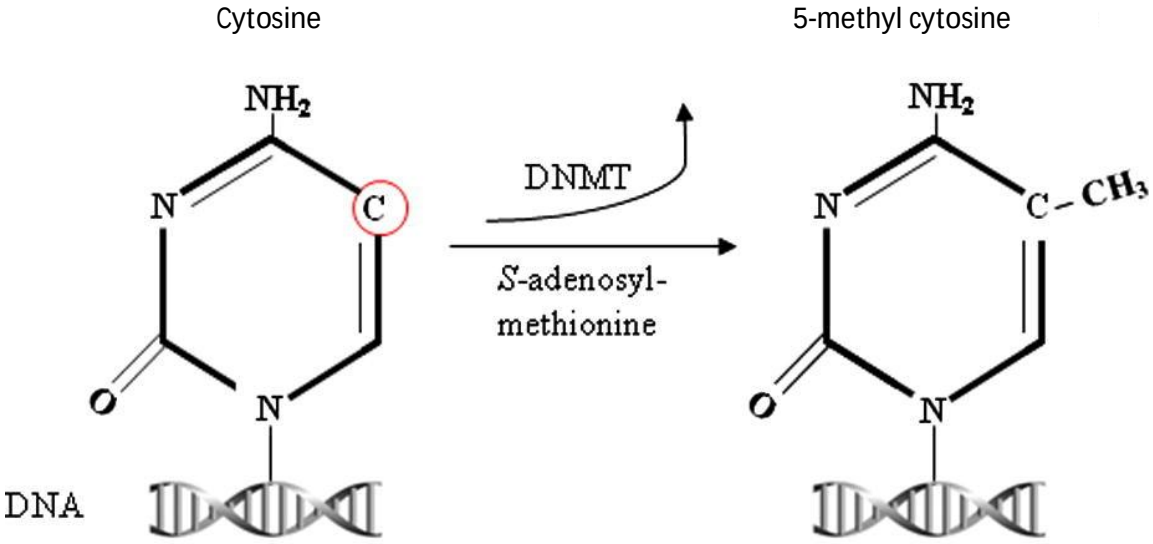

Figure 3: Mechanism of DNA methylation.
Cytosines are methylated at the C^5. This methylation is carried out by DNA methyltransferases (DNMT). DNMTs use S-adenosyl-methionine as methyl-group donor. (From Huang et al. 2011)[15]

In bacteria, DNA methylation serves as a protection mechanism in which restriction endonucleases specifically recognize and digest foreign unmodified DNA, leaving the methylated host DNA undigested.[16] In eukaryotes, most of the DNA methylation occurs at cytosine residues, with only low levels of methylated adenines, which occur mostly in unicellular organisms.[17–19] The level of DNA methylation in eukaryotes vary from nearly undetectable in yeast, to intermediate levels in mammals up to high levels in plants.[20] Increasing levels of DNA methylation correlate with a relative increase in non-coding and repetitive DNA content in higher eukaryotes.[21] In humans, approximately 1 % of all DNA bases are estimated to be 5mC.[22]

DNA methylation occurs in mammals at the palindromic CpG dinucleotide. In fungi and plants methylation occurs not only at the CpG dinucleotide; also other symmetric, asymmetric, and non-CpG methylation are known.[23,24] 60 – 90 % of the CpG sites in the mammalian genome are methylated with an enrichment at noncoding regions and interspersed repetitive elements but not in the CpG island of active genes.[25–27] On the inactivated X-chromosome and imprinted loci, CpG islands are silenced, i.e. the cytosines are methylated.[28–31] In mammals, CpG islands are normally 300 – 3000 base pairs in length and are found in or close to about 60 % of mammalian gene promoters.[32] One general definition of a CpG island is that: it should be at least 200 bp long; the CpG content should be between 50 to 55 %, and finally the observed-to-expected CpG ratio should be greater than 60 %.[33]

DNA methylation is carried out by DNMT.[34] In mammals, there are four DNA methylatransferases: Dnmt1, Dnmt3a, Dnmt3b and Dnmt3L.[35] Different DNMTs have distinct functions, and they are conserved from prokaryotes to eukaryotes.[34] Dnmt1 is the maintenance DNMT. Although, Dnmt1 has significant activity against unmethylated CpGs, its main substrate is hemimethylated DNA.[5,36] This finding was supported by the observation that inactivation of Dnmt1 in mouse embryonic stem cells leads to a genome-wide loss of CpG methylation.[37] Dnmt3a and Dnmt3b are both de novo methyltransferases and dehydroxymethylases.[38,39] Unlike Dnmt1, which has both activities, Dnmt3a and Dnmt3b lack maintenance DNMT activity.[40] Dnmt3L belongs to the Dnmt3 family and is important for imprinting.[41,42] Dnmt3L has no DNMT activity, but supports Dnmt3a and Dnmt3b in their catalytic activity.[43] Dnmt2 (renamed to TRDMT1 (tRNA aspartic acid methyltransferase 1) since 2006), which has sequence homology to the other DNMTs, does not methylate DNA but instead methylate position 38 in aspartic acid transfer RNA.[44] Dnmt2 is ubiquitous expressed.[45]

DNA methylation is generally associated with transcriptional silencing.[46,47] DNA methylation prevents transcription by inhibiting the binding of transcription factors to the DNA. Alternatively, methylation of CpGs attracts methyl-CpG-binding domain (MBD) proteins, which bind to the DNA and associate with co-repressor complexes leading to chromatin structure changes and transcription repression.[48–50]

1.1.2 Chromatin structure

Chromatin is composed of repeating units of nucleosomes.[51] One nucleosome is buildup of a histone octamer (two molecules of each core histone (H2A, H2B, H3 and H4)). Around this histone octamer 147 bp (base pair) of DNA are wrapped. Molecular interactions between the core histones and the DNA could be determined by high resolution X-ray pictures.[52–54] Histones can interact with the negatively charged DNA backbone, because they contain many lysine residues, which are positively charged, allowing the histones to bind the DNA tightly, leading to a compact structure. The nucleosomes with the wrapped around DNA represent the 11-nm fiber. To get the whole genome into a cell the chromatin must be further compacted. The higher compacted form of the 11-nm fiber is the 30-nm fiber. The evidence is growing that the 30-nm fiber is arranged in a more open zigzag model, which adopts higher order self-assembly with two stacks of nucleosome particles that are connected with a linker DNA, instead of the solenoid model (where the single nucleosomes are gradually coiled around a single axis).[54,55] In the compaction of the chromatin structure, histone modifications play a crucial role. Due to electric charges, they can either compact the chromatin or open the chromatin structure depending on the modification of the histone tail.[56–59] The 30-nm fiber compacts the DNA only about 50-fold. Therefore, more levels of higher-order chromatin exist. New DNA labeling techniques could reveal that the higher order chromatin is dynamically changed by positive and negative chromatin remodeling factors for states compatible with gene expression.[60–62] This dynamic higher-order chromatin structure is represented by the 300 – 700-nm fiber. Only during nuclear division the 1.5-µm chromosome is present, representing the most compact structure. Figure 4 gives an overview to the described chromatin structures.

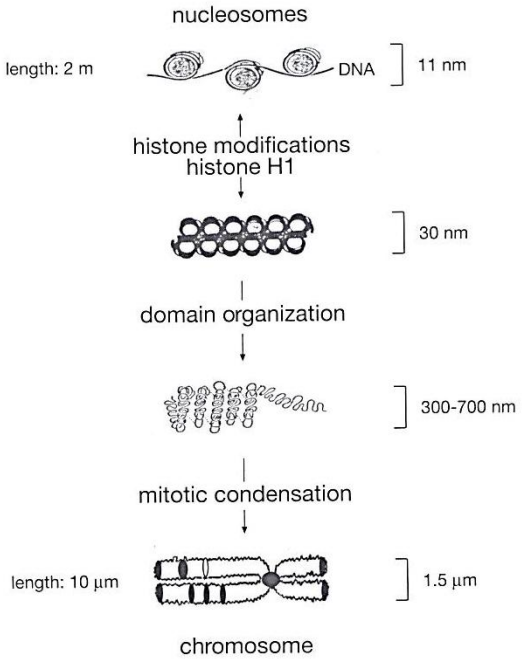

Figure 4: Higher order chromatin structure.
The 11-nm fiber represents the DNA wrapped around the nucleosomes. In this state the length of the total DNA will be 2 meters. A 2 meter long DNA does not fit into the cell, therefore the chromatin is further compacted into the 30-nm fiber. This compaction is carried out by histone modifications and the linker histone H1. In this figure the 30-nm fiber is organized in the solenoid model, although there is increasing evidence that the 30-nm fiber is arranged in a more open zigzag model.[54,55] The 300 – 700-nm fiber represents dynamic higher-order chromatin looping, which occurs in both interphase and metaphase chromatin. The highest compacted chromatin structure (1.5 µm) is only present during cell division (mitosis or meiosis). (From Allis at al. 2007)[2]

The chromatin structure can be modified by three different mechanisms: (i) ATP dependent chromatin remodeling, (ii) modification of histones and (iii) incorporation of histone variants.[63] Modifications of histones will be described in section 1.1.3.

1.1.2.1 Histone variants

Not only have chemical posttranslational modifications of the histone tails an important role on the chromatin structure but histone variants play a crucial role, too. All histones, apart from histone H4, have sequence variants.[64,65] Histone variants can be grouped according to their dependence on DNA replication and/or the cell cycle for their incorporation into chromatin.[66] Replication-dependent histones are H2A, H2B, H3.1, H3.2, H3 and H4. These are typically input together during DNA replication. The histone variants build in independently of DNA replication are H3.3, CenH3, H2A.Z and H2A.X. These variants are incorporated in response to ongoing mechanisms like transcriptional activation or stress signals like DNA damage or nutritional starvation. Histone variants are replaced by chromatin remodeling complexes or exchanger complexes that are specific for distinct histone variants, like H3.3, H2A.Z, or H2A.X.[64,65,67] For example H3 is replaced by H3.3 via the action of histone regulator A (HIRA) exchanger complex[68] and H2A is replaced by H2A.Z through the activity of the Swi2/Snf2-related ATPase 1 (SWR1) chromatin remodeler complex.[69] Sequence variants of the different histones serve for different purpose. Histone H3.1 and histone H3.2 are typically incorporated into DNA during DNA replication.[68,70] The histone variant H3.2 is associated with gene silencing.[70] The replication-independent histone variant H3.3 is incorporated into transcribed

regions.[71] The three previous described sequence variants of histone H3 are distributed throughout the whole genome, whereas the variant CenH3 is found nearly exclusively in centromeres.[72] This histone variant serves as the attachment point for the spindle apparatus.[73] There is a testis specific variant of histone H3, H3.1t, too.[74]

Another histone with several variants is histone H2. The variant H2A.Z is involved in transcriptional regulation and is localized at chromatin boundaries and nucleosome free regions at the promoters of genes.[75–77] H2A.Z can be associated with gene silencing or gene activation and it is very likely that H2A.Z contributes to the machinery that establishes borders between euchromatin and heterochromatin.[63] The variant H2A.X plays an important role in DNA double-strand repair.[78,79] Around double-strand breaks H2A.X is rapidly phosphorylated (γH2A.X).[80] γH2A.X surrounds the double-strand break up to megabase distances.[81–83] It is believed that γH2A.X is an epigenetic mark, which recruits chromatin remodeling complexes and damage recognition and repair proteins to the double-strand break. Many DNA repair and damage recognition proteins contain BRCA1 C-terminal domains (BRCT), which bind γH2A.X.[84,85] The binding of these proteins recruit additional DNA repair factors to the double-strand break.[84] macroH2A is localized at the inactive mammalian X chromosome.[66,86,87] macroH2A co-localizes with Xist RNA along the X chromosome.[88,89] The incorporation of macroH2A inhibits the binding of the chromatin remodeling complex SWI/SNF[90] and inhibits transcription.[91] In contrast to macroH2A, H2A.Bbd (Barr body deficient) is found at the active X chromosome.[92] H2A.Bbd co-localizes with acetylated histone H4 and is found at transcriptionally active sites.[93,94]

The linker histone H1, which binds between nucleosomes and facilitates higher order structure of chromatin,[95] has sequence variants, too. The H1 variants are thought to change the bulk properties of chromatin that can affect overall compaction.[96] The different Histone H1 variants are H1.1-1.5, H1o and H1t, whereas H1t is a testis specific variant.[97]

It is noteworthy that the histones H3, H2A, H2B and H1 have all testis specific variants.[66,98] All currently known histone H2B variants are testis specific! There are several ideas why there are so many testis specific histone variants. One theory says that the testis specific histone variants affect the global chromatin structure, facilitating recombination during spermatogenesis. Relative to the other histone H1 variants, H1t has the lowest chromatin condensing capacity.[74,99,100] The other theory says that there is a unique testis specific histone code, which helps to drive the unique progression of the genome during sperm development.[98]

1.1.2.2 Chromatin remodeling complexes

Chromatin remodeling complexes are needed to modulate the accessibility of nucleosomal DNA.[101] All proteins belonging to this family have a catalytic ATPase subunit.[102] The best studied ATP-dependent chromatin remodeling complexes belong to three different families: (i) SWI2/SNF2 family, (ii) the ISWI family and (iii) the Mi-2 family.[102,103] All of them have directly demonstrated chromatin remodeling activity.[104–107] Chromatin remodeling activates or represses genes and thereby affects the cell cycle[108] and cell differentiation.[109] The two main models on how the remodeling factors may change the DNA accessibility are (i) “sliding” and (ii) “conformational change”. Sliding is the most obvious mechanism and is carried out by movement of the entry and exit point of the DNA around

the nucleosome in the same direction, resulting in an octamer that is translationally repositioned .[110] The model is shown in Figure 5.

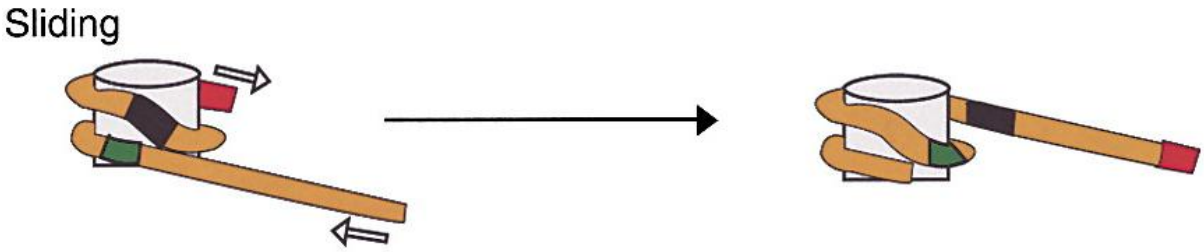

Figure 5: Sliding model of nucleosome repositioning.
DNA is wrapped around the nucleosome. The DNA is moved by the chromatin remodeling complex around the core octamer (indicated by the arrows). This DNA shift results in a translational reposition of the octamer, allowing the transcription of new genes or repression of transcription. (From Narlikar et al. 2002)[102]

This could be shown by analysis of the starting and end positions of nucleosomes on defined DNA fragments, which were moved in *cis* to new position.[111] Further evidence for this model was brought by experiments in which SWI/SNF action on nucleosomes blocked certain restriction enzymes sites in the linker DNA sequence, indicated that SWI/SNF has moved the nucleosomes over the previously accessible sites.[112]

Sliding cannot explain how DNA in dense compact chromatin regions can be made accessible, because sliding needs translational repositioning of single nucleosomes. Sliding therefore does not increase the amount of exposed DNA, it changes only the location of the exposed DNA.[102] A model which might explain this is the conformational change model (see Figure 6). The conformational change model says that there could be either a collapse of the nucleosome to a canonical nucleosome structure, that has a new position, or there could be partial or complete release of the core histone octamer followed by a binding at a new position.[113,114]

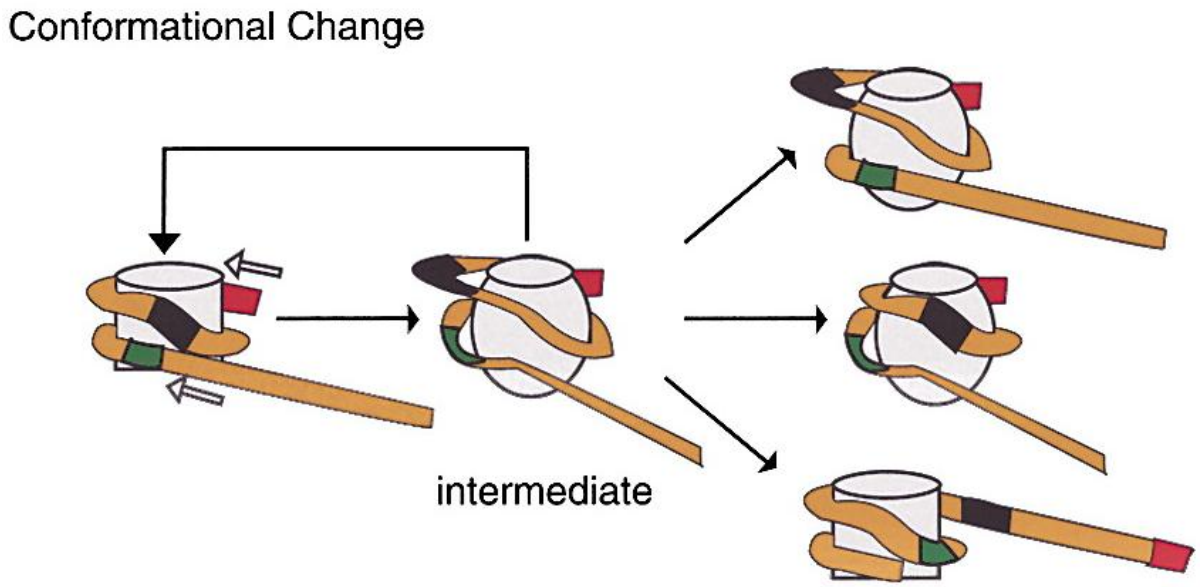

Figure 6: Conformational change model as a mechanism of ATP-dependent nucleosome remodeling.
The ATP-dependent remodeling complexes induce a conformational change of the core octamer. This change leads either to a canonical structure, that has a new position, or to partial or complete release of the core histone octamer. The free octamer binds at a new position leading to changes in accessibility of different DNA sequences. (From Narlikar et al. 2002)[102]

This model is supported by observations by Kinston and Narlikar[101]. They showed that DNA wrapped around a mononucleosome, without flanking DNA sequences, have a higher DNase and restriction enzymes sensitivity when incubated with SWI/SNF members. Further support comes from the fact that site-specific crosslinking of the DNA to the histone octamer, does not prevent remodeling by SWI/SNF.[115] SWI/SNF is more likely to act on chromatin by the conformational change model, whereas the ISWI-based complexes work after the sliding model principle.[116,117]

Two other families which are involved in chromatin remodeling are the polycomb group (PcG) proteins and the trithorax group (trxG) proteins. They were first discovered in Drosophila by their role in the developmental regulation of the Hox gene cluster and homeotic gene regulation.[2] Both have major roles in the epigenetic memory. They can transduce signals to the chromatin structure and thereby maintaining cellular identity.[118] PcG and trxG work antagonistically, i.e. the PcG family establishes a silent chromatin state, whereas the trxG family propagate gene activity.[2] Both families consist of diverse proteins, but they are highly conserved in eukaryotes.[2] DNA-binding proteins like YY1, histone-modifying enzymes (e.g. Ezh2) and other repressive chromatin-associated factors with a chromodomain belong to the PcG gene family.[2] Other trxG family members are transcription factors, ATP-dependent chromatin-remodeling enzymes and histone lysine methyltransferases.[2]

1.1.3 Histone modifications

Histones are part of the nucleosome. Two copies of each histone (H2A, H2B, H3 and H4) form together an octamer around which DNA is wrapped. The histones are needed to condense the genome. The fifth histone H1 helps to condense the genome, by binding to the linker DNA (the free DNA between two nucleosomes).[119] Histones are modified mostly at their tail region, which protrude from the surface of the nucleosome, although there are also modifications within the globular domain.[63] Histone modifications were discovered nearly 50 years ago, when lysine methylation was

reported in histones isolated from calf thymus.[120] As early as histone modifications were discovered they were proposed to play a role in transcriptional regulation.[121] Histones are modified at specific residues of their tail region (see Figure 7 for details). Beside methylation there exist other modifications including acetylation, phosphorylation, ubiquitination, sumoylation, ADP-ribosylation, biotinylation and proline isomerization.[122] Different enzymes conduct the different modifications of the histone residues.

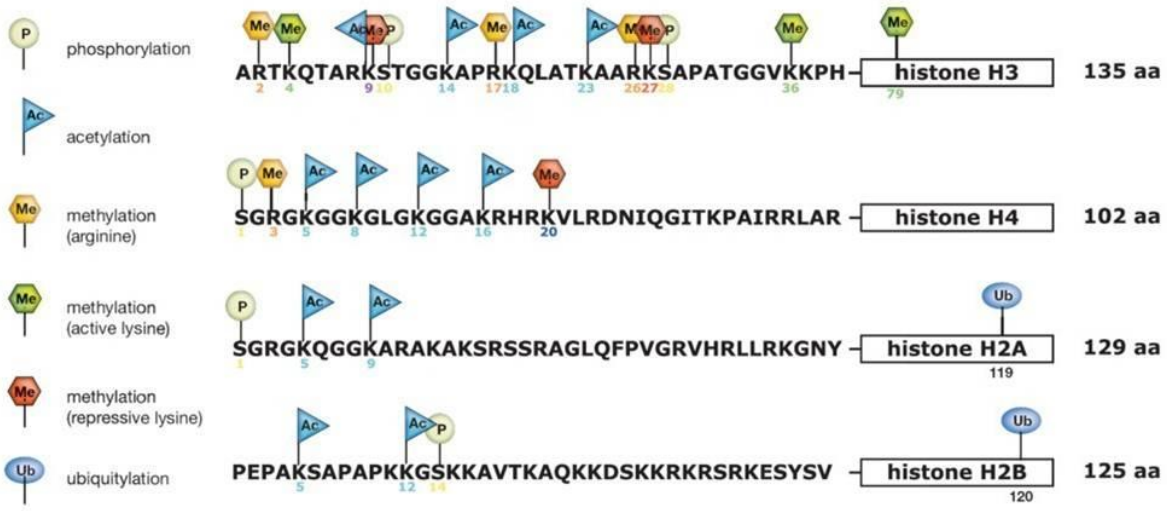

Figure 7: Different histone modifications and their location in the histone tail.
Histones can be modified at different residues in their tail region, but some occur also in the globular domain (boxed). Associated with transcription activation are acetylation (blue Ac flag), arginine methylation (yellow Me hexagon), and some lysine methylation (green Me hexagon). The red Me hexagons represent repressive marks. (From Allis at al. 2007)[2]

Acetylation of specific histone residues are carried out by histone acetyltransferases (HATs).[123] Their action is reversed by histone deacetylases (HDACs).[124] Figure 8 gives an overview of histone modifying enzymes. HDACs are described in more detail in section 1.2. Acetylation of histone residues is associated with active chromatin. This was demonstrated by ChIP experiments, which defined this modification at promoters of active genes.[125] The identification of the first HATs revealed that they are transcriptional co-activators and are components of multiprotein transcription regulatory complexes.[126] This model is supported by the observation that factors of transcription complex contain an evolutionary conserved bromodomain, which preferentially binds to acetylated histone tails, enhancing the probability of transcription.[127,128] Acetylation per se seems to be associated with activation of transcription, but uncontrolled acetylation (inhibition of HDACs) can lead to a block of transcription.[129,130] There is a cross-talk between the different histone modifications and other epigenetic marks.[131]

Phosphorylation of histone residues is carried out by kinases, and many of the kinases have been identified. Phosphorylation is reversed by phosphatases (see Figure 8).[132] Like other histone modifications, phosphorylation can have opposed effects on transcriptional regulation. Phosphorylation of histone H3 at serine 10 is associated with gene activation.[133,134] During mitosis however, histone H3 and H1 become hyperphosphorylated on condensed mitotic chromosomes.[135]

Phosphorylation of the histone variant H2A.X plays an important role in DNA double-strand break repair (see 1.1.2.1).

Nearly all histone modifications are correlated with active or repressive function, respectively, depending which amino acid residue is modified. Synergistic as well as antagonistic pathways have been described, which can induce combinations of active marks and thereby counteracting repressive marks.[136–138] Methylation, like phosphorylation, was found in transcriptional silencing as well as in transcription activation. Adding of a methyl group to a lysine residue does not change the overall positive charge of the lysine like acetylation or phosphorylation, but it does chemically alter the residue in a different way. Unlike the other modifications, which can be modified only once, there can be added up to three methyl groups to the ε-amino group of the lysine, hence there can be a mono-, di- or trimethylation at the lysine residue.[139] The incorporation of more methyl groups led to an increase in basicity and hydrophobicity, which led to a higher affinity of the histone tail for the DNA backbone, resulting in non-permissive nucleosomes.[140,141] The trimethylated lysine residues seem to be capable to be stably propagated during cell division.[142] There are two classes of methylating enzymes (see Figure 8): the protein arginine methyltransferases (PRMTs), whose substrate is arginine[143] and histone lysine methyltransferases (HKMTs), which act on lysines.[144] Arginine methylation can be reversed indirectly by deiminases, which convert methyl-arginine to a citrulline residue.[145] Because the methylations of the lysine residues are more stable, the methylation cannot be reversed so easily. There are two known mechanisms how the lysine residue can be demethylated: (i) by the action of an amino oxidase and (ii) by hydroxylases or dioxygenases. The lysine-specific demethylase LSD1 was described as an amino oxidase, which is able to remove the methylation of H3K4.[146] The mechanism of action of the hydroxylases or dioxygenases is more potent, working by radical attack.[147] There are around 30 enzymes in the mammalian genome, which contain the conserved jumonji domain, which is necessary for the radical attack, which can destabilize methylated lysines.[148,149] Other histone methyltransferases contain a so called SET-domain (Su(var)3-9, Enhancer of zeste E(z), Trithorax, TRX), but not all show methyltransferase activity.[150]

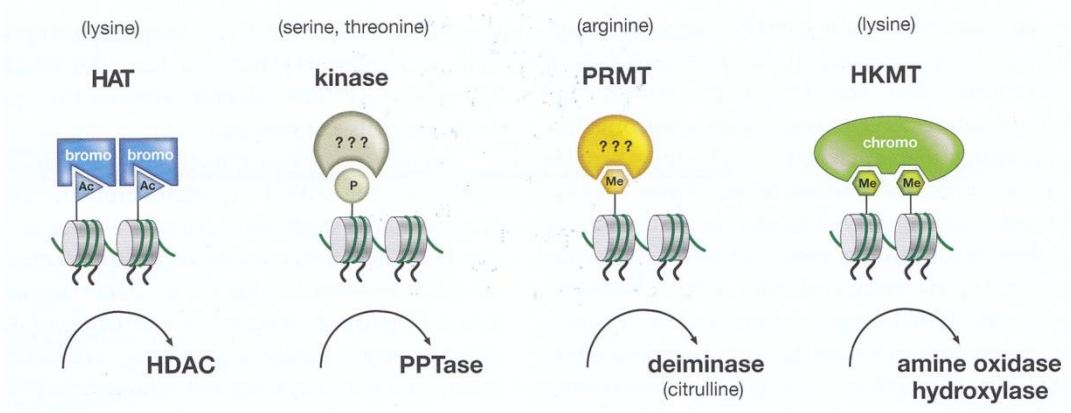

Figure 8: Histone modifying enzymes.
Modifications of histones are carried out by different enzymes, depending on the modification. Histone acetyltransferases (HATs) add acetyl groups (Ac) to distinct lysine residues. This action is reversed by histone deacetylases (HDAC). Different kinases have been identified which transfer phosphate groups (P) to histones. The reaction is reversed by protein phosphatases (PPTase). Protein arginine methyltransferases (PRMT) transfer methyl groups (Me) to arginine residues and histone lysine methyltransferases (HKMT) to lysine residues. The reactions are reversed by deiminases and amine oxidase or hydroxylase, respectively. (From Allis at al. 2007)[2]

ADP-ribose-polymerases, with NAD^+ as a co-factor, transfer ADP-ribose molecules to arginine residues.[151] ADP-ribosylation is found in all histone types.[152] Due to its size, more than 100 ADP-ribose molecules can be added. It is one of the most drastic post-translational modification of histones.[63,151] Mono-ADP-ribosylation has a repressive effect on transcription[153], whereas poly-ADP-ribosylation has effects on DNA repair, gene expression, DNA replication, apoptosis and genomic stability.[154] ADP-ribosylation is found at hyperactylated histones, indicating a role in the histone code.[155] The modification itself is rapidly degraded by poly-ADP-ribose glycohydrolase (PARG), indicating an important role in the adaption of the cell to environmental changes.[156]

The 76-amino acid (~ 8.5 kDa) protein ubiquitin is added to a lysine residue in ubiquination. Normally polyubiquination is associated with degradation by the 26S proteasome complex.[157] Ubiquitinated H2A and H2B are the most abundant ubiquitin conjugated proteins in higher eukaryotes.[158] Monoubiquitination is associated with transcriptional activation or silencing[159] and shows the interplay between different histone modifications. Rad6p can monoubiquinate H2B at lysine 123, this modification is necessary for the methylation of H3K4 by Set1p.[160]

SUMO stands for small ubiquitin-related modifier. Therefore, it is not surprisingly that SUMOylation behaves in the same way as ubiquitination in adding a bulky structure to their substrates.[63] SUMOylation plays a role in transcriptional silencing[161] and is added covalently to the histone by Ubc9. Heterochromatin protein 1 (HP1) and histone deacetylases are attracted by SUMOylation of the histone.[161]

The binding of biotin to histones is catalyzed by holocarboxylase synthetase. It could be shown that biotinylation is enriched in repeat regions and repressed loci, participating in the maintenance of genome stability and gene regulation.[162]

Proline isomerization, a rare studied histone modification (only 7 articles found on PubMed (www.ncbi.nlm.nih.gov/pubmed) retrieved on 16.4.2013) is involved in transcriptional regulation by

interacting with histone lysine methylation. Responsible for proline isomerization is the proline isomerase Fpr4, by binding to the histone tails. If proline P38 in histone H3 is isomerized by Fpr4, the histone methyltransferase Set2 cannot methylate H3K36.[163]

There is cross-talk between the different histone modifications (see Figure 9). On histone H3, 13 amino acids can be modified.[164] 78% of active transcribed genes have at least one active mark and only half of active genes have only active marks![164] One modification can affect other modifications in cis. For instance, methylation of H3K4 prevents methylation of H3K9 (see Figure 9 lower panel).[164]

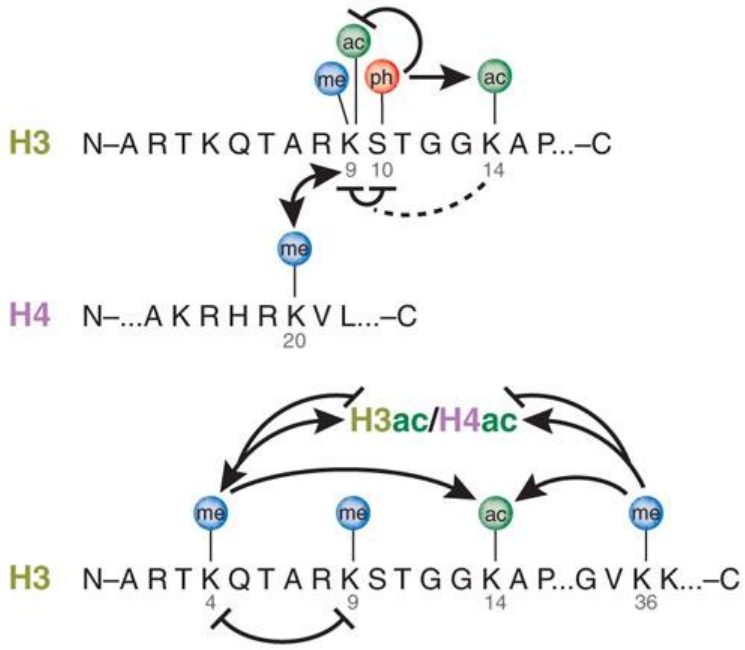

Figure 9: Histone modification cross-talk.
Histone modifications have influence on their surrounding modifications. Modifications of histone H3 (H3) at one amino acid residue can influence modifications at other residues of histone H3. Phosphorylation at serine 10 blocks acetylation of lysine 9, but favors acetylation of lysine 14. Modifications of lysine 9 exclude modifications of serine 10 and vice versa. Methylation of histone H4 at lysine 20 has influence on the modification of lysine 9 of histone H3. Methylation of H3 lysine 4 excludes methylation of H3K9 and vice versa. Methylation of H3K4 favours acetylation of H3K14.(From Latham *et al.* 2007)[164]

1.1.4 RNA interference

RNA interference (RNAi) is a natural mechanism to control the activity of genes. Two classes of RNA molecules could carry out the RNAi pathways (Figure 10). These molecules are either small interference RNAs (siRNAs) or micro RNAs (miRNA). siRNAs are generally synthetic, exogenous, dsRNA that do not correspond to protein coding regions and do not have the potential to arise from hairpin characteristics of miRNA precursors. In contrast, miRNAs are encoded in the genome and have the potential to arise from foldback structures characteristic of miRNA precursor hairpins. Both types of small interfering RNAs have in common that they are about 21 nucleotides long and are processed in the cell in similar ways. miRNAs are generally transcribed by polymerase II (pol II) to pri-

miRNAs[165] although some miRNAs are transcribed by polymerase III.[166] The pri-microRNAs, made from pol II, have a 7-methylguanosine cap and are polyadenylated.[165] The pri-miRNAs are processed by Drosha and DGCR8 into ~60 nucleotide long precursor miRNAs (pre-miRNAs). It could be shown that DGCR8 plays an essential role in the biogenesis of miRNAs.[167]
The pre-miRNAs form an imperfect stem-loop structure. They are transported into the cytoplasm by exportin 5 and are then processed by Dicer into mature miRNAs, which are then loaded into the RNA-induced silencing complex (RISC).[63] The complex of miRNA/RISC downregulates specific gene products by translational repression by binding to partially complementary sequences in the 3'UTR of the target mRNAs or over directing mRNA degradation through binding to completely complementary sequences.[63,168,169] These two mechanisms are known as post-transcriptional silencing. However, RNAi also plays a role in heterochromatin formation, known as transcriptional gene silencing.[170] The evidence that heterochromatin formation and RNAi are tied together came from studies in *Schizosaccharomyces pombe*.[171] In these studies, it could be shown that mutations of any component of the RNAi machinery lead to failures in chromosomal segregation.[172,173] In the first step, double-stranded RNA is generated from heterochromatic regions, by transcription of the two DNA strands. The double-stranded RNA is then cleaved by Dicer to produce siRNA. These siRNAs are then incorporated into the RNA-induced transcriptional silencing complex (RITS). One enzyme in the RITS is a histone methyltransferase, which methylates H3K9, after it was guided to the target sequence by the siRNA incorporated into the RITS complex.
The methylated histone H3 attracts Swi6 (ortholog to mammalian HP1), which diminishes the transcription capacity.[174,175] Similar mechanisms on chromatin structure could be detected in mammals, too. RNase A treatment of mammalian cells removes the heterochromatin mark histone H3 lysine 9 trimethylation (H3K9me3), indicating that RNA is a structural component of the pericentromeric heterochromatin.[176] When siRNA processing factors are removed from the cell, H3K9 methylation is impaired and binding of HP1 at pericentromeric heterochromatin is inhibited.[177] Beside RNA-induced heterochromatin formation, RNA-directed DNA methylation was observed.[8,178] Like the other RNAi mechanisms, RNA-directed DNA methylation requires dsRNA as well as DNA 5-cytosine methyltransferase and histone modifying enzymes. While RNA-induced heterochromatin formation affects large regions (several kilobases), RNA-directed DNA methylation leads to silencing of single genes, i.e. promoters which have sequence homology with the siRNA.[8,178] RNAi plays also a role in genomic imprinting. The non-coding RNAs originate from imprinting centers and target histone modifications, which then trigger transcriptional silencing of the surrounding genes.[179] The best characterized example is *Xist* RNA, which spreads around the inactive X chromosome and triggers gene silencing in the flanking regions of the *Xist* locus.[180]

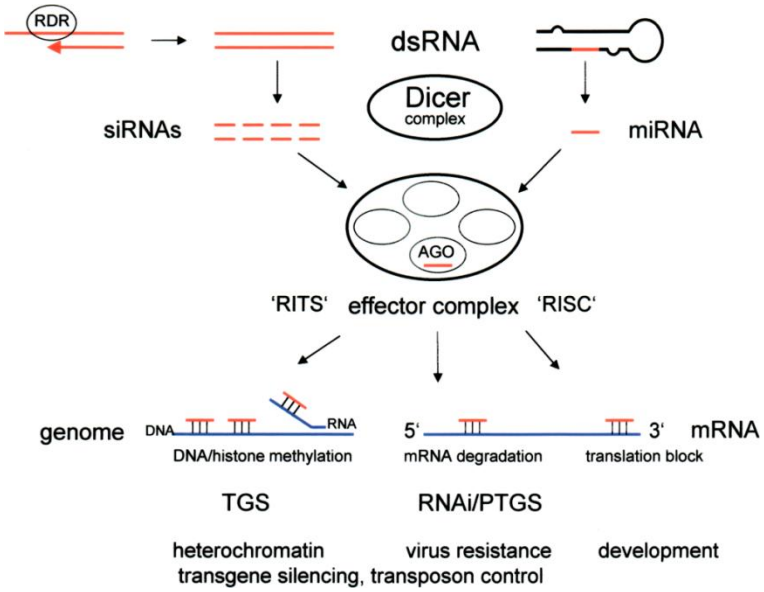

Figure 10: RNA interference overview.
Short RNAs (red lines) derived from Dicer cleavage of dsRNA are incorporated into multiprotein effector complexes, such as RISC (RNA induced silencing complex) and RITS (RNA-induced transcriptional silencing) and lead to mRNA degradation, translation inhibition, or transcriptional gene silencing and genome modifications (target nucleic acids are blue lines). ARGONAUTE (AGO) proteins bind short RNAs and bring them to the effector complex RITS or RISC. Both transcriptional gene silencing (TGS) and RNAi/posttranscriptional gene silencing (PTGS) can result in heterochromatin formation and other functions mentioned at the bottom of the figure. Proteins are ovals and RDR stands for RNA-dependent RNA polymerase. (From Matzke and Matzke 2004)[181]

1.2 Histone deacetylases

Histone deacetylases (HDACs) remove the acetyl group from the ε-amino group of lysine side chains on the histone protein. HDACs counteract histone acetyltransferases (HATs), which use acetyl-CoA as a cofactor, and transfer an acetyl group to the lysine moiety. Histone deacetylation is generally associated with transcriptional silencing, because it promotes higher order chromatin structures and the recruitment of silencers.[182] Although they are named histone deacetylases, they can also deacetylate non-histone proteins, like transcription factors or molecular chaperones influencing their activity or stability.[183,184] Today 18 different HDACs are known in mammals and are divided into four classes, based on phylogeny.[185,186] Figure 11 shows the classification of the HDACs according to sequence homology.

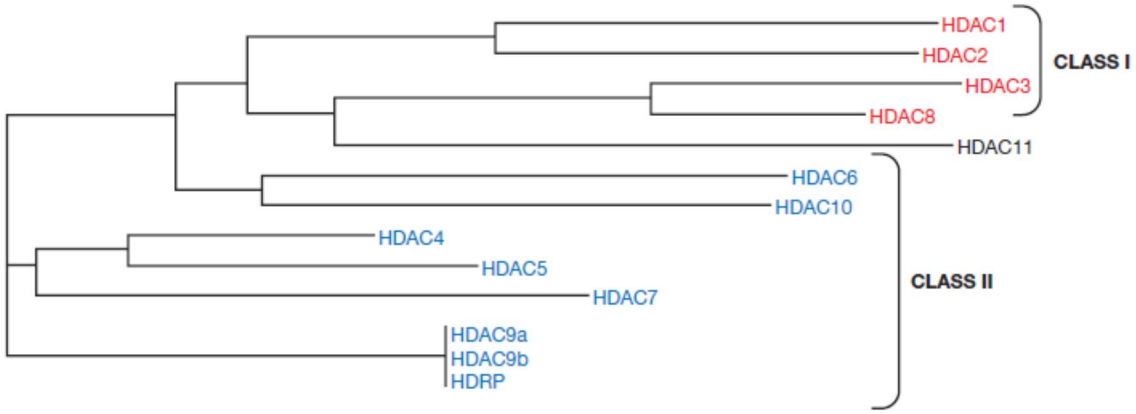

Figure 11: Phylogenetic tree of HDACs.
HDACs are group based on sequence homology. Class I HDACs are HDAC1, HDAC2, HDAC3 and HDAC8. Class II HDACs are HDAC4, HDAC5, HDAC6, HDAC7, HDAC9 and HDAC10. HDAC11 is the only member of class IV. (From de Ruijter *et al.* 2003)[186]

Class I consists of HDAC1, HDAC2, HDAC3 and HDAC8. All of the class I HDACs are found mainly in the nucleus, whereas HDAC3 can be found in the cytoplasm and membrane bound, too.[186,187] HDAC4 to HDAC7, HDAC9 and HDAC10 belong to class II. This class is further dived into two subclasses, depending on the number of catalytic domains. With one catalytic domain, HDAC4, HDAC5, HDAC7 and HDAC9 build up class IIa and HDAC6 and HDAC10 are placed in class IIb, containing two catalytic domains.[188] Class IV has only one member, namely HDAC11. Class I, II and IV are Zn^{2+}-dependent and are now referred to as classical HDACs.[186] Class III is composed of NAD^{+}-dependent deacetylases called Sirtuins (Sirtuin1 – Sirtuin7), which are not related to the other three classes. Those HDACs that use histones as substrate belong mainly to class I, whereas Class IIa members function as signal transducers involved in nucleocytoplasmic trafficking and class IIb members function as cytoplasmic regulators.[189] It seems that the HDAC activity of class IIa HDACs comes from the recruitment of enzymatically active complexes containing HDAC3.[190] HDACs are mainly found and are functional in multiprotein complexes, which support the catalytic domain of the HDACs to bind the specific chromatin site.[191] Little is known about HDAC11, but it could be shown that HDAC11 may play an essential role in Hodgkin lymphoma and inhibition of HDAC11 may produce a favorable anti-tumor response.[192]

The HDAC forms a hydrophobic cavity with the Zn^{2+} ion at its end. The C-terminal domain of the acetylated lysine is buried in this cavity. The acetyl group interacts with the Zn^{2+}. Another important amino acid is an aspartate residue located at the rim of the active site tunnel, which interacts with the backbone of the peptide substrate, imposing a constrained *cis*-conformation. The interaction of the aspartate locks the histone tail in the correct position for the deacetylases reaction at the acetyl group.[193] After binding of the acetylated lysine to the HDAC, a nucleophilic attack by an enzyme-activated water molecule on the carbonyl carbon of the ε-acetyl group takes place, leading to a tetrahedral intermediate. The tetrahedron intermediate is broken down by protonation of the amide nitrogen.[194,195]

HDAC1 and HDAC2 share high sequence similarity and show activity only when they are in a complex of proteins.[196] In these complexes are proteins, which can modulate the HDAC activity of HDAC1 and HDAC2, support DNA binding, and mediate the recruitment of HDACs to the promoters of genes.[197] HDAC1-null mice show embryonic lethality at day 10.5 and show severe proliferation defects and general growth retardation.[198,199] Mouse HDAC1-null embryonic stem cells show a significant reduction in total HDAC activity and modest hyperacetylation of histones H3 and H4.[200] But surprisingly, 3 % of genes are downregulated and about 5 % of genes are upregulated in these HDAC1-null embryonic stem cells.[201] These results indicate that HDAC1 does not function as a global transcription repressor, but instead regulates different genes by regulating promoter activity.[200] Such a differential effect on gene regulation is only observed by HDAC1 deletion, but also when HDAC inhibitors are used.[202,203] These results speak for a more complex regulation of gene expression by HDACs than only transcriptional repression due to hypoacetylation of the promoter regions. There are different reports about the influence of HDAC2 on development. One study showed that HDAC2-null mice died within the first 24 hours after birth with severe cardiac malformations.[199] However, other studies reported that the mice are viable, when they have a *lacZ* insertion in the *Hdac2* gene, creating a null mutation.[204]

HDAC3 has the highest sequence identity with HDAC8.[186] It is noteworthy, that the unconserved C-terminal domain of HDAC3 is required for deacetylases activity and transcriptional repression.[186] Together with the nuclear export signal, which all class I HDACs possess, HDAC3 has an additional nuclear export signal, which might play a role depending on cell type and environmental signals.[205] Like HDAC1 and HDAC2, HDAC3 coexist in multisubunit complexes (SMRT (silencing mediator for retinoic acid and thyroid hormone receptor) and N-CoR (nuclear receptor co-repressor)), but others than HDAC1 and HDAC2 (Sin3, NuRD (nucleosome remodeling and deacetylating) and Co-REST).[186] SMRT and N-CoR have a deacetylases-activating domain for HDAC3 activation.[206] HDAC3 mutant mice die at embryonic stage E9.5 due to defects in gastrulation.[207–209] If HDAC3 is lost in the liver a disrupted lipid and cholesterone homeostasis occurs, leading to an accumulation of lipids and a decrease in glycogen storage.[207] HDAC3 is important for endothelial cell survival.[210,211] The knockdown of HDAC3 in the heart, leads to cardiac disease, due to massive cardiac hypertrophy.[209]

HDAC7 belongs to class IIa and is closely related to HDAC4 and HDAC5.[186] HDAC7 is able to interact with SMRT/N-CoR and the co-repressors BCoR (Bcl-6-interacting co-repressor) and CtBP (C-terminal binding protein) and thereby interacts with HDAC3.[212,213] HDAC7 might function as a link between DNA-binding recruiters and the HDAC3-containing HDAC-complex.[190,205,212] The N-terminus of HDAC7 interacts specifically with MEF2, a DNA-binding transcription factor essential for muscle differentiation, and inhibits MEF2 function.[214] Knockdown of HDAC7 leads to embryonic lethality due to loss of vasculature.[215] HDAC7 is specifically expressed in endothelial cells during development. Knockdown of HDAC7 leads to a loss of integrity of endothelial-cell interactions and consequent rupture of blood vessels and haemorrhaging[215], which is the cause for the embryonic lethality.

How important HDACs are, can be seen in knockout experiments. Knockout of HDAC1, HDAC3 and HDAC7 leads to embryonic lethality and knockout of HDAC2 or HDAC4 results in lethality with 24 hours after birth or within 7 days, respectively. HDAC5 and HDAC9-null mice are viable, but have cardiac defects. HDAC6-null mice are viable and without an apparent phenotype. For HDAC8, HDAC10 and HDAC11 knockout animals, no data about the phenotype are available.[216]

1.3 HDAC inhibitors

HDAC inhibitors inhibit, as stated by their name, HDAC. In this study three histone deacetylase inhibitors were used, scriptaid, suberoylanilide hydroxamic acid (SAHA) and trichostatin A (TSA). All these inhibitors are hydroxamic acids. HDAC inhibitors can be divided into several classes and hydroxamic acids are one of these. Hydroxamic acids are the most potent HDAC inhibitors, compared with the other classes[217]. The inhibitors used in this study are classical HDAC inhibitors; this means they only inhibit class I, II and IV of HDAC. Table 1 shows the half maximal inhibitory concentration (IC_{50}) of scriptaid, SAHA and TSA against different HDACs. Today, two HDAC inhibitors are approved by the U.S. Food and Drug Administration (FDA). These two are Vorinostat (SAHA), which was licensed 2006 for treatment of cutaneous T-cell lymphoma (CTCL) and Romidepsin, which belongs to another class of HDAC inhibitors (depsipeptides). Romidepsin was approved by the FDA in 2009 against, like Vorinostat, CTCL. A lot of other HDAC inhibitors undergoing clinical trials belong to different classes of HDAC inhibitors.[216]

Table 1: IC_{50} values of HDAC inhibitors used in this study against selected HDAC isoforms (modified from Blackwell *et al.* 2008)[218]

	IC_{50}							
Inhibitor	HDAC1	HDAC2	HDAC3	HDAC8	HDAC4	HDAC6	HDAC7	HDAC10
Scriptaid	0.17	0.64	0.03	2.3	0.2	0.004	0.16	0.17
SAHA	0.1	0.44	0.02	2.2	0.05	0.02	0.05	0.1
TSA	0.005	0.021	<0.005	1.1	<0.014	<0.005	<0.014	0.005

Hydroxamic acids interact with the Zn^{2+} ion in the active site of the HDAC. The Zn^{2+} ion is coordinated by two aspartates, one histidine and the bidentate hydroxamic acid of the inhibitor through the carbonyl oxygen and the hydroxyl oxygen (see Figure 12).[193,219,220] This means that all HDAC inhibitors occupy the acetyl-lysine channel, blocking interaction with the substrate.[221] Selectivity of the HDAC inhibitors is mediated by interactions at the surface-rim and at the foot-pocket next to the catalytic site.[222] Potency and selectivity are driven by chelation of the Zn^{2+} ion at the metal-dependent catalytic site.[223] Figure 12 shows the binding of SAHA to the catalytic site of a HDAC-like protein.

HDAC inhibitors are used for therapy, because increased acetylation of histones and non-histone proteins are linked with the arrest of tumor growth, apoptosis, and anti-angiogenesis.[224,225] Both hydroxamic acids and the sulfhydryl group chelate the catalytic Zn^{2+}, but show little specificity between the different HDACs, although it has been reported that Vorinostat preferentially inhibits HDAC1, HDAC2, HDAC3 and HDAC6 and Romidepsin prefers HDAC1, HDAC2, HDAC3 and HDAC8.[223]

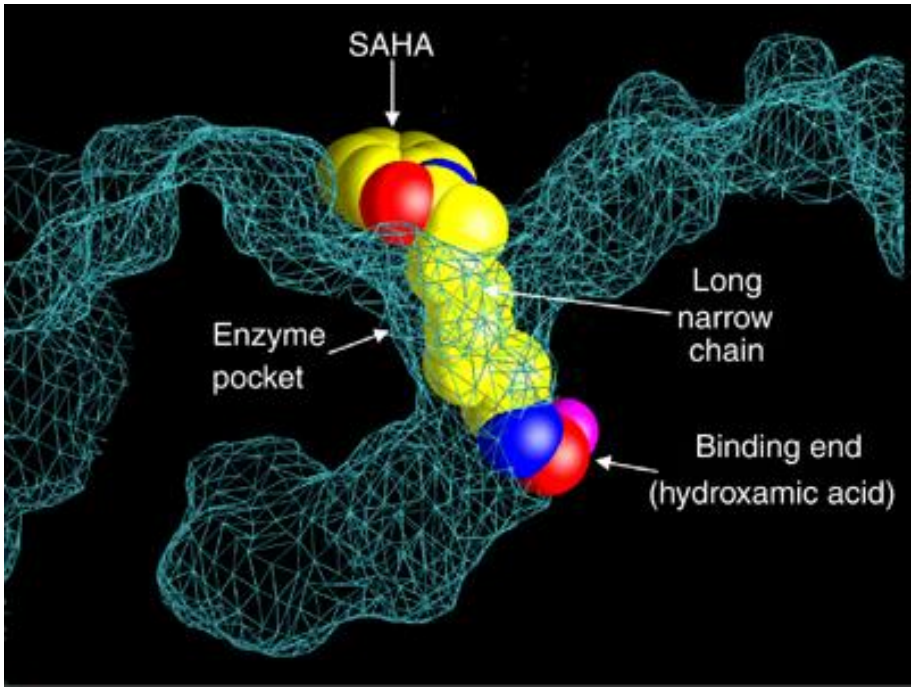

Figure 12: Binding of SAHA to the catalytic site of a histone deacetylases-like protein.
SAHA inhibits HDAC activity by binding to the catalytic site of this protein. The hydroxamic moiety of SAHA binds to the zinc atom (pink). Through this binding SAHA makes contact to residues at the rim, wall and bottom of the pocket. The hydroxamic group, most of the aliphatic chain and part of the phenyl amino group of SAHA are buried in the active site of the enzyme. Trichostatin A and scriptaid, another 2 hydroxamic acid HDAC inhibitors, similarly insert into the catalytic pocket of HDACs binding to zinc. (From Marks *et al.* 2001 and Richon 2006)[226,227]

1.4 NADPH oxidases (Nox)

Oxidative stress is associated with all known cardiovascular risk factors, and a large body of evidence indicates that it is implicated in many of the processes of atherogenesis.[228] Reactive oxygen species (ROS) are oxygen-derived small molecules, including oxygen radicals.[229] ROS generation is generally a cascade of reactions that starts with the production of superoxide.[229] ROS can be produced by several enzyme systems in the vascular wall, including Nox, xanthine oxidase, uncoupled endothelial nitric oxide synthase (eNOS), enzymes of the respiratory chain, and cytochrome P450 monooxygenases.[230] Although all of these enzymes contribute to the oxidative burden, evidence is accumulating that the initial generation of ROS by NADPH oxidases triggers the release of ROS by the other enzymes (e.g., xanthine oxidase and eNOS).[231,232] ROS have an important physiological roles in signaling, host defense, angiogenesis and wound healing.[233–235] An overproduction of ROS, however, leads to oxidative stress and is associated with pathological processes such as aging and apoptosis.[236–238] NADPH oxidase-mediated oxidative stress is involved in the development and progression of atherosclerosis.[239] In diseased human coronary arteries, about 60% of the superoxide has been shown to be derived from NADPH oxidases.[240]

NADPH oxidases are enzyme complexes, which transfer electrons across biological membranes and thereby produce ROS.[229] The Nox complex consists of two membrane-bound catalytic subunits (the p22phox and a Nox protein) and several cytosolic regulatory subunits (p47phox, p67phox, p40phox and the small GTPase Rac).[241] Cardiovascular tissues express the Nox isoforms Nox1, Nox2, Nox4,

and Nox5.[232,242] Nox4 is the predominant Nox isoform in endothelial cells[243,244] and also makes a significant contribution to Nox activity in vascular smooth muscle cells[245] as well as in cardiac tissues.[232] Figure 13 gives an overview of the different NADPH oxidase family members and their subunits. Nox3 is mainly found in the inner ear[246] and the dual oxidase (Duox) 1 and 2 are mainly found in the thyroid.[247]

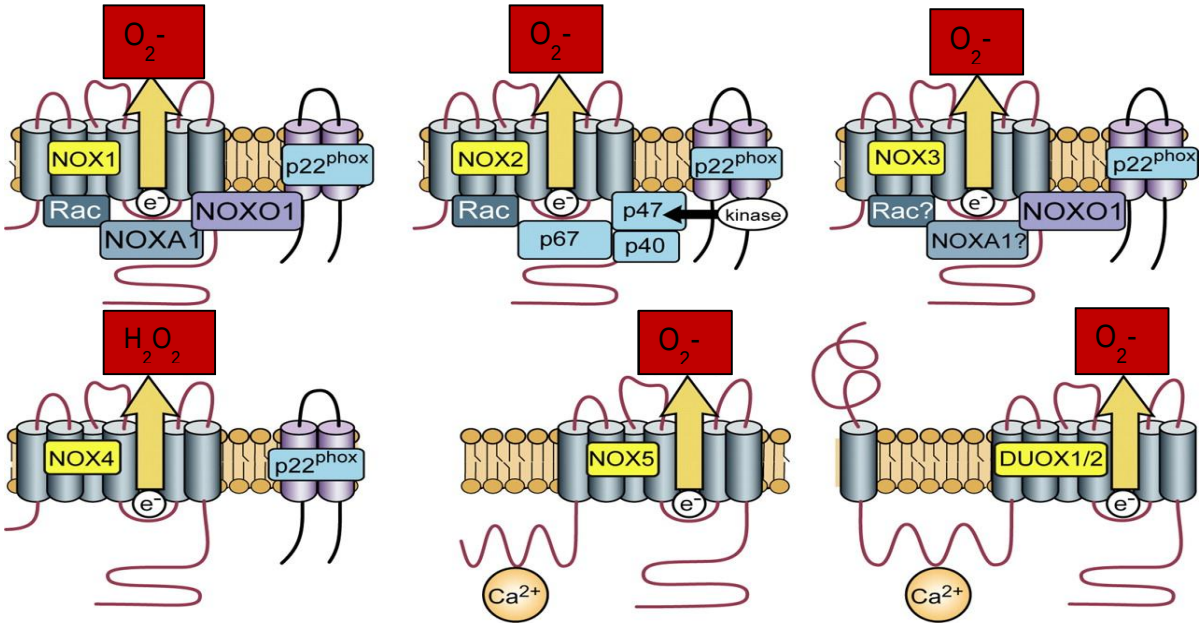

Figure 13: NADPH oxidase enzyme family.
Despite their similar structure and enzymatic function, Nox family enzymes differ in their mechanism of activation. Nox1 activity requires $p22^{phox}$, NOXO1 (NADPH organizer 1 or possibly $p47^{phox}$ in some cases) and NOXA1 (NADPH activator 1), and the small GTPase Rac. Nox2 requires $p22^{phox}$, $p47^{phox}$, $p67^{phox}$, and Rac; $p47^{phox}$ phosphorylation is required for Nox2 activation. Nox3 requires $p22^{phox}$ and NOXO1. In some species NOXA1 may be required, too, and the requirement of Rac is still debated. Nox4 requires only $p22^{phox}$ to function. Nox5, DUOX1, and DUOX2 are activated by Ca^{2+} and do not appear to require subunits. (Modified from Bedard, K. and Krause, K. 2007)[229]

Compared to other Nox proteins, Nox4 has unique features. All other NADPH oxidase family members generate superoxide, whereas Nox4 produces predominantly hydrogen peroxide.[248] The activity of Nox4 requires p22phox protein (see Figure 13).[249] The cytosolic regulatory subunits, however, are not required for Nox4 activity. Therefore, the activity of Nox4 depends mainly on its expression levels.[229] It could be shown that the type and origin of the released ROS are crucial for whether the ROS is beneficial or detrimental to the vascular system.[250] Overexpression of Nox1 or Nox2, both produce O_2^-, in endothelial cells leads to vascular dysfunction[251,252], whereas endothelial-specific overexpression of Nox4 promotes vasodilatation due to increased H_2O_2 release.[253] It seems that Nox4 may have beneficial effects to the vascular system.

1.5 Aim of the study

The aim of the study was to investigate

(i) Whether Nox4 expression is regulated by HDAC,
(ii) Which HDAC isoforms play a role, and
(iii) What are the molecular mechanism

2 Materials and Methods

2.1 Cell culture

The term cell culture is general referred to the fact when cells are removed from the tissue. When these cells are cultivated under the appropriate conditions and supplied with essential nutrient they need, they continue to grow. Cell culture is an artificial process and it occurs *in vitro*. In such *in vitro* culture one single cell can act as an independent organism. They divide, increase in size and, depending on the cell type and supply with nutrients, a single cell colony can nearly grow unlimited. There are a lot of advantages using cell culture. Cells are easier to handle than animals, grow faster and are cheaper. With different cells in culture the effect of different chemical compounds can be tested and it can be seen what effects different compounds have on different cell types. Cells can be modified genetically easily, what is not always the case with animals. The disadvantages are that cells can adapt to different culture conditions, and after a period of continuous growth they may change their characteristics and maybe physiological behavior, which differ from the original population.

In this study two cell lines were used. These are EA.hy926 cells and human umbilical vein cells (HUVEC). Most works were done with EA.hy926 cells. Key findings were verified in HUVEC. The characteristics of each cell line are pointed out below. All works with cell culture were performed under sterile conditions in a biosafety cabinet.

2.1.1 EA.hy926

The EA.hy926 cell line is a hybridoma cell line, i.e. it is a fusion product of two cell lines: HUVEC with a thioguanine-resistant clone of A549 by exposure to polyethylene glycol (PEG)[254]. A549 cells are adenocarcinomic human alveolar basal epithelial cells[255]. EA.hy926 cells grow adherent and have the morphology of endothelial cells. Further, it could be shown that EA.hy926 cells contain Weibel-Palade bodies. These bodies serve for storage of multimerized von Willebrand factor. This shows that this continuously replicating cell line has characteristics of differentiated endothelial cell functions such as regulation of angiogenesis, homeostasis/thrombosis, blood pressure and inflammation[256].

EAh.hy926 cells are cultivated at 37 °C with 5 % carbon dioxide (CO_2). The basal growth medium is Dulbecco's Modified Eagle's Medium (DMEM) (D5921, Sigma-Aldrich, Hamburg, Germany). To ensure optimal conditions, additional supplements are added to the basal medium: fetal bovine serum (FBS) (A15-151, PAA Laboratories, Cölbe, Germany), sodium pyruvate (11360, Gibco/ Life Technologies, Darmstadt, Germany), penicillin-streptomycin solution (15140, Gibco/ Life Technologies, Darmstadt, Germany) for prevention of cell culture contamination, HAT (5 mM sodium hypoxanthine, 20 µM aminopterin, 0.8 mM thymidine) supplement (21060, Gibco/ Life Technologies, Darmstadt, Germany) as a post-fusion selective medium to eliminate unfused or self-fused HGPRT (hypoxanthine-guanine phosphoribosyltransferase) -myeloma cells and finally L-glutamine (M11-004, PAA Laboratories, Cölbe, Germany). For an overview of the supplements and their final concentration see Table 2. FBS is the most widely used serum-supplement because it has

very low antibodies level and contains a lot of growth factors, allowing for versatility in many different cell lines. One critical point about FBS is that it is not a chemically defined medium, i.e. the ingredients like growth factors can differ from batch to batch. Medium is renewed every two to three days.

Table 2: Additional supplements for EA.hy926 cultivation.

Supplement	Final concentration
Fetal bovine serum	10 %
Sodium pyruvate	1 mM
Penicillin-streptomycin	100 U/ml; 100 µg/ml
HAT supplement	5 mM / 20 µM / 0.8 mM
L-glutamine	2 mM

EA.hy926 cells were cultivated in T75 cell culture flask in the above described medium. When the cells achieved confluence they were split at a subcultivation ration of 1:6 to 1:10. Prior to subculturing or transferring the cells in 24-well plates or petri dishes for experiments, the whole medium in the T75 flask was aspirated and the cells are washed with 10 ml pre-warmed Dulbecco's phosphate-buffered saline (DPBS) (14190, Gibco/ Life Technologies, Darmstadt, Germany) to remove all traces of serum, which may inhibit trypsinization. To detach the cells, 1 ml of trypsin-EDTA (L11-004, PAA Laboratories, Cölbe, Germany) was rinsed over the cells and dispensed carefully to cover the whole surface with the cell layer. The flask was placed in the incubator at 37 °C for several minutes. The detachment of the cells was observed under the inverted light microscope. After the cell layer is dispersed, 4 ml of growth medium was added to the flask and the cells were suspended by gentle pipetting. For subcultivation, an appropriate volume (1:6 or 1:10 ration) was used. As mentioned, for experiments cells were transferred from the flask to 24-well plates. In plates, the HAT supplement was replaced by HT (5 mM hypoxathine, 0.8 mM thymidine) supplement.

2.1.2 Human umbilical vein endothelial Cells (HUVEC)

HUVEC were isolated from umbilical vein from caesarean section born babies to guarantee semi sterility. HUVEC cells from passages four to six were used in the present study.

2.1.2.1 Isolation

The umbilical cord was kept cold (4 °C/ or on ice) in 500 ml DPBS containing 1 g glucose and 5 ml of penicillin-streptomycin solution prior to cell isolation.

The isolation of the HUVEC from the umbilical cord was performed under biosafety cabinet. The cord was placed in a bin covered with paper towels and aluminum foil. The cord was then cleaned with ethanol and patted dry. At both ends of the umbilical cord 1 cm was cut off. Then, the umbilical vein, the largest of the three vessels in the umbilical cord, was carefully expanded with forceps. A Vasofix® Safety 16-gauge needle (4268172S-01, Braun, Melsungen, Germany) was carefully inserted into the widened vein. The plastic cover of the needle was not removed; the needle was placed into the vein only with the plastic cover to avoid punctures of the vein. A three-way-stopcock (394602, BD, Helsingborg, Sweden) was affixed onto the Vasofix® Safety needle. On this three-way stopcock a syringe was placed and the umbilical vein was washed two times with 20 ml DPBS to eliminate the remaining blood. Then, the opposite end of the umbilical cord was closed tightly with a surgical

suture. To elute the endothelial cells, collagenase B from *Clostridium histolyticum* (11088807001, Roche Diagnostics, Mannheim, Germany) was used. Three mg collagenase was dissolved in 12 ml Medium 199 with Earle's Salts (E15-834, PAA Laboratories, Cölbe, Germany). The collagenase solution was warmed for 30 minutes in a 37 °C water bath. The total volume of the warmed collagenase solution was then injected into the umbilical vein through the three-way stopcock. After injection, the stopcock was closed and the umbilical cord was placed in a beaker filled with 37 °C DPBS. There should be enough DPBS in the beaker to cover the umbilical vein. The beaker was placed in a water bath (37°C) and left there for 15 minutes. After the incubation time, the umbilical cord was put back into the biological safety cabinet. To ensure detachment of the endothelial cells, the umbilical cord was carefully massaged. Afterwards, the collagenase solution was collected in a 50 ml falcon tube. The vein was washed with DPBS and this was collected in the same falcon tube as the collagenase solution. The tube was then centrifuged at room temperature for 15 minutes at 1000 rpm. The supernatant was discarded carefully.

2.1.2.2 Cultivation

HUVEC are cultivated in Medium 199 with Earle's Salts (E15-834, PAA Laboratories, Cölbe, Germany). Additional supplements are FBS (A15-151, PAA Laboratories, Cölbe, Germany), penicillin-streptomycin (15140, Gibco/ Life Technologies, Darmstadt, Germany) and Endothelial Cell Growth Supplement with Heparin (ECGS/H) (C-30120, Promocell, Heidelberg, Germany). For an overview of the supplements and their final concentration see Table 3. The ECGS/H is a growth supplement and contains necessary growth factors and hormones in an appropriate concentration. This aqueous protein extract is from mixed-sex bovine hypothalami. Heparin, as an additional supplement, enhances the growth promoting effect on endothelial cells.

For optimal isolation conditions DPBS and gelatin were placed in a water bath set to 37 °C before isolation.

Before the isolated HUVEC (see 2.1.2.1) are transferred to the culture flask, the flask bottom should to be coated with gelatin, because HUVEC proliferate better in coated flasks. For this, gelatin solution (G1393, Sigma-Aldrich, Hamburg, Germany) was mixed with DPBS in a 1:1 ratio and then distributed over the surface of the culture flask. After 30 minutes the gelatin solution was aspirated. The cell pellet obtain from 2.1.2.1 was resuspended in 5 ml culture medium and then transferred to the t25 tissue culture flask coated with gelatin. The culture medium was changed on the second day. After that, the medium was changed two to three times a week and the subcultivation ratio was 1:2 or 1:3. The subcultivation protocol equals that of EA.hy926 cells (for details see 2.1.1); with differences in the growth medium used and that the tissue culture flask was coated with gelatin.

Table 3: Additional supplements for HUVEC cultivation.

Supplement	Final concentration
Fetal bovine serum	20 %
Penicillin-Streptomycin	100 U/ml; 100 µg/ml
Endothelial Cell Growth Supplement with Heparin	0.02 %

2.2 Histone deacetylase inhibitors

In this study, three histone deacetylase inhibitors were used, Scriptaid (BML-GR326, Enzo Life Sciences, Lörrach, Germany), suberoylanilide hydroxamic acid (SAHA) (10009929, Cayman Chemical, Ann Arbor, MI, USA) and trichostatin A (TSA) (BML-GR309, Enzo Life Sciences, Lörrach, Germany). All of these inhibitors are hydroxamic acids. All histone deacetylase inhibitors were dissolved in dimethylsulfoxid (DMSO) (A994, Carl Roth, Karlsruhe, Germany). Table 4 shows the different concentration of the histone deacetylase inhibitors used in this study. Scriptaid has a lower cytotoxcicity than TSA and the optimal concentration recommended by the supplier is 6 - 8 µM.

Table 4: Concentration of the different histone acetylase inhibitors used in this study.

Substance	Concentrations (µM)
Scriptaid	10, 5, 3 and 1
SAHA	10, 3 and 1
Trichostatin A	1, 0.3 and 0.1

2.3 Messenger RNA stability assay

Regulation of mRNA stability is one of the mechanisms controlling expression levels of proteins. In this study, 5,6-dichloro-1-β-D-ribofuranosylbenzimidazole (DRB, D1916, Sigma-Aldrich, Hamburg, Germany) was used to block transcription elongation by polymerase II. The cells were cultured to confluence and then treated with 3 µM scriptaid for 2 hours. After this incubation time, 60 µM of DRB was added for 3 or 6 hours, respectively. The effect of scriptaid on Nox4 mRNA was measured by qPCR (2.5) after isolating RNA from the cells (2.4.1.1).

2.4 Nucleic acid isolation

Either spin columns (peqGOLD Total RNA Kit (S-Line), 12-6834, PEQLAB Biotechnologie, Erlangen, Germany) or peqGOLD TriFast (30-2020, PEQLAB Biotechnologie, Erlangen, Germany) method were used to isolate total RNA. For plasmid isolation, two kits were used. The peqGOLD XChange Plasmid Midi Kit (12-7401, PEQLAB Biotechnologie, Erlangen, Germany) was used to isolate small quantities of plasmids, to test if the bacteria have uptaken the plasmid, and to determine if the plasmid has the correct size, i.e. plasmids are intact and not broken, which was determined by electrophoresis (as described in 2.7.2.3). If the bacteria have uptaken the correct plasmid, the peqGOLD XChange Plasmid Maxi-EF Kit (12-7404, PEQLAB Biotechnologie, Erlangen, Germany) was used to isolate lager amounts of plasmids, which then were used for transfection of the eukaryotic cells (as described in 2.8). The EF-kit allows the preparation of plasmids from bacteria without endotoxin contaminations. Genomic DNA was used to determine the methylation state of different CpG sites in the human Nox4 promoter by pyrosequencing (as described in 2.12 and 2.12.4). The genomic DNA was isolated with the GenElute™ Mammalian Genomic DNA Miniprep Kit (G1N70, Sigma-Aldrich, Hamburg, Germany).

2.4.1 Spin columns

The principle of the spin column technology is based on binding of nucleic acids to the silica membrane. This is solid a phase extraction method. Chaotropic salts not only help to lyse the cells,

but also support the nucleic acids to bind to the silica membrane, by destabilizing hydrogen bonds, van der Waals forces and hydrophobic interactions. Alcohol helps the binding of the nucleic acids to the membrane, too, that is the reason why ethanol or isopropanol are normally added to the binding buffer. The washing steps serve to remove proteins and salts from the silica membrane. The first washing buffer generally has a low amount of chaotropic agents to get rid of remaining proteins from the membrane, which are not passed through the column in the binding step. After removing the proteins, a wash step with ethanol follows to carry away the chaotropic salts. Because the removal of the chaotropic agents is important; this kit uses a second ethanol wash. If the salts are not washed away completely, the yield and purity of the nucleic acids is low, resulting in a high A230 value. After all contaminants are erased from the membrane, the now pure nucleic acids are eluted either in water or TE-buffer. It is noteworthy that for DNA the water should sit longer on the membrane, than for RNA, because the high molecular weight DNA does not rehydrate as easy as RNA [257,258].

2.4.1.1 RNA isolation

The peqGOLD Total RNA Kit is a silica-membrane based technology, which allows isolating total RNA from cells and tissues fast and easily. Cells were cultivated in 24-well plates until confluency and then treated with different compounds (as described in 2.22.2). RNA was isolated according to the manufacturer's protocol. All steps are carried out at room temperature. After treatment of the cells, the cell culture medium was aspirated and 400 µl of RNA Lysis Buffer T was added directly into the wells. After a short incubation/lysis time, the solution from the wells was transferred to a 1.5 ml sample tube. 400 µl of 70 % ethanol (A3678, Applichem, Darmstadt, Germany) was added to the 400 µl lysate obtained from one well of the 24-well plate. The ordered ethanol was absolute ethanol, which was diluted to 70 % prior to use of the kit . For this, 35 ml of absolute ethanol was mixed with 15 ml diethylpyrocarbonate (DEPC)-treated water. The DEPC-water was produced by mixing 0.1 ml DEPC (D-5758, Sigma-Aldrich, Hamburg, Germany) in 50 ml water at room temperature for 1 hour, then autoclaved and cooled again to room temperature). After the addition of the equal volume of ethanol, the tube was mixed thoroughly by vortexing. A spin column was placed on a 2.0 ml collection tube (supplied with the kit) and the lysate was added directly on the membrane. Then, the spin columns are placed in a microcentrifuge and spinned down for 1 minute at 10,000 x g. The flow-through was discarded. In the next step 500 µl of RNA Wash Buffer I was added on the membrane, followed by a centrifugation for 15 seconds at 10,000 x g. Again the flow-through was discarded. After this, 600 µl of RNA Wash Buffer II was added to the membrane and centrifuged at 10,000 x g for 15 seconds. Then, the washing step with the RNA Wash Buffer II was repeated. After the three washing steps the silica membrane with the RNA was dried to remove all the ethanol from the column. After that, the spin column was placed in the micocentrifuge and centrifuged for one minute at 10,000 x g. The spin column was then placed on a new 1.5 ml collection tube. 50 µl of 70°C hot distilled H_2O (dH_2O) was added to the center of the membrane and incubated for 5 minutes, followed by a centrifugation step for one minute at 5,000 x g to elute the RNA.

2.4.1.2 Plasmid isolation

In this study, plasmids were used for promoter analysis. Therefore, promoter fragments were cloned in front of the luciferase reporter gene. For closer information about the plasmids used see 2.7.2.

As described above, the peqGOLD XChange Plasmid Midi and peqGOLD XChange Plasmid Maxi Kits were used. As the protocols differ only slightly, only the procedure of the peqGOLD XChange Plasmid Maxi kit is described here. The isolation of the plasmids was performed according to the manufacturer's protocol. The transformed bacteria were cultivated in LB medium (lysogeny broth; 10 g peptone (8952, Carl Roth, Karlsruhe, Germany), 5 g yeast extract (2363, Carl Roth, Karlsruhe, Germany) and 10 g sodium chloride (NaCl) (9265, Carl Roth, Karlsruhe, Germany) for one liter) in an overnight culture (37°C with shaking 250 rpm) with ampicillin (0.1 mg/ml). For the peqGOLD XChange Plasmid Maxi Kit, 100 ml overnight culture was prepared. Overnight culture was pelleted by centrifugation at 4,000 x g for 20 minutes at 4°C. The supernatant was discarded. 12 ml Solution I-EF/RNase A (0.5 mg/ml) were added to the bacterial pellet. The cells were resuspended by vortexing. For high yields of plasmid DNA, it is important to completely resuspend the cell pellet. Then 12 ml of Solution II was added and mixed by inverting 6-8 times, followed by incubation at room temperature for 5 minutes. Next, 12 ml pre-cooled (4 °C) Solution III was added and mixed by inverting until a white flocculate formed, followed by a 5 minute incubation on ice. During this incubation time, the XChange column is equilibrated with 4 ml Buffer EQ (100 mM Tris-HCl, 15 % EtOH, 1 M KCl; pH 8.5). A filter was placed in a funnel and pre-wetted with a few drops of Buffer EQ. The bacterial lysate was then loaded on then filter and the flow-through collected. The filter cleared supernatant was then loaded on the equilibrated column and allowed to pass the column by gravity flow. The XChange Maxi column was then washed with 24 ml DNA Wash-EF I Buffer, followed by 2 x 12 ml DNA Wash-EF II Buffer; every time the flow-through is discarded. In total, there are four washing steps for the maxi kit to get the plasmids endotoxin free, compared to one washing step for the midi kit. 15 ml Elution buffer were added directly on the matrix for the maxi columns. The flow-through was collected. 3.5 ml of isopropanol (6752, Carl Roth, Karlsruhe, Germany) was added to the eluate to precipitate the plasmid DNA, carefully mixed and centrifuged at 10.000 g for 30 minutes at 4°C. To the eluate from the maxi kit 11 ml of isopropanol are added and mixed to precipitate the plasmid DNA, followed by a centrifugation at 10,000 x g for 30 minutes at 12°C. After the centrifugation step the supernatant is discarded. 1 ml of 70 % ethanol is added to the pellet. The pellet is then transferred to a 2.0 ml collection tube and another milliliter of 70 % ethanol is added. The collection tube is than centrifuged for 10 minutes at 15,000 x g at room temperature. After the centrifugation the supernatant was discarded and the pellets were dried at room temperature for half an hour. After drying, 50 µl H_2O-EF was added to the pellet and the tube with the pellet was then placed on a 3D-shaker for 60 minutes to re-dissolve the DNA.

2.4.1.3 Genomic DNA isolation

For the isolation of genomic DNA, cells were cultured in a 24-well plate until confluency and treated with 5 µM scriptaid for 24h (for details see 2.2). The isolation was performed using the GenElute™ Mammalian Genomic DNA Miniprep Kit (G1N70, Sigma-Aldrich, Hamburg, Germany) according to the manufacturer's protocol. After treatment, cells were washed with Dulbecco's Phosphate-Buffered Saline (DPBS) (14190, Gibco/Life Technologies, Darmstadt, Germany), because Ca^{2+} and Mg^{2+} in the cell culture media as well as proteins in the FBS inhibit the following trypsinization. Cells were detached from the well with 50 µl trypsin-EDTA (L11-004, PAA Laboratories, Cölbe, Germany). EDTA is a chelating agent and protects trypsin by "sequestering" metal ions. When the cells were detached, one milliliter of medium was added to stop the trypsin. The cells were then transferred to a 1.5 ml collection tube for a centrifugation at 300 x g for 5 minutes. The culture medium was

removed and discarded. The cell pellet was resuspended in 200 µl of Resuspension Solution. To obtain RNA-free genomic DNA, 20 µl of RNase A Solution was added and incubated for two minutes at room temperature. After RNA digestion, 20 µl of Proteinase K solution (20 mg/ml) was added to the sample followed by 200 µl of Lysis Solution C, thoroughly vortexed and incubated for 10 minutes at 70°C on a thermoshaker incubator. For each sample, a pre-assembled GenElute Miniprep Binding Column was needed. To maximize the binding of the DNA to the membrane, 500 µl of the Column Preparation Solution was added to each column, followed by a centrifugation step at 12,000 x g for one minute. The flow-through was discarded. 200 µl of absolute ethanol was added to the lysate. The lysate was than vortexed thoroughly because a homogenous solution is essential. The entire lysate was then loaded onto the pre-treated binding column and centrifuged 6,500 x g for one minute. For the first washing step, 500 µl of Wash Solution was added to each column and then centrifuged 1 minute at 6,500 × g. The flow-through was discarded. Another 500 µl of Wash Solution was added to the binding column followed by a centrifugation for three minutes at maximum speed to dry the membrane. The flow-through was discarded and another centrifugation step for one minute at full speed was performed. For elution, the spin column was placed in a new 2.0 ml collection tube and 200 µl of Elution Solution (10 mM Tris-HCl, 0.5 mM EDTA, pH 9.0) was added onto the middle of the membrane to elute the DNA. Prior to centrifugation for one minute at 6,500 x g, there was an incubation step of five minutes at room temperature to increase the elution efficiency.

2.4.2 Phenol-chloroform extraction (TriFast™)

Like the above described spin column method, the phenol-chloroform extraction method serves to isolate nucleic acids. In this case, the nucleic acids are not bound to a membrane, but collected and divided from proteins by phase separation. Phenol dissolves proteins and lipids and leaves water soluble matters, like carbohydrates and nucleic acids, in the aqueous phase. Because phenol is denser, the organic phase is at the bottom of the tube, and the aqueous phase sits on the organic phase. Between these two phases an interphase can be seen. Because phenol is less polar than water, and nucleic acids are polar due to their negatively charged phosphate backbone, nucleic acids are soluble in water but not in phenol. When water and phenol are mixed, the nucleic acids remain in the aqueous phase, because polar molecules are best solved in polar solvents and non-polar molecules dissolve better in non-polar solvents. Chloroform is added to make sure that the phenol and water will mix again. At last, RNA is in the aqueous phase, DNA in the interphase and proteins are in the organic phase. Proteins have different side chains with different polarity. In the cytoplasm the proteins are mainly folded in the way that the amino acids with the polar side chains are on the outside and the hydrophobic side chains are away from the polar solvent, in case of the cytoplasm water. When proteins come in contact with a less polar solvent than water, in this case phenol, the non-polar side chains from the amino acids in the inside of the molecule want to get in contact with the new solvent, whereas the hydrophilic amino acids want to avoid the contact with the phenol. In phenol proteins are denatured and that is the reason while proteins and nucleic acids can be separated by phenol[259,260].

Cell were cultivated and treated in 24-well plates. After treatment, the cell culture medium was aspirated and replaced with 250 µl TriFast™ per well. It is essential to use enough TriFast™ reagent, because an insufficient amount may cause contamination of your RNA with DNA. The TriFast™ reagent contains phenol and guanidine isothiocyanat. Phenol lowers the pH and dissolve the

proteins, whereas guanidine isothiocyanat lyses the cells and denatures proteins, because it is a chaotropic salt. After cell lysis and homogenization with the 250 µl of TriFast™ reagent, an incubation time of five minutes follows to ensure the dissociation of the nucleotide complexes. After the incubation, the sample was transferred to a 1.5 ml sample tube and 50 µl of chloroform (A1585, Applichem, Darmstadt, Germany) are added. The samples are shaken fiercely and then incubated for 5 minutes at room temperature.
Then, the samples were centrifuged for 5 minutes at 13,000 x g. In the next step, the 70 µl of the aqueous phase, i.e. upper phase, are transferred to a new sample tube and 125 µl of isopropanol (6752, Carl Roth, Karlsruhe, Germany) was added. To support the precipitation of the RNA, 1 µl GlycoBlue™ (AM9515, Ambion/ Life Technologies, Carlsbad, California, USA) was added to each sample. GlycoBlue™ is a blue dye covalently linked to glycogen and serves as a coprecipitant or carrier for nucleic acids. A useful side effect is that GlycoBlue™ labels the pellet blue, so it is easier seen in the sample tubes. The samples were vortexed thoroughly for about 15 seconds and then placed at -20°C for 10 minutes. After the precipitation, a centrifugation step (at 4°C for 20 minutes at 13,000 x g) followed. The RNA pellet could now be seen as a small dot at the bottom of the tube. The isopropanol supernatant was discarded carefully and the RNA pellet was washed twice with 500 µl 75 % ethanol at 4°C for 5 minutes at 13,000 x g. After each washing step the supernatant was discarded and the samples was placed head down to dry for 30 minutes under a chemical hood. Finally the dried RNA pellets were resuspended in 20 to 50 µl dH_2O, depending on the cell type and the cell number.

2.4.3 Concentration measurement of nucleic acids (NanoDrop™)

To determine the concentration of the isolated nucleic acids by the methods described above (2.4) the NanoDrop™ 1000 (Thermo Scientific, Wilmington, DE, USA) was used. All nucleotides absorb light at a maximum wavelength of 260 nm; this is due to nitrogen atoms in the purines and pyrimidines. That is the reason why the concentration of nucleic acids can be determined spectrophotometrically. The mathematical principles (from the NanoDrop™ 1000 manual) are a modified Lambert-Beer equation for nucleic acids to give $c = (A * \varepsilon)/b$. Where c is the nucleic acid concentration in ng/ml, A is the absorbance in absorbance unit (AU), ε is the wavelength-dependent extinction coefficient in ng-cm/ml and b is the path length in cm. The generally accepted extinction coefficients for nucleic acids are:

- Double-stranded DNA: 50
- Single-stranded DNA: 33
- RNA: 40

Contaminants like proteins or phenol absorb light at 280 nm, because of their aromatic side chains. To determine the purity of nucleic acids the ratio of absorbance at 260 nm and 280 nm is used. A ratio of 1.8 is accepted as pure DNA, whereas a ratio of 2.0 is accepted for RNA. The NanoDrop™ was first blanked with the appropriate elution buffer. One 1.5 µl of each sample are measured. For a more detailed description see NanoDrop™ 1000 manual.

2.5 Quantitative reverse transcription polymerase chain reaction

The reverse transcription polymerase chain reaction (RT-PCR) serves to transcribe RNA into cDNA. In this reaction two enzymatic steps are involved. In the first step with a reverse transcriptase, this

converts the RNA into cDNA. In the second step, in which the cDNA is amplified in a PCR reaction, the enzyme needed is a Taq polymerase. The Taq polymerase is a heat stable enzyme derived from the thermophilic bacterium *Thermus aquaticus*[261,262]. There are two different forms of RT-PCR, one-step and two-step. In the one-step RT-PCR everything takes place in the same tube. Because the both enzymatic reactions occur in a single tube, the one-step RT-PCR minimizes experimental variation. However, because RNA is prone to rapid degradation if not handled properly, the on-step method is not suitable for applications in which the same sample is used over a long period of time[263]. It has also been reported that the one-step RT-PCR is not as sensitive as two-step RT-PCR[264]. The two-step RT-PCR separates the reverse transcription from the PCR amplification. They take place in different tubes. Because the steps are separated this allows different real-time PCR reactions from the same cDNA sample. A two-step RT-PCR is highly reproducible and should be preferred when using SYBR green or similar dyes[265]. Because there are more pipetting steps, the two-step method is more prone to DNA contamination than the one-step method[263].

2.5.1 Reverse transcription

The reverse transcriptase allows the transcription of RNA into DNA (see Figure 14 for schematic overview). The reverse transcriptase was discovered by Howard Temin[266] and David Baltimore[267], independently. At that time the existence of a reverse transcriptase was discussed controversially because in contradicted the central dogma of molecular biology[268,269]. Nowadays reverse transcription is commonly used to transcribe RNA into cDNA for subsequent applications like PCR. This is necessary, because the PCR technique works only with DNA. The reverse transcription can be primed with random primers, oligo(dT), or a gene-specific primer. Random primers are good for the detection of non-coding RNAs, because they can detect all kinds of RNA, they anneal at a random point in the RNA sequence, depending on sequence specificity. Because of their random binding, the cDNA of mRNAs will not be full length. Another disadvantage is that ribosomal RNA will be amplified as well, which may lead in some cases to lower reverse transcription of target mRNA. Oligo(dT) primers have a high specificity for RNAs with a poly(A) tail. The problem can be that the reverse transcription does not reach the 5' end of long transcripts.

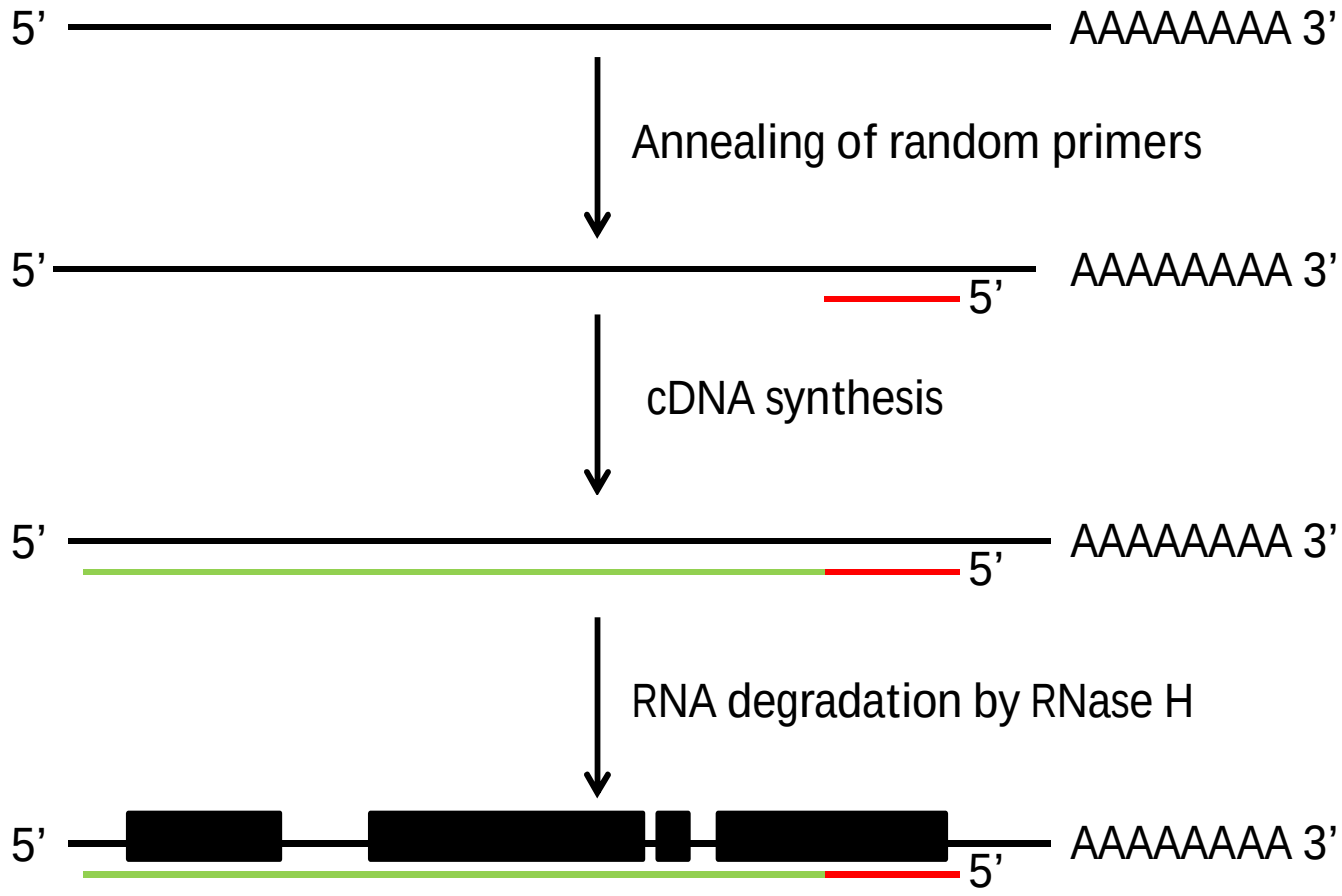

Figure 14: Schematic overview of reverse transcription.
cDNA synthesis occurs in several steps. The random primers (red) anneal, depending on sequence specificity, on a random point of the mRNA (blue). After annealing the reverse transcriptase creates a cDNA strand (green). By its RNase H activity the reverse transcriptase itself, degrades the RNA strand of the RNA:DNA hybrid. The result is a single strand cDNA which can be used for qPCR or other downstream applications. Oligo(dT) primers will anneal to the poly(A) tail.

In this study the high-capacity cDNA reverse transcription kit (4368813, Applied Biosystems/Life Technologies, Darmstadt, Germany) was used. Up to 2 µg of total RNA can be used, in a 20 µl reaction, to be converted into single stranded cDNA. The reverse transcriptase used in this kit is the MultiScribe™ MuLV (murine leukemia virus) reverse transcriptase. MuLV reverse transcriptase is a recombinant RNA-dependent DNA polymerase that uses single-stranded RNA as a template in the presence of a primer to synthesize a cDNA strand. The reverse transcriptase has a weak RNase H activity, which means it can hydrolyze the RNA in RNA:DNA hybrid strands, leaving behind single stranded cDNA. For each sample 10 µl of RNA (up to 2 µg) are used. After the isolation of the RNA (see 2.4 for details) the RNA concentration was measured with the NanoDrop™ (see 2.4.3). If necessary RNA was diluted with dH_2O so that 10 µl could be used in each reaction without getting over the limit of 2 µg per reaction. According to Table 5 a master mix for the required number of reactions was calculated and then prepared.

Table 5: Master mix for reverse transcription

Component	Volume/reaction (µl)
10x reverse transcription buffer	2
25x dNTP Mix (100mM)	0.8
10x random primers	2
MultiScribe™ reverse transcriptase	1
Nuclease-free H_2O	4.2
Total volume per reaction	10

The master mix was placed on ice and the MultiScribe™ reverse transcriptase was added at the last moment, before the mix was added to the RNA. 10 µl of RNA was added into 0.2 ml PCR tubes. The tubes with the RNA were placed on ice. After the addition of the reverse transcriptase to the master mix, the master mix was mixed gently. The 10 µl of the master mix were added to each PCR tube containing the 10 µl RNA, sealed with a cap, mixed and centrifuged. All tubes were then placed in a thermocycler and the program as shown in Table 6 was started to convert the total RNA into single stranded cDNA.

Table 6: Thermal cycling conditions for reverse transcription

	Step 1	Step 2	Step 3	Step 4
Temperature	25 °C	37 °C	85 °C	4 °C
Time	10 minutes	120 minutes	5 minutes	∞

2.5.2 Quantitative real-time polymerase chain reaction (qPCR)

The qPCR is an effective method to amplify, simultaneously detect and quantify one or more target DNAs in real-time[270]. The qPCR method works similarly to a normal PCR reaction, with the difference that the amplification of the target(s) can be monitored in real-time with a fluorescence detection system. There are different techniques to generate the fluorescence signal [271]. The first option is to use double-stranded DNA binding dyes such as SYBR Green I. SYBR Green I binds to the minor groove of double-stranded DNA, thus causing fluorescence of the dye. Because the amount of double-stranded DNA increases in each PCR cycle, the fluorescence intensity increases proportionally. The increase in fluorescence can be measured and this allows quantification of DNA concentration (shown in Figure 15). The disadvantage is, that SYBR Green I binds not only target double-stranded DNA, but also primer-dimers or other unspecific PCR products, which can interfere with quantification of the target DNA. Another detection opportunity is the probe based method. This technique is more accurate than the SYBR Green I method, because the probe binds only to its specific sequence, thereby avoiding false signals like primer-dimers. By labeling different probes with different dyes, more target genes can be detected simultaneously in a multiplex PCR. The principle is the same as with SYBR Green I; an increase of the specific PCR product leads to an increase in fluorescence signal. The probes are labeled with the fluorescence dye at their 5' end and a quencher at the 3' end. The quencher is necessary to avoid auto-fluorescence of the probe. Only after the degradation of the quencher by the Taq polymerase, the close proximity of the quencher to the dye is broken and fluorescence can be detected[272]. The negative aspect of the probe based method is that for every target, a new probe has to be designed.

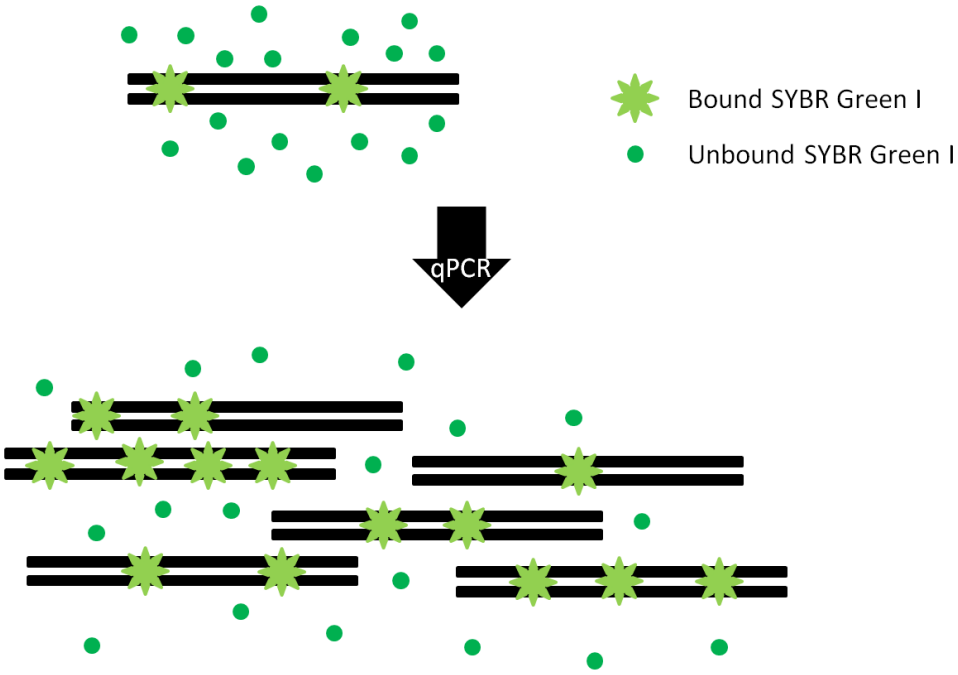

Figure 15: Schematic view of SYBR Green I chemistry.
SYBR Green I binds to double-stranded DNA and thereby increasing its fluorescence. The amplification of new double-stranded DNA during every PCR cycle increases the fluorescence signal, because more SYBR Green I can be bound to the newly synthesized double-stranded DNA products.

Real-time PCR can be quantified in two ways. Either in an absolute quantification, which uses external standards to determine the absolute value of target DNA. But in this study the relative quantification was used, which calculates the ratio between the target and an internal control (housekeeping gene). This internal control is normally a housekeeping gene, which should not differ in concentration in various experimental states. Every fluorescence probe has background fluorescence. This is true for SYBR Green I, too. To account for the background fluorescence, a threshold for every DNA-based fluorescence, is set over the background. The number of PCR cycles, at which the DNA-based fluorescence is over the background, is called the cycle threshold (C_t). During the exponential amplification phase, the amount of the target DNA doubles every cycle. To calculate the relative expression, the ΔC_t value has to be calculated first. For this, the control C_t is subtracted from the target C_t (C_t target - C_t control). Then, the ΔC_t value of the treated group is subtracted from the ΔC_t value of the untreated group ($\Delta\Delta C_t$= ΔC_t untreated - ΔC_t treated). Using this method the $\Delta\Delta C_t$ of the untreated group is 0. To calculate the n-fold expression of the target gene the following formula is used:

$$\text{Fold}_{\text{untreated to treated}} = 2^{-\Delta\Delta Ct}$$

The untreated control is then 1. If for the treated group the $\Delta\Delta C_t$ is -1, this means that the doubled amount of the target gene is expressed under these conditions. If the $\Delta\Delta C_t$ is 1, this means that with this treatment the expression of the target gene is halved. It is important to know that both primer pairs (for the housekeeping gene and for the target gene) should have nearly the same efficiency if using this method.

In this study, the SYBR® Green JumpStart™ Taq ReadyMix™ (S4438, Sigma-Aldrich, Hamburg, Germany) was used. Prior to use the obtained cDNA from 2.5.1 was diluted with dH_2O to 10 ng/µl. Because RNA concentration was measured with the NanoDrop™ (2.4.3) and 10 µl of RNA was used and the total volume of the reaction was 20 µl, the required quantity of water could be calculated easily. To achieve best reproducibility, a reaction master mix was prepared (see Table 7). The sequences of the primers used in this study are shown in Table 9. For details about primer design see 2.14. The reference gene was β-Tubulin because it fulfilled all the characteristics for an acceptable reference gene, i.e. the expression of β-Tubulin was stable even after treatment. The data were normalized to β-Tubulin.

Table 7: Master mix for qPCR

Component	Volume/reaction (µL)
2x SYBR® Green Jump Start Taq ReadyMix	10
Forward primer	0.2
Reverse primer	0.2
H_2O	7.6
Total volume per reaction	18

The qPCR was performed in a 96-well plate. 2 µl (20 ng) of every sample was placed in a 96-well plate and 18 µl of master mix was added. The plate was sealed with an optical film and spinned down. After this the plate was placed in a real-time PCR thermal cycler and the following program (Table 8) was used.

Table 8: Thermal cycling conditions for qPCR

	Temperature	Time	Number of cycles
Initial denaturation	94 °C	2 minutes	1
Denaturation Annealing, extension, and read fluorescence	94 °C 60 °C	15 seconds 1 minute	40

If necessary (e.g. in SYBR Green technique), a melt curve was added at the end of the run to analyze the PCR product. Data were analyzed using the software provided with the real-time PCR thermal cycler. Excel was used to calculate the relative expression with the $\Delta\Delta C_t$ method.

Table 9: Primers used in qPCR for comparison of mRNA expression.

Target	Orientation	Sequence
β-Tubulin	forward	CCAAGTTCTGGGAGGTGATCA
	reverse	ACGCCAAGAAACAGTGATGCT
Nox4	forward	TTTTCTCAGGCGTGCATGTG
	reverse	CATTCAGTTCAACAAAGTCTTCACTGT
HDAC3	forward	TGGCTTCTGCTATGTCAACG
	reverse	CCCGGTCAGTGAGGTAGAAA
c-Jun	forward	TAACAGTGGGTGCCAACTCA
	reverse	TTTTTCTCTCCGTCGCAACT
c-Fos	forward	GACCTTATCTGTGCGTGAAACA
	reverse	AATACACACTCCATGCGTTTTG
HDAC1	forward	TTGGAAAGGTGCCCTTATTG
	reverse	CCAGTGGGAAGGTACGAAAA
HDAC2	forward	GAAGCAGACAAATGGGGGTA
	reverse	AATGTGGGCCTGACAAAAAG
HDAC4	forward	TGAAGAATGGCTTTGCTGTG
	reverse	ATCTTGCTCACGCTCAACCT
HDAC5	forward	TCTGTGAGGAGGGCTGTCTT
	reverse	CCCACACACTTTCACCCTCT
HDAC6	forward	CGAGCTGATCCAAACTCCTC
	reverse	GGTCCTGAGACTCCCAATCA
HDAC7	forward	CAGCTTTTTGCCTCCTGTTC
	reverse	TCAGGTTGGGCTCAGAGACT
HDAC8	forward	GTGGGAATTGGCAAGTGTCT
	reverse	ATAGCCTCCTCCTCCCAAAA
HDAC9	forward	CAGGCTGCTTTTATGCAACA
	reverse	CAGCAGGGGAAGAGTGAGTC
HDAC10	forward	AGAAACACGGGCTACACAGG
	reverse	CGGTGCCAGGAGAAGTAAAG
HDAC11	forward	GAGCTGGCCCTTCCTCTACT
	reverse	CTATGGGCTGGTGACTTCGT
DICER1	forward	TTGGCTTCCTCCTGGTTATG
	reverse	CACATCAGGCTCTCCTCCTC

2.6 Western blot

Western blot is a commonly used technique to identify distinct proteins out of a homogenous protein mixture. Protein immunoblotting uses different techniques to separate the proteins and later quantify and identify them. The protein mixture from tissue or cells is first separated by electrophoresis, transferred to a nitrocellulose membrane or polyvinylidene fluoride membrane and then detected with a specific antibody against the protein of interest. As mentioned, the separation of the proteins is carried out by gel electrophoresis. The proteins can be separated by isoelectric point, molecular weight or charge. A combination of the different separation methods is possible, too. For protein analysis, a polyacrylamide gel electrophoresis (PAGE) is used normally. Polyacrylamide separated the proteins by molecular weight, due to its uniform pore size. Electrophoresis can be done under denaturing conditions, which means the secondary, tertiary and

quaternary structures of the proteins are not maintained. The protein structure is determined by hydrophobic interactions, hydrogen bonds and disulfide bonds, just to mention some of these. Under denaturing conditions, normally provoked with sodium dodecyl sulfate (SDS), a strong reducing agent, proteins and other macromolecules lose their natural structure. In their denatured form they can be separated by molecular weight. In the gel electrophoresis the proteins migrate to the anode, because they are covered with the negatively charged SDS.

Smaller molecules migrate faster than larger molecules through the polyacrylamide gel in an electric field, because they can pass easier through the gel matrix. Higher polyacrylamide content (e.g. 2%) allows a better separation of small molecules, because the pores are thinner, but large molecules migrate slower and their separation might be difficult. By reducing the amount of polyacrylamide (e.g. 0.8%) larger molecules are separated better, because the gel matrix has larger pores, but smaller molecules may migrate out of the gel, because they can pass easily the pores and therefore migrate fast. Depending on the size of the macromolecule of interest, the percentage of the polyacrylamide gel should be chosen. After the separation of the proteins in the electric field, they are transferred to a membrane.

The membrane consists of nitrocellulose or polyvinylidene fluoride. The blotting is necessary to make the proteins accessible to antibodies. Again, an electric current is used to blot the proteins from the gel onto the membrane, thereby keeping the layout of the gel intact, this means the proteins are still separated on the membrane as they were on the gel. Nitrocellulose as well as polyvinylidene fluoride bind proteins non-specific. The membrane is placed close to the anode and the proteins migrate in the electric field to the plus pole. The membrane binds the protein in an unspecific manner by hydrophobic interactions and charge interactions between the protein and the membrane. After the transfer, the membrane is stained with Ponceau S, to verify whether all proteins are transferred evenly to the membrane. Ponceau S is a water soluble dye and can be easily washed away afterwards. Antibodies are used to detect the proteins of interest, but antibodies are proteins, too, i.e. the antibodies can bind to the membrane, because the membrane binds protein in a non-specific manner. To avoid this, blocking solution is used prior to the addition of the antibody. The blocking solution contains bovine serum albumin (BSA) or non-fat dry milk to block the membrane. They interact with the membrane and therefore prevent unspecific binding of the antibodies to the membrane.

Blocking the membrane with the blocking solution diminishes the background and false positive results. The antibody solution is left on the membrane between 60 minutes and overnight. After binding of the primary antibody, the membrane is rinsed with Tris-buffered saline containing Tween 20 as a detergent, to wash unbound primary antibodies away. A second antibody is used to detect the species-specific portion (fragment crystallizable region (Fc region)) of the primary antibody. The secondary antibody is linked to biotin or to a reporter enzyme like horseradish peroxidase (HRP). The horseradish peroxidase for example cleaves a chemiluminescent agent, and the product of this reaction produces light, which can be detected on a photographic film. Depending on the amount of protein the produced light is proportional. On the photographic film the target protein appears as a band and can be quantified with computer software.

2.6.1 Protein isolation

Cells were seeded in 6-well plates. When the cells were confluent, they were treated with scriptaid for 24 hours. In each well, 120 µl of lysis buffer (composition see Table 10) was added. Every component in the lysis buffer has a different effect. Sodium pyrophosphate (NaPPi) is a chelating agent and blocks protease and DNAse activity, because it binds metal ions with a 2^+ charge and many proteases and DNAses need these metal ions to function. The protease and phosphatase inhibitors instead inhibit the activity of the enzymes. Triton X is a detergent; this means it is an amphipathic molecule. Amphipathic molecules can dissolve fats (like in the cell membrane) by forming micelles, i.e. the hydrophobic part of the amphipathic molecule point toward the fat molecule. Tris-HCl and NaCl (Table 11) are buffering agents and they prevent protein degradation. Sodium fluoride (NaF) is a Serine/Threonine phosphatase and acidic phosphatase inhibitor. NaF mimics the nucleophilic hydroxyl ion in the active site of the enzyme and thereby inhibiting its activity.

Table 10: Western blot cell lysis buffer formula

Component	Supplier	Volume (µl) per 1 ml
5x pre-lysis buffer (see Table 11)		200
Triton X (10%)	6683, Carl Roth, Karlsruhe, Germany	100
Protease and Phosphatase Inhibitor Cocktail	78442, Thermo Fisher Scientific, Waltham, MA, USA	10
H_2O		690

Table 11: 5x pre-lysis buffer

Component	Supplier	Concentration (mM)*
Tris-HCl, pH 7.5	9090, Carl Roth, Karlsruhe, Germany	20
NaCl	3957, Carl Roth, Karlsruhe, Germany	150
NaPPi		10
NaF		20

* dissolved in H_2O

After addition of the lysis buffer to each well, a rubber policeman is used to scrape the well. The lysate was then transferred to a 1.5 ml sample tube. The sample tubes were then incubated on ice for 10 minutes, followed by a centrifugation at 4 °C at 13,000 revolutions per minute (rpm) for 10 minutes. The cell debris was discarded and the supernatant was transferred into a new sample tube.

2.6.2 Bicinchoninic acid assay

The bicinchoninic acid (BCA) assay was used to determine protein concentration[273], thereby a color change from green to purple can be seen and measured with colorimetric techniques. Proteins can reduce Cu^{2+} to Cu^+ in an alkaline medium. Peptides with three or more amino residues form a light blue colored chelate complex with cupric ions. This reaction is temperature depended. The amount of protein in the solution is proportional to the amount of reduced cupric ions. In the next step two

molecules of BCA chelate with one cuprous ion, leading to a strong purple-colored complex. The color formation reaction is strongly dependent on amino acid residues (cysteine or cystine, tyrosine, and tryptophan). The formed purple-colored complex absorbs light at a wavelength of 562 nm. The BCA reaction is 100 times more sensitive than the light blue complex formed by the reduction of Cu^{2+} to Cu^{+} by the proteins. Peptide bonds assist in forming the BCA/copper complex at higher temperatures, which leads to a higher increase assay sensitivity while minimizing the variances caused by unequal amino acid composition[274]. To determine the protein concentration, the absorption of the sample is compared to the absorption of samples with a known protein concentration.

The protein concentration is measured colorimetric with the Sunrise™ microplate reader (Tecan Group, Männedorf, Switzerland) at a wavelength of 562 nm. The Magellan™ software (Tecan Group, Männedorf, Switzerland) was used for data analysis. A standard curve of bovine serum albumin Franktion V (BSA) (K41-001, PAA Laboratories, Cölbe, Germany) was used (see Table 12) to determine the protein concentration in each sample. The standard curve is done in replicates, in total 18 wells are needed for the standard curve.

Table 12: Standard curve for determination of protein concentration

	Well								
Component (µl)	1	2	3	4	5	6	7	8	9
BSA (1mg/ml)	0	1	2	5	10	20	30	40	50
H_2O	50	49	48	45	40	30	20	10	0

For each sample, 5 µl are added to one well, filled up with 45 µl of H_2O. Prior to starting the reaction, a master mix was prepared containing 196 µl BCA and 4 µl $CuSO_4$ per well. 200 µl of BCA/copper solution was added to each well and the plate was placed in an incubator at 37 °C for 30 minutes. Then, the plate was read in the microplate reader.

2.6.3 Gel electrophoresis and immunoblotting

After the protein isolation (2.6.1) and determination of the protein concentration (2.6.2), the same amount of protein (normally ≈ 30 µg) from every sample was transferred into a new tube and stored on ice. A 12 % resolving Bis-Tris gel (see Table 13) was used for electrophoresis (according to Tim Corson, PhD, Indiana University School of Medicine (http://iueye.iu.edu/corson). The 12 % resolving is suitable to separate proteins in a range of 20 – 150 kilo Dalton (kDa), and all the proteins examined in this study fall into this range (Nox4: ≈ 67 kDa, c-Jun: ≈40 kDa, HDAC3: ≈ 50 kDa and GAPDH: ≈ 40 kDa). The 3.5 x buffer for the gel contains 52.32 g Bis (2-hydroxyethyl) amino-tris (hydroxymethyl) methane (Bis-Tris) (B9754, Sigma-Aldrich, Hamburg, Germany) dissolved in H_2O and adjusted to pH 6.5 - 6.8 with HCl (4625, Carl Roth, Karlsruhe, Germany). To create the 10 % ammonium persulfate (APS) solution 10 mg APS are dissolved in 1ml H_2O.

Table 13: Components for a 12 % resolving gel

Component	Supplier	Volume (µl)
3.5 x buffer		5680
30 % acrylamide	A1672, Applichem, Darmstadt, Germany	8000
H_2O		6320
10 % APS	A2941, Applichem, Darmstadt, Germany	100
TEMED	A1148, Applichem, Darmstadt, Germany	20

The resolving gel was prepared according to Table 13 and filled between a 1.5 mm spacer plate (165-3312, Bio-Rad Laboratories, Hercules, CA, USA) and a short plate (165-3308, Bio-Rad Laboratories, Hercules, CA, USA); the glass plates were fixed in a casting frame (165-3304, Bio-Rad Laboratories, Hercules, CA, USA) on a casting stand (165-3303, Bio-Rad Laboratories, Hercules, CA, USA) prior to gel casting. The resolving gel was left for polymerization.

Table 14: Components for a stacking gel

Component	Volume (µl)
1 x buffer*	2000
30 % acrylamide	920
H_2O	4080
10 % APS	80
TEMED	40

* The 3.5 x buffer from Table 13 was diluted to get the 1 x buffer

When the resolving gel has polymerized, a stacking gel (see Table 14 for components) was cast on the resolving gel and a comb was placed between the spacers into the still liquid stacking gel. Again the gel was left for polymerization. The proteins of the samples were mixed in a 1:1 ration with 2x Laemmli buffer[275] (see Table 15), heated for 10 minutes at 95 °C and spinned down at 4°C. The polymerized gels were transferred into a blotting chamber (Bio-Rad Laboratories, Hercules, CA, USA). The chamber was filled with 1x MOPS-SDS (50 mM MOPS, 50 mM Tris base, 1 mM EDTA, and 0.1% SDS) Running Buffer (10530007, bioWORLD, Dublin, OH, USA).

Table 15: 2x Laemmli buffer

Component	Concentration
Tris-HCl, pH 6.8	0.125 M
Sodium dodecyl sulfate	2 %
Glycerol	20%
2-mercaptoethanol	10%
bromphenol blue	0.03 %

The samples were loaded on the gel. A PageRuler™ Prestained Protein Ladder (SM0671, St. Leon-Rot, Germany) was used as a reference to determine protein size. The chamber was placed on ice and the electrophoresis was performed with 80 V until the running front reached the end of the glass

plate. Then, the gel was removed of the glass plates and the stacking gel was cut off. In the next step, the proteins were transferred on a nitrocellulose membrane; therefore a transfer sandwich was prepared containing soak sponges and blotting paper. The nitrocellulose membrane, soak sponges and blotting paper are equilibrated in transfer buffer prior to use.

Table 16: 20x transfer buffer

Component	Amount (g) for 500 ml
Bicine	40.8
Bis-Tris	52.32
EDTA, disodium	3.8
When diluting to 1 x, include 20 % (final) methanol (4627, Carl Roth, Karlsruhe, Germany)	

The blotting sandwich was prepared as follows: the basis was built by a plastic grid. On the grid, two soak sponges and three layers of blotting paper were placed. On the blotting paper, the nitrocellulose membrane was placed and the gel was carefully laid on the nitrocellulose membrane. The membrane was covered with three layers of blotting paper and two pieces of soak sponge. To ensure stability, a second grid is put on the top of the whole sandwich. Air bubbles were rolled out with a glass bar. The blotting sandwich was then placed in a blotting chamber with the nitrocellulose membrane closest to the positive electrode (anode, red). The blotting chamber was filled with 1x transfer buffer containing 20 % (final) methanol. The transfer is carried out over night at 4 °C at 45 V. On the next day, the membrane was stained in Ponceau S (0.5 g Ponceau S, 1 ml acetic acid filled up with H_2O to 100 ml) for five minutes and then rinsed with water to make the bands visible. In the next step, the gel was cut into pieces, i.e. unnecessary parts are discarded. To prevent unspecific reaction of the primary antibody with the membrane, the membrane was placed in blocking solution (5 % skim milk powder in Tris-buffered saline + Tween 20 (TBST, 10 mM Tris-HCl, pH 7.4, 150 mM NaCl with 0.1% Tween 20) for one hour. The antibodies (Table 17) were diluted in 5 % skim milk powder in TBST in dilutions as stated in Table 17. The antibody solution was left on the membrane at 4 °C overnight in a covered bin. On the next day, the antibody solution was removed and saved (stored at – 20 °C until further use) and the blots were washed several times in TBST for five minutes each. After the washing steps, the secondary antibody solution (5 % skim milk in TBST with anti-rabbit IgG HRP-linked antibody; Table 17) was added to the blot and incubated on an orbital shaker for one hour at room temperature. Then, the antibody solution was discarded and the blot was again washed for several times with TBST for five minutes.

Table 17: Antibodies used for Western blot analyses.

Target	Supplier	Dilution
Nox4	NB-110-58851, Novus Biologicals, Littleton, CO, USA	1 : 1,000
c-Jun	ab31419, Abcam, Cambridge, United Kingdom	1 : 1,000
HDAC3	ab7030, Abcam, Cambridge, United Kingdom	1 : 1,000
GAPDH	2251-1, Epitomics, Burlingame, CA,USA	1 : 20,000
Anti-rabbit	7074, Cell Signaling, Danvers, MA, USA	1 : 5,000

The last washing step, before detection of the bands on a photographic film, was performed with TBS. After that, the membrane was removed from the bin, drained and placed on a glass plate. The membrane was then covered with Western Lightning Plus-ECL enhanced chemiluminescence substrate (NEL105001EA, Perkin Elmer, Waltham, MA, USA). The Western Lightning solution contains two components (Enhanced Luminol Reagent and Oxidizing Reagent), which were mixed in a 1:1 ratio and incubated for one minute prior to use. In a dark room, the Amersham Hyperfilm ECL (28906837, GE Healthcare, Little Chalfont, United Kingdom) was placed on the membrane as long as necessary to get clear bands of the target proteins. The hyperfilm was placed in Kodak GBX developer solution (5158621, Kodak, Rochester, NY, USA) until black bands appeared, washed in water und finally placed in Kodak GBX fixer solution (5158639, Kodak, Rochester, NY, USA) for a couple of minutes. After fixation, the film was washed again and dried. Densitometric analysis was performed using the Quantity One software (Bio-Rad).

2.7 Microbiological methods

2.7.1 Bacteria

2.7.1.1 Strains

Two different *Escherichia coli* (*E. coli*) strains, DH5α and Top10, were used in this study. *E. coli* DH5α was a modified form of *E. coli* DH5[276] and first generated by the Bethesda Research Laboratories in 1986[277]. The *E. coli* DH5α have the following genotype: F- ϕ80lacZΔM15 Δ(lacZYA-argF)U169 recA1 endA1 hsdR17 (rk-, mk+) phoA supE44 thi-1 gyrA96 relA1 λ-. The DH5α strain transforms with high efficiency. The endA1 mutation inactivates an intracellular nuclease. The lacZΔM15 is an alpha acceptor allele needed for blue-white screening. recA1 eliminates homologous recombination. supE44 is an amber suppressor. *E. coli* DH5α were used for transformation of small plasmids (up to 5 kb). *E. coli* Top10 was first described in 1980[278] and has the following genotype: F- mcrA Δ(mrr-hsdRMS-mcrBC) ϕ80lacZΔM15 ΔlacX74 recA1 araD139 Δ(araleu) 7697 galU galK rpsL (StrR) endA1 nupG. The Top10 are very similar to DH10β. nupG is regulatory gene that allows constitutive expression of deoxyribose synthesis genes. This allows the uptake of large plasmids. galU and galK

mutations result in the inability to metabolize galactose and are resistant to 2-deoxygalactose. *E. coli* Top10 were used to transform larger plasmids (over 5 kb).

2.7.1.2 Preparation of competent bacteria

For the bacteria to take up plasmids, they were first made competent. Competent means that the bacteria are ready to take up DNA from their surrounding environment. Some bacteria are naturally competent but others must first be made competent. Transformation serves to bring genetic change, which help the bacteria to adapt to new environmental situations. DNA is a hydrophobic molecule and cannot pass through the bacterial cell wall itself. To take up DNA, small holes in the bacteria cell wall must be created. This can be done with calcium chloride in high concentrations. By incubating the bacteria and the DNA on ice together, followed by heating the solution to 42 °C (heat shock) and replacing it on ice, the DNA can enter the bacteria. It is important that the bacteria are chilled on ice and then get a heat shock to force them to take up the DNA. Another method to bring the DNA into the cells is by electroporation. In this method, the cells are made permeable with an electric field. In this electric field the lipid formation of the membrane changes, making the membrane permeable for DNA.

In the present study, the bacteria strains were made competent using the following protocol. E. coli were grown on an LB-Agar Petri dish (1.5 % agar (A0949, Applichem, Darmstadt, Germany) over night. No antibiotic was added to the plate. A single colony was selected and grown in 100 ml LB medium (lysogeny broth (10 g peptone (8952, Carl Roth, Karlsruhe, Germany), 5 g yeast extract (2363, Carl Roth, Karlsruhe, Germany) and 10 g sodium chloride (9265, Carl Roth, Karlsruhe, Germany) at 37 °C until an OD_{600} (optical density to measure of cells/ml) of 0.35 (cell number 10^8 cells/ml). Within this range, the bacteria are in the logarithmic growth phase and thereby being the healthiest bacteria. When the cells have achieved this density, the medium was transferred to two sterile, ice-cold 50 ml falcon tubes and chilled on ice for 10 minutes. Then, they are centrifuged for 10 minutes at 4 °C and 2,700 x g and the medium was removed. Each cell pellet was then resuspended in 30 ml of ice-cold suspension buffer (80 mM $MgCl_2$ and 20 mM $CaCl_2$) followed by a centrifugation step at 2,700 x g for 10 minutes at 4 °C. Medium was discarded and the pellets were resuspended in 2 ml of ice-cold 0.1 M $CaCl_2$. To every 2 ml of 0.1 M $CaCl_2$ solution 70 µl DMSO (A994, Carl Roth, Karlsruhe, Germany) was added, gently mixed on ice for 15 minutes. After the incubation, another 70 µl DMSO are added into each tube, gently mixed and returned on ice. The prepared suspension was divided into 50 µl aliquots. The 50 µl are added into chilled reaction tubes and immediately put into liquid nitrogen and then stored at – 80 °C until further use.

2.7.2 Plasmid preparation

Plasmids are circular DNA molecules that replicate independently of the host genome inside the cells. Naturally occurring plasmids contain genetic information, like resistance to antibiotics, which help the bacteria to grow and survive. Plasmids used in molecular biology are design and contain beside the resistance to antibiotics other characteristics. One of the most important is the multiple cloning site (MCS), this site contains recognition sequences of different restriction enzymes, which allows the researcher to open the plasmid and to clone other DNA molecules, i.e. promoters, 3'UTRs into the plasmid. If the plasmids are used to express proteins or for 3'UTR studies, a viral promoter (*Cytomegalovirus* (CMV) or *Simian virus 40* (SV40)) can be part of the promoter to ensure continuously transcription. For luciferase reporter studies, like in this study, the plasmid contains a

gene encoding for luciferase (either from the firefly *Photinus pyralis* or from the sea pansy *Renilla reniformis*). The luciferases are recombinant but their origins are from the species mentioned above. For higher stability of the transcripts, the poly(A) signal is included, too. If plasmids are used in genetic engineering they are called vectors. The vectors used in this study are pGL3 basic (Figure 16) containing a human Nox4 promoter fragment of 649 bp (- 497 - + 151, which was cloned into the backbone at the multiple cloning site) and the PathDetect pAP-1-Luc Cis-Reporter Plasmid (Figure 17). The AP-1 luc reporter contains 7 AP-1 binding sites $(TGACTAA)_7$ in the enhancer element (219074, Stratagene/Agilent Technologies, Santa Clara, CA, USA).

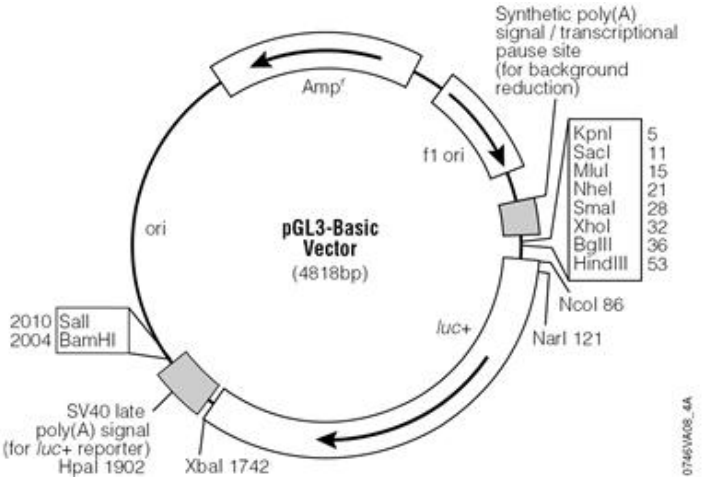

Figure 16: pGL3-basic vector.
The pGL3-Basic Vector lacks eukaryotic promoter and enhancer sequences, allowing maximum flexibility in cloning putative regulatory sequences. Expression of luciferase activity in cells transfected with this plasmid depends on insertion and proper orientation of a functional promoter upstream from luc+ (cDNA encoding the modified firefly luciferase). Potential enhancer elements can also be inserted upstream of the promoter or in the BamHI or SalI sites downstream of the luc+ gene. Amp^r is the gene necessary for ampicillin resistance. f1 ori, origin of replication derived from filamentous phage; ori, origin of replication in E. coli. Arrows within luc+ and the Amp^r gene indicate the direction of transcription; the arrow in the f1 ori indicates the direction of ssDNA strand synthesis. (From Promega homepage)

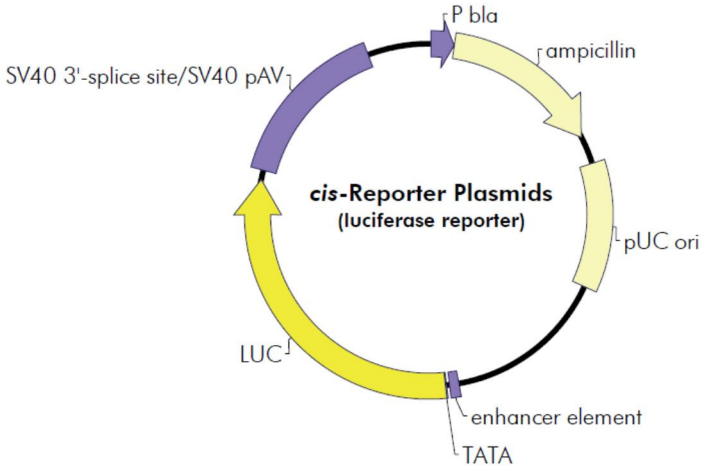

Figure 17: Cis-reporter plasmid.
The cis-reporter plasmid contains a luciferase gene (LUC) and the ampicillin resistance (ampicillin). In the enhancer element multiple binding sites for transcription factors are present. In the AP-1 luc reporter, 7 AP-1 binding sites are in the enhancer element. (From Agilent Technologies homepage)

The pGL3 basic_Nox4 promoter was used to determine the effect of scriptaid on the Nox4 promoter activity, whereas the AP-1 luc reporter was used to test the activity of AP-1 transcription factor. A stimulation of the Nox4 promoter should result in a higher light signal, whereas a repression of the Nox4 promoter should be detected with a lower light signal, because less luciferase is made. The Ap-1 luc reporter can be used to show activity of the AP-1 pathway after a stimulus.

The human Nox4 promoter fragment was created using PCR technique, therefore primer with restriction sites (BamHI in the forward primer and NcoI in the reverse primer) were designed (see Table 18). The restriction sites are marked in blue in Table 18. The nucleotides shown in red in Table 18 are necessary for the restriction enzymes to cut properly. The creation of the pGL3 basic_huNox4 -497 was performed by Katja Steinkamp-Fenske (PhD thesis)[279]. The control vector for the AP-1 luc reporter was created by cutting the pNF-κB-Luc Cis-Reporter Plasmid (219078, Stratagene/Agilent Technologies, Santa Clara, CA, USA) at SacII (R0157, New England Biolabs, Frankfurt am Main, Germany) and BsmBI (R0580, New England Biolabs, Frankfurt am Main, Germany), thereby cutting out the enhancer element with the NF-κB binding sites, leaving a promoter less vector behind.

Table 18: Human Nox4 promoter primers

Primer	Orientation	Sequence
hNox4_prom_5P2_2	forward	ccggatccgggcaaggggataaagaaac
hNox4_prom_3P2	reverse	ggccatggaccgagggtcaaagactgag

2.7.2.1 Transformation

After preparation of the plasmids (2.7.2), they were brought into competent bacteria (2.7.1.2). The frozen competent bacteria were thawed on ice, and then 10 µg of plasmid was mixed with 100 µl competent bacteria and left on ice for 30 minutes. After the incubation, a heat shock was induced by placing the sample tube on a thermomixer set at 42 °C for two minutes. After that, the samples were replaced on ice for another five minutes. Then, 500 µl of LB-medium (free of antibiotics) was added to each tube and incubated for one hour at 37 °C allowing the bacteria to express antibiotic resistance. After this incubation, 250 µl of the bacteria suspension was spread on an agar plate containing ampicillin (100 µg/ml) and left over night at 37 °C.

2.7.2.2 Isolation

From the colonies obtained in 2.7.2.1, one colony was picked and incubated in 100 ml LB-medium with ampicillin (100 µg/ml) over night. Then the plasmids were isolated using the peqGOLD XChange Plasmid kits. For details see 2.4.1.2

2.7.2.3 Electrophoresis

Agarose electrophoresis was used to determine whether the isolated plasmids (2.4.1.2 and 2.7.2.2) had the correct size or to separate DNA fragments after restriction (2.7.2.5). For this, a 1.5 % agarose gel was prepared. 1.5 g agarose was added to 100 ml TAE buffer and boiled in the microwave to melt the agarose. 20 µl of ethidium bromide (10 mg/ml, 2218, Carl Roth, Karlsruhe, Germany) was added to the 100 ml solution before it was filled in a gel casting rack for formation (agarose and agar gels form by gellation through hydrogen bonding and electrostatic interactions, not through polymerization like SDS gels). The solid gel was transferred into a horizontal electrophoresis chamber containing TAE buffer. To determine the size of the plasmids a reference ladder was run

together with the plasmids. Before the plasmids were filled into the pockets of the gel running buffer was added. The electrophoresis was performed at room temperature at 100 V until a sufficient separation occurred. Because ethidium bromide intercalates with the DNA double helix, and is fluorescent. Ethidium bromide has ultraviolet (UV) light absorbence maxima of 300 nm and 360 nm wavelength, respectively. The absorbed energy is emitted at 590 nm wavelength (orange). The fluorescence of ethidium bromide is stronger when intercalated with DNA and so the plasmids can be seen as orange bands under UV light.

2.7.2.4 Gel extraction

To isolate the separated plasmid from the electrophoresis (2.7.2.3) the NucleoSpin Extract II kit (740609, Machery-Nagel, Düren, Germany) was used. This is based on the spin column principle described in 2.4.1. The DNA was extracted according to the manufacturer's protocol. The band with the plasmid was sliced out of the agarose gel and placed in a sample tube with 200 µl buffer NT per 100 mg agarose gel. The gel slice together with buffer NT was heated at 50 °C until the gel slice was completely dissolved. The sample was then loaded onto the spin column, centrifuged for 1 minute at 11,000 x g and the flow-through was discarded. In the next step, 700 µl of wash buffer NT3 was loaded on each column followed by a centrifugation step for 1 minute at 11,000 x g. Again the flow-through was discarded. To remove any residual wash buffer and to dry the membrane, the column was centrifuged for 2 minutes at 11,000 x g. Prior to elution, the column was heated to 70 °C for 5 minutes to remove any residual ethanol. The elution buffer was prewarmed to 70 °C to increase the DNA yield and 50 µl of elution buffer NE was added onto the membrane. The spin column was placed in a new collection tube prior to elution. After addition of the elution buffer NE, the spin column was incubated for one minute at room temperature, again to increase the yield of DNA, and then centrifuged for 1 minute at 11,000 x g. The eluate contains the plasmid of interest which can then be re-ligated as described in 2.7.2.5. Concentration of the plasmid was measured using the NanoDrop™ (2.4.3).

2.7.2.5 Blunting and Ligation

As described above the pLuc control vector was created by cutting out the enhancer element of the pNF-κB-Luc Cis-Reporter Plasmid. After restriction with SacII and BsmBI a self-ligation is not possible because no compatible ends had been created. Linear plasmids run on a gel and were isolated as described in 2.7.2.4. For ligation, the plasmid first was blunted and then ligated, using the Quick Blunting™ and Quick Ligation™ Kits (E0542, New England Biolabs, Frankfurt am Main, Germany) according to the manufacturer's protocol. The blunting reaction is necessary to convert DNA with incompatible 5' or 3' overhangs to 5' phosphorylated blunt-ended DNA for efficient ligation. The DNA was blunted by the T4 DNA polymerase. The T4 polymerase has both 3'→ 5' exonuclease activity and 5'→ 3' polymerase activity. Additionally, a T4 polynucleotide kinase is included to phosphorylate the 5'-ends, because for ligation phosphorylated 5'-ends are necessary. Up to 5 µg of restriction enzyme digested and gel extracted DNA can be used in the blunting reaction. The blunting reaction was mixed as shown in Table 19 and incubated at room temperature for 15 minutes, followed by enzyme inactivation with a heat shock at 70 °C for 10 minutes.

Table 19: Blunting reaction

Component	Volume (µl)
DNA (up to 5 µg)	1-19
10x Blunting Buffer	2.5
1 mM dNTP Mix	2.5
Blunt Enzyme Mix	1
H_2O	variable
Total Volume	25

Directly after the enzyme inactivation, the ligation step followed. 50 ng of the blunted vector was used. If an insert should be cloned into the vector, the insert should be in a 3-fold molar excess. In this study no insert was ligated into the vector, so no insert was added to the ligation reaction mix. The ligation mix was prepared according to Table 20, mixed thoroughly, spinned down and incubated at room temperature for 5 minutes. Ligation products can be stored at -20 °C or used directly for transformation. Transformation was performed by using 10 ng of ligated vector (4 µl of ligation reaction) according to the transformation protocol described in 2.7.2.1.

Table 20: Ligation reaction

Component	Volume (µl)
50 ng vector	Variable
Insert (3-fold molar excess)	Variable
H_2O	Variable
Volume	10
2x Quick Ligation Reaction Buffer	10
Quick T4 DNA Ligase	1
Total Volume	21

To avoid self-ligation of the vector, Antarctic phosphatase (M0289, New England Biolabs, Frankfurt am Main, Germany) can be used. The Antarctic phosphatase removes phosphate groups from the 5'-ends, because this 5' phosphate group is need for the ligase to ligate the ends, removing of the 5' phosphate group decrease the vector background.

2.8 Plasmid transfection

Transfection is a process to bring foreign DNA into mammalian cells. The uptake of DNA by eukaryotic cells resembles the transformation process of bacteria, but the term transformation is used to describe the conversion of cells to the malignant state. Therefore, transfection is a widely used term to describe the uptake of foreign DNA into eukaryotic cells. Transfection of cells with reporter plasmids, like luciferase assay plasmids described above, is a useful tool in molecular biology to study promoter activity, signal transduction, miRNA effects, mRNA stability, etc.

50,000 cells/well were seeded the day prior to transfection in a 24-well cell culture plate. As transfection reagent, Nanofectin (Q050-005, PAA Laboratories, Cölbe, Germany) was used according to the manufacturer's protocol. The principle is to bring the plasmid into cells, where they can be

transcribed. Nanofectin consists of two components. The first component is a positively charged polymer, which has capacity to bind the negatively charged DNA. This polymer is embedded in a porous nanoparticle, the second component. The complete nanoparticle complex protects the DNA from degradation by nucleases. Due to its unique size, the nanoparticle complex can be taken up by the cells. 500 ng of plasmid DNA was diluted with the diluent solution (included in the kit) to a final volume of 50 µl in a 1.5 ml reaction tube. In a second tube, 1.6 µl of Nanofectin was mixed with diluent solution to a final volume of 50 µl. The 50 µl of Nanofection solution was added to the 50 µl DNA solution. It is important not to mix the solutions in the reverse orders! The solution was then vortexed, spinned down and incubated for 20 minutes at room temperature. In the meantime, the cell culture medium of each well was replaced with 500 µl of fresh serum containing medium. After the incubation time, the 100 µl DNA/Nanofectin complex was added drop-wise into each well. The cells were placed in an incubator at 37 °C for two hours, and then 500 µl serum containing medium was added into the wells. After another two hours the medium was sucked up and replaced with 1 ml medium. 24 hours after transfection, cells were treated with HDAC inhibitors for another 24 hours. The experiment was then stopped by adding passive lysis buffer (2.9).

2.9 Luciferase reporter assay

Luciferase reporter assays are a commonly used tool in molecular biology to study gene expression. For promoter studies, the promoter of the gene of interest is cloned in front of the firefly luciferase gene. The firefly luciferase converts luciferin into oxyluciferin, thereby producing light (see Figure 18). The luciferase reporter assay is very sensitive because there is no background luminescence in the cells. To prolong the light signal, coenzyme A (CoA) is added to the reaction. The emission of light occurs after the formation of oxyluciferin, because oxyluciferin is in an electronically excited state, and a photon of light is released when oxyluciferin returns to its ground state.

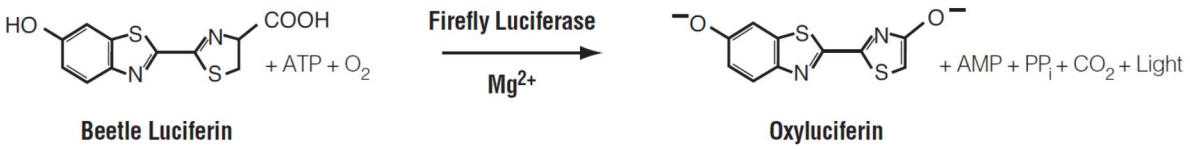

Figure 18: Firefly luciferase reaction.
The firefly luciferase catalyzes the reaction of luciferin into oxyluciferin. Luciferin together with ATP is converted to oxyluciferin, AMP, PPi and light. The measured light signal is proportional to the built luciferase in the cell. (Promega, Madison, WI, USA)

After transfection (2.8) and treatment, the cells were lysed in passive lysis buffer (E194, Promega, Mannheim, Germany). The lysis solution of each well was transferred into a new 1.5 ml collection tube, vortexed, and incubated on ice for 10 minutes. After incubation, the samples were centrifuged for 10 minutes at 12,000 x g at 4 °C. The supernatant was transferred into a new tube. Protein concentration was measured using the BCA assay (2.6.2). The luciferase enzyme present in the samples needs substrates to work. A 2x luciferase assay buffer containing 60 mM tricine (T0377, Sigma-Aldrich, Hamburg, Germany), 0.2 mM ethylenediaminetetraacetic acid (EDTA) (CN06, Carl

Roth, Karlsruhe, Germany), 30 mM $MgSO_4$ (105886, Merck, Darmstadt, Germany) and 20 mM dithiothreitol (DTT) (A2948, Applichem, Darmstadt, Germany) was prepared. Luciferase substrate solution was prepared in an extra tube containing 25 mM d-luciferin (A1029, Applichem, Darmstadt, Germany), 27 µM Coenzyme A (A0813, Applichem, Darmstadt, Germany) and 100 mM adenosine triphosphate (ATP) (A1348, Applichem, Darmstadt, Germany) in H_2O. The luciferase assay buffer and luciferase substrate solution were mixed in a light protection tube. From each sample, 10 µl were pipetted into a 96-well plate. Measurement of the light emission was done using a Centro LB960 Luminometer (Berthold, Bad Wildbad, Germany). The luminometer added 200 µl of the luciferase assay substrate solution in each well. The light intensity was measured and normalized to protein content of the samples.

2.10 small interference RNA transfection

The transfection of cells with siRNA to knock-down specific genes is a commonly used method.

All siRNAs used in this study are obtained from Sigma-Aldrich, Hamburg, Germany.

Table 21: List of siRNAs used in the present study

siRNA target	siRNA ID (Sigma-Aldrich)
Nox4	SASI_Hs02_00349918
HDAC3	SASI_Hs01_00136351
c-Jun	SASI_Hs02_00333461
c-Fos	SASI_Hs01_00184572
HDAC1	SASI_Hs01_00079968
HDAC7	SASI_Hs02_00318889
DICER1	SASI_Hs01_00160748

The day before transfection with siRNA, 50,000 cells/well were seeded in a 24-well cell culture plate. Cells should be 50 - 80 % confluent for transfection. siRNA was diluted in sterile water to a concentration of 20 µM. As transfection reagent, Saint-Red (SR-1003, Synvolux Therapeutics, Groningen, Netherlands) was used. Saint-Red was mixed with HBS to obtain the Saint-Red solution. For each transfection reaction, 5 µl of Saint-Red was mixed with 20 µl HEPES (4-(2-hydroxyethyl)-1-piperazineethanesulfonic acid)-buffered saline (HBS, provided with Saint-Red). In Table 22 all components for the Saint-Red master mix are listed. All components were mixed together in a sample tube and kept aside until further use. The serum containing culture medium was sucked up and the cells were washed with Dulbecco's phosphate-buffered saline (DPBS) (14190, Gibco/ Life Technologies, Darmstadt, Germany). After this, 250 µl of the master mix was added drop-wise into each well. The cells were then placed in an incubator at 37 °C for 3 – 4 hours. After the incubation, 750 µl of fresh serum containing medium was added to each well. The cells were then incubated for additional 48 hours before testing the knock-down efficiency of the siRNA by western blot (2.6) or qPCR (2.5.2). The final concentration of the siRNA was 50 nM.

Table 22: Components of Saint-Red master mix

Substance	Volume (µl)
HBS	24.4
siRNA (20 µM stock)	0.6
Incubation 1 to 5 minutes at room temperature	
Saint-Red solution	25
Serum free medium	200

Saint-Red transfection reagent is based on the synthetic amphiphilic delivery system. With Saint-Red, the siRNA is wrapped into a lipid mixture and thereby chemically stabilized. Furthermore, Saint-Red enhances the intracellular release of the wrapped siRNA.

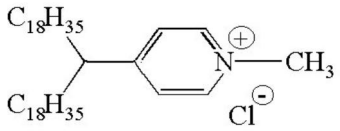

Figure 19: Chemical structure of Saint-Red.
In this figure the chemical structure of the Saint-Red reagent is shown.

2.11 Chromatin accessibility assay (EpiQ™)

Chromatin accessibility studies enables to determine the chromatin structure at a specific point in the genome. The chromatin structure is essential for the expression profile of a gene. A dense or closed chromatin structure (heterochromatin) is associated with silenced genes, whereas an open chromatin structure (euchromatin) is associated with genes that may be transcriptionally active or inactive. Heterochromatic sites can be divided into permanently silenced (constitutive heterochromatin) or facultative heterochromatin. The latter contains genes that are rarely expressed or repressed during a specific cell stage or developmental stage.

The chromatin structure is controlled by an armada of different proteins. DNA methylation and histone modifications play a role in determine the chromatin status. There is a strong cross-talk between DNA methylation and histone modification and both interact with each other. The EpiQ™ chromatin analysis kit (172-5400, Bio-Rad Laboratories, Hercules, CA, USA) enables to investigate the chromatin structure of the gene of interest by qPCR. Control cells and treated cells are treated with and without a nuclease. If the chromatin is accessible, the nuclease will cut the DNA at this site and a shift in the ΔCt-value of this region can be seen in the qPCR. If the gene is in a more silenced region, i.e. the chromatin is denser packed, the nuclease cannot get access to the DNA in this region and therefore cannot digest it. No shift in the ΔCt-value in the qPCR can be seen. Measuring the chromatin accessibility by DNA digestion is an easy way to determine chromatin structure. DNA methylation and histone modification are not always suitable parameters to determine the status of the chromatin in a distinct region.

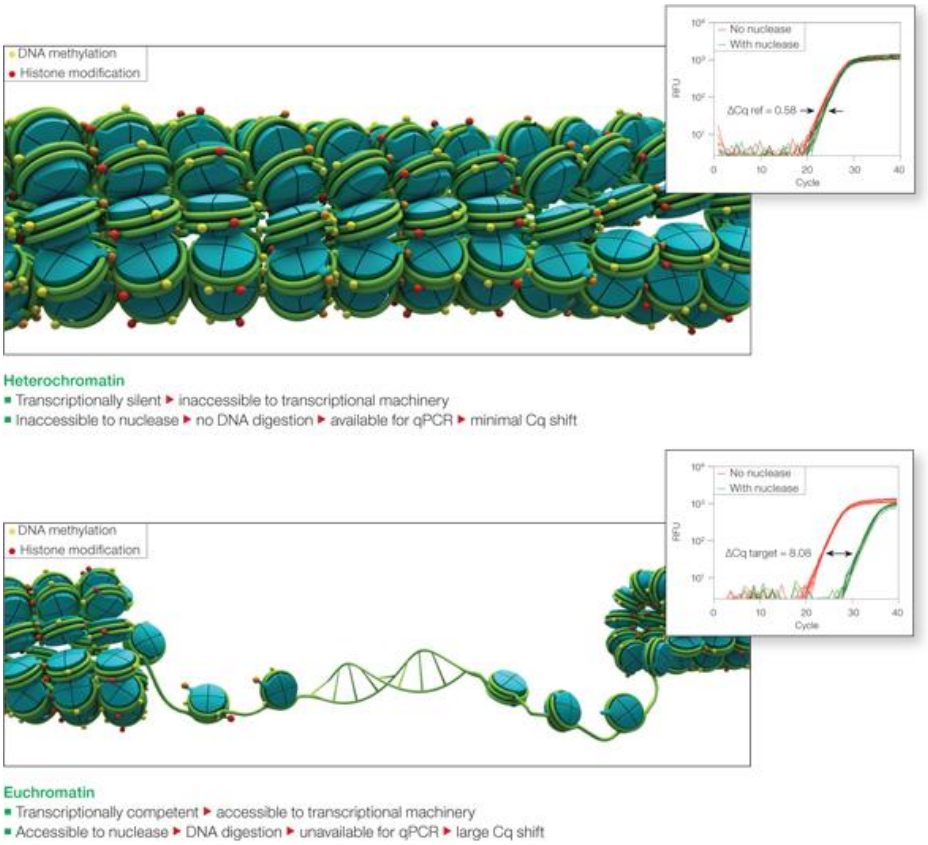

Figure 20: Schematic diagram showing the principle of the EpiQ™ chromatin accessibility assay.
This figure shows heterochromatin (upper picture) and euchromatin (lower picture). Heterochromatin is a dense and closed structure. The nuclease has no chance to digest the DNA, because the DNA is not accessible. In the qPCR run no shift in the ΔC_t (in the figure ΔCq, picture from Bio-Rad) can be detected (upper right picture). The lower picture shows the open euchromatin structure. In this case the nuclease can digest the DNA, resulting in a shift of the ΔC_t (lower right picture).

Cells were cultured in a 48-well plate and treated as needed. After that, half of the samples were treated only with chromatin buffer and another half with chromatin buffer and nuclease. Experiment was performed according to the manufacturer's protocol. The cell culture medium was aspirated and 100 µl of chromatin buffer added, with or without nuclease. The buffer should cover the whole well, and the plate was then incubated for one hour at 37 °C. After the incubation, 25 µl of stop solution was added to each well. The plate was replaced in the incubator at 37 °C for another 10 minutes. After this incubation, the cell lysate from each well was transferred to the 1.5 ml tubes containing the DNA lysis solution. Tubes were mixed by inverting and then spinned down. Next 100 % ethanol (A3678, Applichem, Darmstadt, Germany) was added to each tube, and mixed by inverting. Genomic DNA was then isolated using a spin-column (2.4.1).
The whole content of the tube was transferred to a spin-column and centrifuged at 12,000 rpm for one minute. The flow-through was discarded. After this, 650 µl of DNA low-stringency wash-solution was added onto each column, followed by a centrifugation step at 12,000 rpm for 1 minute. The flow-through was discarded and 650 µl of high-stringency wash-solution was added to each tube and the centrifugation was repeated. Then, each column was washed two more times with 650 µl of DNA low-stringency solution with centrifugation at 12,000 rpm for one minute. After the washing steps, the columns were spinned dry at 12,000 rpm for three minutes. After drying, the columns were

placed in 2 ml tubes and 52 µl of preheated DNA elution solution was added to the center of each column and incubated for two minutes followed by a centrifugation step at 12,000 rpm for two minutes. Elution was repeated as described and collected in the same tube. The concentration of the DNA was then measured using the NanoDrop™ (2.4.3) and then diluted to a final concentration of 1 ng/µl in Tris/EDTA (TE) buffer, pH 8. To determine the accessibility of the chromatin 5 ng of genomic DNA was used (5 µl). The master mix for a 20 µl reaction can be seen in Table 23. SYBR® Green JumpStart™ Taq ReadyMix™ (S4438, Sigma-Aldrich, Hamburg, Germany) was used in the qPCR reaction (Table 24).

Table 23: EpiQ qPCR master mix

Reagent	Volume (µl)
Genomic DNA sample	5
Primer mix (forward and reverse)	5 (2.5 forward and 2.5 reverse)
2x SYBR® Green JumpStart™ Taq ReadyMix™	10

Table 24: Thermal cycling conditions for EpiQ qPCR

Step	Temperature	Time	Repeats
Initial denaturation	94 °C	2 minutes	1
Denaturation Annealing, extension, and read fluorescence	94 °C 60 °C 80 °C	15 seconds 1 minute 30 seconds	40
Melt curve	70 - 96 °C	0.2 °C increment, 5 second hold	

The primers used in the qPCR for the chromatin accessibility analysis of the human Nox4 promoter are listed in Table 25. The primers for the reference gene and the control gene were provided by Bio-Rad. The reference gene is rhodopsin (RHO). In endothelial cells this gene should be epigenetically silenced. It is used as a negative control, because of the silent state of the chromatin of this gene the DNA should not be accessible to nuclease digestion and no or only a slight shift in the ΔC_t should be observed. The control gene instead is glyceraldehyde 3-phosphate dehydrogenase (GAPDH). GAPDH is ubiquitously expressed, and can therefore be used as a housekeeping gene. It serves as a positive control in this study, because due to its expression profile it should be in an epigenetically active state, i.e. the DNA should be accessible for transcription factors and for the nuclease, too. For GAPDH there should be a clear shift in the ΔC_t-value due to its open chromatin structure. An alternative reference gene is hemoglobin beta (HBB), which is provided by the kit, too.

Table 25: Primers used in qPCR for determination of chromatin accessibility

Target	Orientation	Sequence
Reference Gene (RHO)	forward	AGGTCACTTTATAAGGGTCTGGGGG
	reverse	AGTTGATGGGGAAGCCCAGCACGAT
Control gene (GAPDH)	forward	ACCTCCCATCGGGCCAATCTCAGTC
	reverse	GGCTGACTGTCGAACAGGAGGAGCA
Human Nox4	forward	CACACAAAAGGCTGTTTCCGGCTCA
	reverse	TCTGCCCACTCAGCTGCCCAGAC

2.12 DNA methylation study

Cytosine methylation, in the genome, occurs mainly at the site of the CpG dinucleotide. This epigenetic modification is an essential signal for imprinting, gene regulation, and development. Bisulfite conversion and DNA sequencing (like pyrosequencing 2.12.4) is the method of choice because it provides detailed information on the methylation pattern of individual DNA molecules at single CpG site resolution. As mentioned, the methylation state of a single CpG site can be best determined by using sodium bisulfite. The treatment of DNA with sodium bisulfite results in a conversion of unmethylated cytosines to uracil, whereas methylated cytosines remain unchanged (see in Figure 21).

	Original sequence	After bisulfite treatment
Unmethylated DNA	N-C-G-N-C-G-N-C-G-N	N-U-G-N-U-G-N-U-G-N
Methylated DNA	N-**C**-G-N-**C**-G-N-**C**-G-N	N-**C**-G-N-**C**-G-N-**C**-G-N

Figure 21: DNA sequence changes after treatment with sodium bisulfite.
The changes of the DNA sequence after the sodium bisulfite treatment can be seen in this figure. Unmethylated cytosine residues are converted into uracil, whereas methylated cytosines are protected from this conversion. Sequencing can then reveal if the cytosine was methylated or not (thymidine is incorporated for uracil and cytosine remains cytosine). (From Qiagen EpiTect Bisulfite Handbook)

The most critical step is the conversion of all unmethylated cytosines; unconverted unmethylated cytosines may lead to wrong results. To reduce false positive, the reaction is performed in high sodium bisulfite salt concentrations at high temperature and low pH. These harsh conditions, however, lead to degradation of DNA fragments and diminish the overall DNA yield after purification, but DNA purification is necessary to get rid of the sodium bisulfite salts. To counteract DNA fragmentation and low DNA yield, high amounts of starting material is needed.

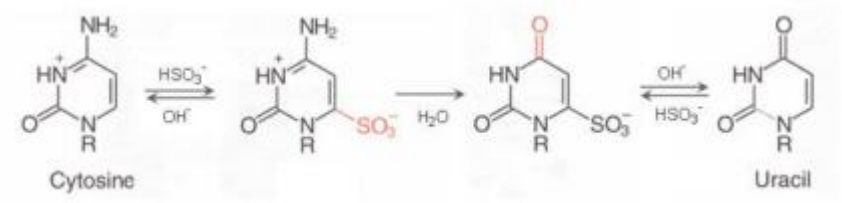

Figure 22: Principle of sodium bisulfite conversion.
In the first step, a sulphonation converts the cytosine into cytosine-sulphonate, followed by a hydrolytic deamination to uracil-sulphonate. In the last step, uracil-sulphonate is converted to uracil by an alkali-desulphonation. (From Deutsches Krebsforschungszentrum)

Figure 22 shows the chemical reaction of the conversion of cytosine to uracil. First the cytosine is converted to cytosine-sulphonate by a sulphonation. A hydrolytic deamination converts the cytosine-sulphonate to uracil-sulphonate and in the final step an alkali-desulphonation converts the

uracil-sulphonate to uracil. Sodium bisulfite preferentially deaminates cytosines in a nucleophilic attack, while the methyl group of methylated cytosines protects the aminogroup from the deamination reaction.

2.12.1 Sodium bisulfite conversion

Sodium bisulfite conversion of genomic DNA was carried out using the EpiTect Bisulfite Kit (59104, Qiagen, Hilden, Germany) according to the manufacturer's protocol. Genomic DNA was isolated as described in 2.4.1.3. Up to 2 µg of genomic DNA can be used for conversion. Table 26 shows the components and their volumes need for a single sodium bisulfite reaction. The reaction was prepared in a 200 µl PCR tube at room temperature.

Table 26: Bisulfite reaction components

Component	Volume (µl)
DNA	Variable (max. 20)
RNase-free water	Variable
Bisulfite Mix	85
DNA Protect Buffer	35
Total volume	140

The bisulfite conversion was performed using a thermal cycler with the cycling conditions shown in Table 27.

Table 27: Bisulfite conversion thermal cycler conditions

Step	Time (min)	Temperature (°C)
Denaturation	5	99
Incubation	25	60
Denaturation	5	99
Incubation	85	60
Denaturation	5	99
Incubation	175	60
Hold	∞	20

2.12.2 Cleanup of bisulfite converted DNA

The sodium bisulfite conversion was followed by a cleanup of the converted DNA to get rid of sodium bisulfite salt. All materials necessary for the cleanup were provided with the EpiTect Bisulfite Kit. Again the cleanup was performed according to the manufacturer's protocol. The PCR tubes with the converted DNA were centrifuged briefly and then transferred to a 1.5 ml microcentrifuge tube. To each sample, 560 µl of Buffer BL was added. The Buffer BL contains 10 µg/ml of carrier RNA. The carrier RNA enhances the binding of the bisulfite converted DNA to the spin column membrane. The whole mixture (140 µl conversion sample + 560 µl Buffer BL) was then transferred to a spin column and centrifuged at maximum speed for one minute. The flow-through was discarded. In the next step, 500 µl of wash Buffer BW was added to the spin column followed by a centrifugation for one minute at maximum speed. Again, the flow-through was discarded. To desulfonate the sample, 500 µl of desulfonation Buffer BD was added to the spin column and incubated for 15 minutes at room temperature. After incubation, the samples were centrifuged at maximum speed for one minute and

the flow-through discarded. The washing step with 500 µl Buffer BW was repeated twice. To remove any residual liquid, the spin column was placed in a new 2 ml collection tube and centrifuged for five minutes at maximum speed. Finally, the spin column was placed onto a new 1.5 ml collection tube and 20 µl of Buffer EB was added to the center of the membrane to elute the converted DNA by centrifugation for one minute at 15,000 x g.

2.12.3 PCR amplification of human Nox4 promoter regions

In this study, three different regions of the human Nox4 promoter were examined. All regions contain CpG sites and the methylation status of these sites after treatment with scriptaid was determined by pyrosequencing (see 2.12.4). Prior to sequencing, the regions of interest needed to be amplified by a PCR reaction. For PCR reaction the Immolase (BIO-21046, Bioline, Luckenwalde, Germany) was used with the components shown in Table 28.

Table 28: PCR master mix for amplification of sodium bisulfite converted target DNA.

Component	Volume (µl)
Buffer	5
dNTPs	0.5
$MgCl_2$	2.5
Forward primer	2.5
Reverse primer	2.5
Taq polymerase	0.4
Bisulfite converted DNA	20
H_2O	16.6

The PCR primers (Table 29) were designed in collaboration with the Institute of Human Genetics. Primer pair 1 covers the CpGs 20 to 25 in the human Nox4 promoter. Primer pair 2 covers the CpGs 31 to 35 and primer pair 3 CpGs 41 to 43, respectively. CpG site 1 is the first CpG site of the CpG island in the Nox4 promoter at the 3' site, i.e. the higher the number of the CpG site the more 5' it is. To separate the double-stranded DNA for sequencing, one primer is biotinylated (for details see 2.12.4). The cycling conditions are shown in Table 30.

Table 29: PCR amplification primers of human Nox4 CpG sites examined in this study.

Primer	Direction	Modification	Sequence
1	Forward		AGGGTTAAAGATTGAGTGGAA
	Reverse	Biotinylated	AAATCCCCACTTTTAATATAAATAACATT
2	Forward	Biotinylated	AGGGTTAAAGATTGAGTGGA
	Reverse		AACAACCACAACAACAAACTC
3	Forward		AGGGTTAAAGATTGAGTGGA
	Reverse	Biotinylated	AAACCTAACAAACCTAAATAAAAACT

Table 30: PCR cycling conditions for Nox4 CpG sites.

Step	Temperature	Time	Repeats
Activation	95 °C	10 minutes	1
Denaturation Annealing Extension	95 °C 53 °C 72 °C	15 seconds 30 seconds 30 seconds	40
Final extension	72 °C	10 minutes	
Hold	10 °C	∞	

2.12.4 Pyrosequencing

Pyrosequencing was developed in Sweden in 1996[280]. Pyrosequencing technology is sequencing by synthesis, a technique that is already used in many second-generation sequencing methods[281]. While the Sanger sequencing method is based on chain termination detection by incorporation of dideoxynucleotides[282], pyrosequencing detects pyrophosphate (PPi) that is released after incorporation of a nucleotide[280]. Like all DNA sequencing methods, a DNA template is needed. In the first step, a complementary primer anneals to the DNA template. To the whole reaction, four enzymes are added, a DNA polymerase, which is needed to incorporate the nucleotides, ATP sulfurylase, luciferase, and apyrase. For chain elongation, deoxyribonucleotide triphosphates (dNTP) are needed and finally the substrates adenosine 5' phosphosulfate (APS), and luciferin are needed. For sequencing, one of the four deoxyribonucleotide triphosphates is added at one time. The primers are hybridized to the single-stranded DNA template and all the enzymes and substrates are added. The first dNTP is added to the mix. If it is complementary to the template strand, the dNTP is incorporated by the DNA polymerase. For incorporation of each dNTP, PPi is released in an equal molarity. The ATP sulfurylase in the reaction serves to convert the PPi into adenosine triphosphate (ATP). For this reaction, APS is needed. The built ATP is needed by the firefly luciferase to convert luciferin into oxyluciferin. By the conversion of luciferin to oxyluciferin, light is generated. The light can be detected by a chip and then appears as a peak on the pyrogram. If the added dNTP is not complementary to the template, it cannot be incorporated, and no peak can be seen on the pyrogram. The nucleotide-degrading enzyme apyrase continuously degrades unincorporated nucleotides and ATP. When the degradation process is completed, the next dNTP is added (see Figure 23). For chain elongation, deoxyadenosine alfa-thio triphosphate (dATP·S) is used instead of ATP. dATP·S is used by the polymerase but not recognized by the luciferase. If ATP instead of dATP·S is used as a substrate, there will be always a signal, whether ATP is incorporated or not! That is the reason why dATP·S is used instead of ATP. Detailed information about pyrosequencing can be found at the Qiagen website or under www.pyrosequencing.com. The limitation of pyrosequencing is that it has only a read length from 300 to 500 bases, which is only half the length of the chain termination method.

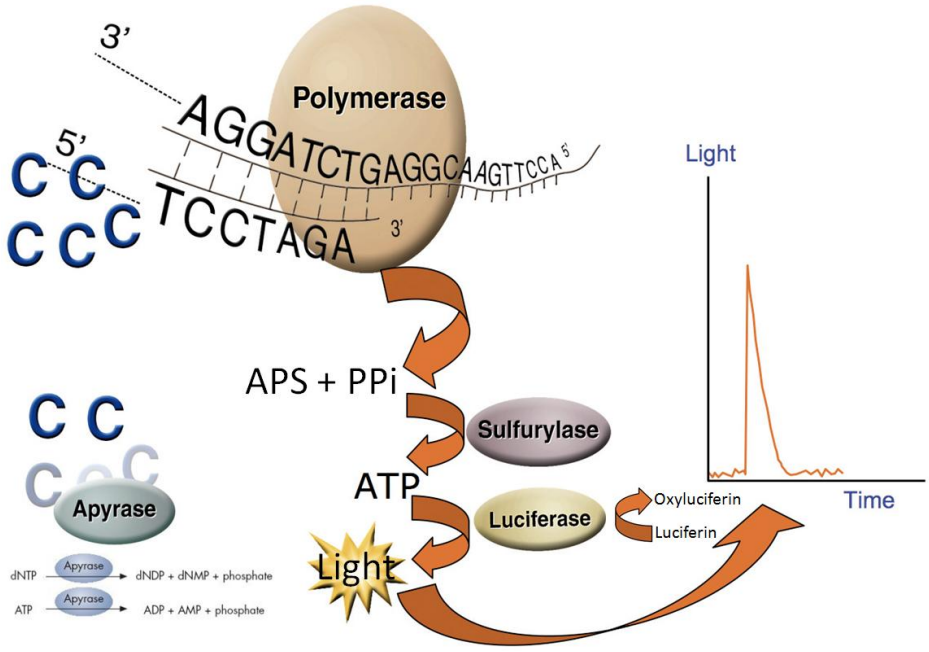

Figure 23: The principle of pyrosequencing.
The enzyme cascade of the pyrosequencing can be seen in this figure. After incorporation of a deoxynucleotide by the DNA polymerase, pyrophosphate (PPi) is released. The PPi together with the adenosine 5' phosphosulfate (APS) serves as the substrate for the sulfurylase, resulting in the formation of ATP. The ATP on the other hand is a substrate for the firefly luciferase. For the conversion of luciferin to oxyluciferin, ATP is needed. In addition to oxyluciferin, light is produced in this catalytic reaction. This light is detected by a photosensitive chip and can be seen as a peak on a pyrogram. The apyrase degrades ATP and other deoxynucleotide triphosphates, allowing starting the reaction again with another dNTP. (From Qiagen homepage, modified by Siuda)

Both the isolated (see 2.4.1.3) and bisulfite converted (see 2.12) genomic DNA are amplified by PCR reaction. One of the two primers is biotinylated. This is necessary to separate the double-stranded DNA in a later reaction with streptavidin-coated sepharose beads. As explained above, a single-stranded DNA is needed as a template in the pyrosequencing reaction. The sequencing reaction was performed according to the PyroMark Q96 Vacuum Prep Workstation manual. After PCR reaction, streptavidin-coated sepharose beads were added to each PCR reaction and incubated for 10 minutes at room temperature on a shaker with 1400 rpm. The PCR amplification was processed at a PyroMark Q96 Vacuum Prep Workstation (9001529, Qiagen, Hilden, Germany). During incubation of the PCR product with the beads, the sequencing primers were diluted (0.4 µM) with annealing buffer (979009, Qiagen, Hilden, Germany). The diluted sequencing primers were then pipetted into wells of an instrument-specific 96-well plate. The workstation has four troughs. According to the manufacturer's layout, they were filled with 70 % ethanol, denaturation solution, wash buffer and high-purity water. The pump was started and a vacuum was applied to the tool by opening the switch. The filter probes (needles at the down-site of the vacuum tool) were flushed with high-purity water in the parking trough. The PCR plate was then positioned on the working station. The vacuum tool was then placed on the PCR plate for 15 seconds to capture the beads with the PCR product. Then, the vacuum tool was placed for five seconds in the ethanol trough, then for five seconds in the trough containing the denaturation solution. After that, the vacuum tool was placed in the trough containing the wash buffer for 10 seconds. Finally, the tool was raised beyond 90° vertical for five seconds to dry the beads. The vacuum tool was passed through the troughs with vacuum on! After

drying, the tool was placed over the plate containing the sequencing primers. The vacuum was switch off and the tool was placed carefully into the wells and shaken to release the beads. In the described process, the DNA strands were separated in the denaturation solution and only the strands bound to the beads were processed. For hybridization of the sequencing primers (see Table 31) to the single-stranded DNA, the plate was placed on a heating block for two minutes at 80 °C.

Table 31: Sequencing primers for pyrosequencing

Primer	Sequence	CpGs analyzed in human Nox4 CpG island
S1	AAGATTGAGTGGAAGT	20-25
S2	AAACAAACTAATACAACCT	31-35
S3	GGTTGTTGTTGTTTAGGA	41-43

The plate was then placed in a PyroMark Q96 ID (9001525, Qiagen, Hilden, Germany) for sequencing. Sequencing enzymes, substrates and dNTPs were filled into the PyroMark Q96 Cartridge (979004, Qiagen, Hilden, Germany). All reagents were obtained from Qiagen (PyroMark Gold Q96 Reagents, 972804, Qiagen, Hilden, Germany). Single-strand binding protein (SSB) was added to the mixture to disrupt secondary structures in the template, thereby increasing sequencing read-length. Depending on the number of cycles and number of incorporated nucleotides, different amounts of enzyme mix, substrate mix and nucleotides were added. If the sequence is unknown the same amount of all nucleotides is added. For Nox4 CpG island analyses, the sequence is known and the nucleotides were added into the cartridge in the amount needed. Because Pyrosequencing is working in an automated system it is important to fill the cartridge in the right manner (see Figure 24).

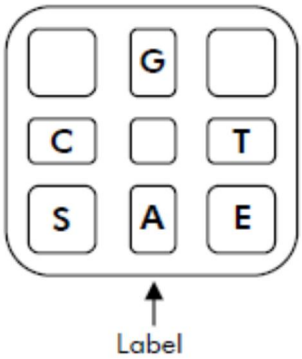

Figure 24: Illustration of the PyroMark Q96 Cartridge seen from above.
Add enzyme mixture (E), substrate mixture (S), and nucleotides (A, T, C, G) according to the volume information given by the PyroMark Q96 ID Software, during run setup. (From Qiagen homepage)

The cartridge was then loaded into the sequencer and the run was started. The results for each well can be detected in real-time. In our experimental setting, the dispensing order of the different nucleotides was provided because the sequence was known. The results can be seen on a pyrogram.

2.13 Chromatin immunoprecipitation (ChIP)

ChIP is a technique used to study protein-DNA interaction within the natural chromatin status of the cell[283,284]. The technique was developed by Gilmour and Lis in the mid-eigthies[285]. It allows studying interactions between specific proteins (like transcription factors) or modified forms of proteins (like histones histones with post-translational modifications) and a genomic DNA region. To perform ChIP, cells are fixed in formaldehyde. This treatment leads to a reversible fixation of the proteins to the DNA, afterwards the cells are lysed and the chromatin is harvested and fragmented by sonication or enzymatic digestion. The fragmented chromatin is then immunoprecipitated with an antibody specific for a particular protein or histone modification. Any DNA sequence that is cross-linked with the precipitated protein or histone modification will be precipitated, too, and enriched by the immunoselection process. After immunoprecipitation, the protein-DNA cross-link is reversed and the proteins are digested, leaving only DNA behind, which is finally purified by the spin column method (2.4.1). The enriched target DNA with a specific sequence can then be detected with methods like qPCR. Figure 25 gives an overview on the ChIP method.

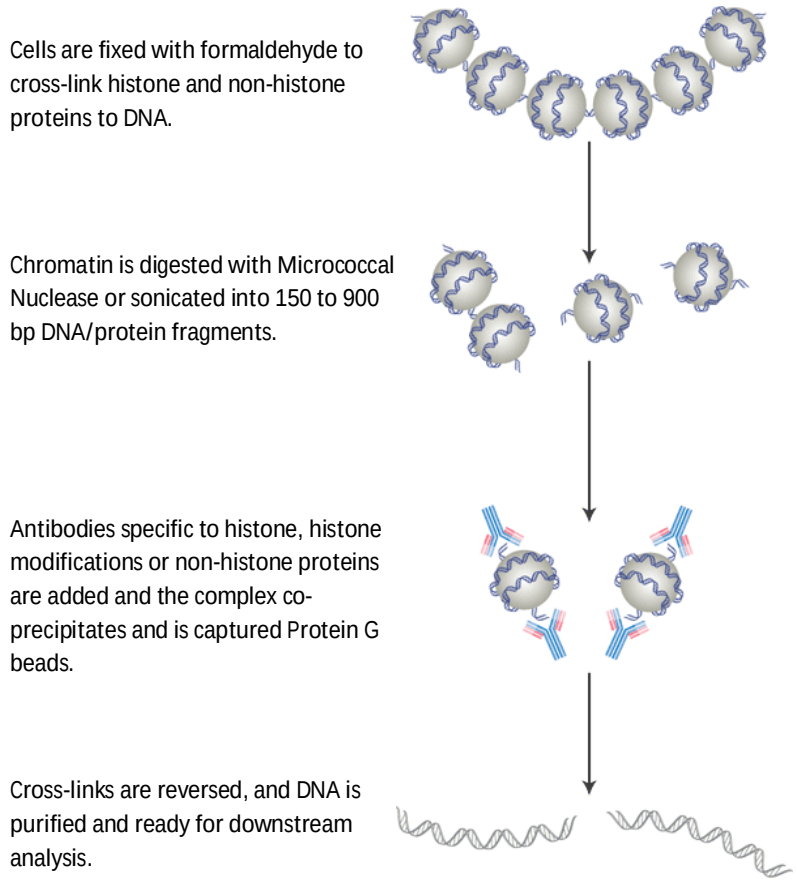

Figure 25: ChIP method overview.
In the first step of ChIP, the proteins are cross-linked to DNA with formaldehyde. After cross-linking, the chromatin is either digested with nucleases or broken by sonication, leading to fragments of 150 to 900 bp size. For immunoprecipitation, a specific antibody against the protein or histone modification of interest is used to immunoprecipitate the protein/DNA complex. The precipitated DNA/protein complex is captured by Protein G beads, leading to an enrichment of the DNA sequence cross-linked with the immunoprecipitated protein. Finally the cross-link is reversed and the DNA is purified and ready for further analysis. (From Cell Signaling Homepage)

In this study ChIP experiments were performed with the SimpleChIP Enzymatic Chromatin IP Kit (9003, Cell Signaling, Danvers, MA, USA) according to the manufacturer's protocol. If not otherwise stated, all reagents were part of the kit. The cells were cultivated in 15 cm culture dishes until confluence and then treated with 3 µM scriptaid for four hours. After the treatment, 540 µl of 37 % formaldehyde was added to 20 ml of culture medium to cross-link the proteins to the DNA, swirled and incubated for 10 minutes at room temperature. After the incubation, 2 ml of 10x glycine was added to the dish, swirled and incubated for five minutes at room temperature. The medium was then removed and the cells washed twice with 20 ml ice-cold DPBS. Afterwards, 2 ml cold DPBS + 20 µl 0.1 M phenylmethansulfonylfluorid (PMSF, A0999, Applichem, Darmstadt, Germany) ware added to the plate and the cells were scraped into ice-cold buffer and transferred into a 2 ml collection tube. The cells in the ice-cold buffer in the collection tube were then centrifuged for five minutes at 1,500 rpm at 4 °C. The supernatant was discarded and the cells resuspended in 2 ml ice-cold Buffer A + 1.25 µl 1 M 1,4-dithio-D-threitol (DTT) + 12.5 µl 200x Protease Inhibitor Complex (PIC) + 25 µl 0.1 M PMSF and incubated on ice for 10 minutes and mixed by inverting the tube every 3 minutes. After the incubation, the nuclei were pelleted by centrifugation at 3,000 rpm for 5 minutes at 4 °C. Again, the supernatant was discarded and the cells resuspended this time in 2 ml Buffer B + 1 µl 1 M DTT. Centrifugation was repeated and the pellet resuspended in 1 ml Buffer B + 0.5 µl 1 M DTT and transferred into a new 1.5 ml collection tube. Then, 1 µl Micrococcal Nuclease was added and incubated at 37 °C on a thermoshaker incubator for 20 minutes. The digestion of the DNA was stopped by adding 100 µl 0.5 M EDTA to the tube and placing it on ice. A centrifugation at 13,000 rpm for one minute at 4 °C served to pellet the nuclei. After centrifugation, the supernatant was discarded and the pellet resuspended in 1 ml 1x ChIP buffer + 5 µl 200x PIC + 10 µl 0.1 M PMSF and incubated for 10 minutes on ice. To break the nuclear membrane, the samples were sonicated after incubation with four pulses for 30 seconds each followed by placing the tube on ice for one minute between the pulses. The lysate was then centrifuged for 10 minutes at 10,000 rpm at 4 °C.

The supernatant containing the cross-linked chromatin was then placed in a new 1.5 ml tube. 50 µl out of it was used for chromatin digestion. To the 50 µl chromatin sample 100 µl nuclease-free water, 6 µl 5 M NaCl and 2 µl RNase A were added, vortexed and incubated for 30 minutes at 37 °C on a thermomixer with light shaking (400 rpm). Then, 2 µl Proteinase K was added to the RNase A-digested sample, mixed by vortexing and incubated for two hours at 65 °C on a thermomixer with slight shaking (400 rpm). After incubation, the DNA was purified using spin columns. To each sample 750 µl of DNA Binding Buffer was added. Then, 450 µl was transferred to the spin column and centrifuged at 14,000 rpm for 30 seconds and the flow-through was discarded. This was repeated with the remaining of the sample. The DNA was then washed by adding 750 µl DNA Wash Buffer on the membrane of the spin column, followed by centrifugation at 14,000 rpm for 30 seconds. Flow-through was discarded. To dry the membrane the collection tube with the spin column was centrifuged for 30 seconds at 14,000 rpm; this time the flow-through and the collection tube were discarded. The spin column was placed in a new 1.5 ml collection tube and 50 µl of DNA Elution buffer was added on the center of the membrane to elute the DNA. Elution was carried out by centrifugation for 30 seconds at 14,000 rpm. Concentration of DNA was determined by the NanoDrop™ method (see 2.4.3). DNA fragment size was determined by electrophoresis (see 2.7.2.3) on a 1 % agarose gel. For this, 10 µl of the sample was used. On the gel, there should be bands in the range from 150 to 900 bp, which correspond to one to five nucleosomes.

For chromatin immunoprecipitation, 1 µg of chromatin was used; additionally an input control sample containing 1 µg of chromatin was prepared. The necessary amount was transferred into a new tube together with 5 µl of antibody. Antibodies used in this study are listed in Table 32.

Table 32: Antibodies used in ChIP experiments.

Target	Order number	Supplier
c-Jun	ab31419	Abcam
Polymerase II	17-672	Millipore
Acetyl-Histone H3K27	17-683	Millipore
Acetyl-Histone H4	17-630	Millipore
Normal rabbit IgG	2729	Cell Signaling

1 µg of chromatin was mixed with 5 µl antibody in a 1.5 ml sample tube and incubated over night at 4 °C with rotation. On the next day, 30 µl of Chip Grade Protein G Magnetic Beads were added to the sample and incubated for two hours at 4 °C with rotation. After incubation with the magnetic beads, the samples were washed three times with low salt buffer and once with high salt buffer. The samples were placed in a magnetic rack to pellet the magnetic beads and the supernatant was carefully removed.
Then, 1 ml low salt wash solution was added (100 µl 10x ChIP Buffer + 900 µl H_2O) and incubated for five minutes at 4 °C with rotation. The washing step was repeated to a total of three low salt washing steps. After removing the third low salt washing solution, 1 ml of high salt washing solution (100 µl 10x ChIP buffer + 900 µl H_2O + 70 µl 5 M NaCl) was added to the sample, incubated for five minutes with rotation. 150 µl of ChIP elution buffer was added to the input sample and placed aside. The samples with the magnetic beads were placed in a magnetic rack to pellet the beads and the supernatant was removed. In the next step, 150 µl of ChIP elution buffer was added to each sample. To elute the chromatin, the tubes were placed in a thermomixer set to 65 °C for 30 minutes with gentle vortexing (1,200 rpm). After incubation, the tubes with the eluted chromatin were placed in the magnetic rack and the supernatant was transferred into a new tube. In the following step, 6 µl 5 M NaCl and 2 µl Proteinase K was added to each sample, including the input sample, and incubated for two hours at 65 °C on a thermomixer with light shaking (400 rpm). Purification of the DNA followed the Proteinase K digestion. For this, 750 µl of DNA Binding Buffer was added. Then, 450 µl was transferred to the spin column and centrifuged at 14,000 rpm for 30 seconds; the flow-through was discarded. This was repeated with the remaining of the sample.
The DNA was then washed by adding 750 µl DNA Wash Buffer on the membrane of the spin column, followed by centrifugation at 14,000 rpm for 30 seconds. The flow-through was discarded. To dry the membrane, the collection tube with the spin column was centrifuged for 30 seconds at 14,000 rpm. The spin column was placed in a new 1.5 ml collection tube and 50 µl of DNA Elution were added on the center of the membrane to elute the DNA. Elution was carried out by centrifugation for 30 seconds at 14,000 rpm.

A qPCR was done to determine the differences of protein-DNA binding in response to treatment with scriptaid. For qPCR, 2 µl of the eluted DNA was used. Two regions in the human Nox4 promoter containing *in silico* determined binding sites for c-Jun were investigated. These two regions are in the distal promoter region (-1287 to -1211) and in the 5'UTR (+15 to + 37). To validate the specificity

of the c-Jun antibody, a positive control[286] (c-Jun positive primer) and a negative control[287] (Igr5-intron3) were included. The sequences of the primers used to amplify the different regions are listed in Table 33. The master mix for the qPCR was prepared as shown in Table 34 using the settings for the thermocycler as shown in Table 35. The obtained data from qPCR were evaluated using the $\Delta\Delta C_t$ as described in 2.5.2.

Table 33: Primers used for ChIP experiments

Target	Orientation	Sequence
c-Jun +15 to +37	forward	GTCTGGGCAGCTGAGTGG
	reverse	AGACCGAGGGTCAAAGACT
c-Jun -1287 to -1211	forward	CACCAGTGCATCCCAGAAT
	reverse	GCTCTAAATCTTTCTGAAGTT
c-Jun positive	forward	AGGGAAAAGTGGTCCAAAGG
	reverse	GGTGCACGGTAGACATTCCT
Igr5-intron3	forward	TCTGCCTCAGGCTTACATGGA
	reverse	CACAAGAATTCTGCAGCACATTT

Table 34: ChIP qPCR master mix

Component	Volume/reaction (µL)
2x SYBR® Green Jump Start Taq ReadyMix	10
Forward primer	0.2
Reverse primer	0.2
H_2O	7.6
Total volume per reaction	18

Table 35: ChIP qPCR thermocycler settings

	Temperature	Time	Number of cycles
Initial denaturation	94 °C	2 minutes	1
Denaturation Annealing, extension, and read fluorescence	94 °C 60 °C	15 seconds 1 minute	40

2.14 Primer design

For comparison of mRNA expression, primers (Table 9) were designed as follows. First the mRNA sequence was obtained from the National Center for Biotechnology Information (NCBI) web site[288]. Then, the mRNA sequence was copied to Primer3 software[289]. The primer3 software is an easy to use online tool; the mRNA sequence can be copied directly into the user interface. Product size of the resulting PCR product was set to 80 to 150 base pairs (bp). The optimal primer length should be 20 bases, with a minimum of 18 bases and a maximum of 27 bases. The melting temperature of each primer should lie between 57 °C and 63 °C, with an optimum at 60 °C. The temperature optimum is important because the qPCR runs at 60 °C (see Table 8). After all settings are chosen, Primer3 shows different primer pairs which can then be chosen by the user. To do an *in silico* PCR with the possible primers, the primers were pasted to the University of California Santa Cruz (UCSC) Genome Browser

PCR tool[290]. In this tool, the reference genome was chosen and the forward and reverse primers were entered in the corresponding fields and the *in silico* PCR was started. If the annotation was successful, the amplified PCR product was displayed in a new window and the exact genomic position could be seen by clicking on it. If no PCR product could be detected another primer pair was tried. When the genome browser window with the genomic position of our primer pair appeared, the primer binding sites were check whether they contained one or more single nucleotide polymorphisms (SNPs). If this was the case, the SNP was examined for its frequency and then the primer pair was either ordered or discarded and a new primer pair was tested the same way as described.

For the chromatin analyses with the EpiQ (2.11), special conditions are required for the primers. They should lie in the region between -300 to +100 of the target gene. This is important because the chromatin accessibility is measured around the transcription start site. For this, the DNA sequence was not obtained from NCBI but from genome browser directly and copied to the primer3 software. The range of the amplicon was set to 200 to 350 bp. The optimal primer length should be 25 bases, with a minimum of 22 bases and a maximum of 27 bases. The melting temperature (T_m) for each primer was set to 72 °C in this application. The primers generated by the primer3 software were *in silico* tested and checked for SNPs like the mRNA primers.

For CHIP primers, some special features must be considered as well. The T_m and the primer length were the same as for the cDNA primers. The DNA sequence was obtained from the genome browser directly and analyzed for transcription factor (TF) binding sites (2.16). When potential binding sites of interest were detected, the binding sites were marked with square brackets ([...]) to indicate for the primer3 software that this region must be included in primer design.

Pyrosequencing and Nox4 CpG site enrichment primers were design using the PyroMark primer design software. The primers were designed in cooperation with the Institute of Human Genetics.

2.15 Cytotoxicity

The use of cytotoxicity assay is essential for cell culture, when working with different chemical compounds. These compounds were used to induce biological changes in the cells but they should not kill them. Determination of non-toxic, but still functional, concentrations is therefore necessary. When the cells are treated with chemical compounds at a cytotoxic dose, they may undergo necrosis, stop growing and dividing or finally may activate apoptosis pathways. Necrotic cells lose membrane integrity, shut down their metabolism, and release cellular contents into the cell culture medium. Apoptosis is a well characterized event. The cells start a genetic program, which leads to cleavage of the DNA, cell shrinking, and nuclear condensation, only to mention a few. In cell culture, cells that undergo apoptosis maybe undergo secondarily necrosis; they shut down their metabolism and lose their membrane integrity. The determination of membrane integrity is the most common way to measure cytotoxicity. Fluorescent dyes like propidium iodide cannot cross the membrane of healthy cells. However, when the membrane of the cells is damaged they can easily enter the cells and stain intracellular components. The other way is to measure substances that are normally inside the cells and do not appear in the extracellular media.

2.15.1 Membrane Integrity Assay

The lactate dehydrogenase (LDH) is one of the most commonly measured molecules. The CytoTox-ONE™ Homogeneous Membrane Integrity Assay (G7890, Promega, Mannheim, Germany) used in this study is based on the detection of LDH (Figure 26). The released LDH converts the provided lactate and nicotinamide adenine dinucleotide (NAD+) to pyruvate. Thereby, the NAD+ is reduced to nicotinamide adenine dinucleotide (NADH). NAD+ stands for the oxidized form, NADH for the reduced form. Resazurin, a dye, and diaphorase are added to the assay, too. The diaphorase catalyzes the reduction of resazurin. Resazurin functions as a hydrogen acceptor from the NADH. NADH leaves the reaction as NAD+ and resazurin is converted into the fluorescent resorufin. The fluorescence of resorufin can then be measured in a fluorometer. The resorufin production is proportional to the amount of released of LDH.

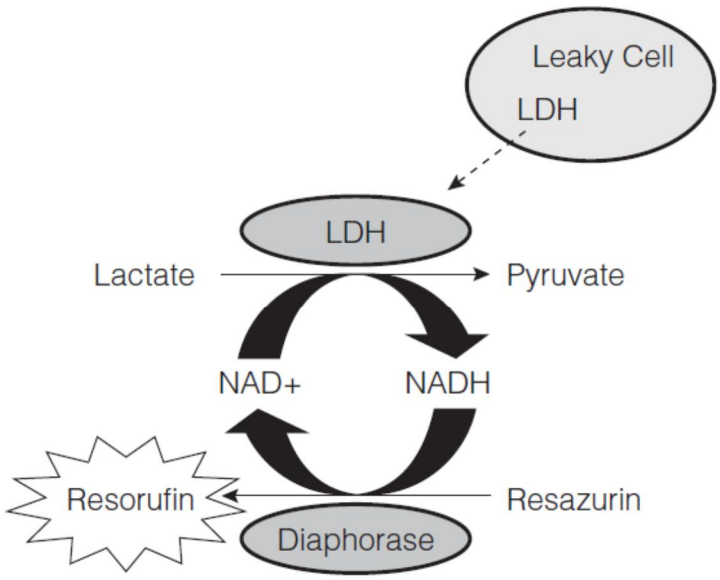

Figure 26: Principle of the CytoTox-ONE™ Homogeneous Membrane Integrity Assay.
Dead or dying cells have a leaky membrane. Through this membrane cellular components like lactate dehydrogenase (LDH) are released into the culture medium. The released LDH converts the provided lactate into pyruvate. For this reaction, nicotinamide adenine dinucleotide (NAD+) is needed as oxidizing agent. NAD+ accepts electrons from the lactate and is thereby reduced to NADH. NADH is a cosubstrate for diaphorase, which converts resazurin into the fluorescent resorufin. The generation of resorufin is proportional to the amount of released LDH. (From Promega homepage)

The experiment was done according to the manufacturer's protocol. Cells (30,000 cells/well) were seeded in 96-well format plate and treated with scriptaid for 24 hours. To the wells used as positive control with maximum LDH-release, 2 µl of lysis solution per 100 µl medium was added. Other cells received an equal volume of CytoTox-ONE™ reagent as the volume of cell culture medium and were incubated at 22 °C (room temperature) for 10 minutes. Then, 50 µl of stop solution was added to each well. To ensure total stop of the reaction, the plate was shaked for 10 seconds. Fluorescence was then measured with an excitation wavelength of 560 nm and an emission wavelength of 590 nm. Cytotoxicity was calculated with the following formula:

$$\text{Percent cytotoxicity} = 100 \text{ x } \frac{(Experimental - Cultural\ Medium\ Background)}{(Maximum\ LDH\ Release - Culture\ Medium\ Background)}$$

2.15.2 Muse™ Cell Analyzer

The apoptotic state of EA.hy926 cells after treatment with 5 µM scriptaid for 24 hours was additionally analyzed with the Muse™ Cell Analyzer (0500-3115, Millipore, Billerica, MA, USA) using the Muse Annexin V and Dead Cell Kit (MCH100105, Millipore, Billerica, MA, USA). The principle of this method is that Annexin V is a calcium-dependent phospholipid-binding protein. Annexin V has a high affinity for phosphatidylserine, which is normally found on the cytosolic side of cell membranes. Early in the apoptotic pathway, phosphatidylserine molecules are translocated to the outer surface of the cell where Annexin V can bind them. The second component of the kit is 7-Amino-actinomycin D (7-AAD), which interacts with double-stranded nucleic acid. Normally, 7-AAD cannot pass the intact cell membrane. Dead or dying cells have a permeable cell membrane so that 7-AAD can enter into the nucleus. In this assay, four populations of cells can be distinguished. Live cells have neither a 7-AAD nor an Annexin V signal. Early apoptotic cells show an Annexin V signal but no 7-AAD signal, whereas late stage apoptotic or dead cells have positive signals for both Annexin V and 7-AAD.

The cells were cultured to confluence and then treated with 5 µM scriptaid for 24 hours. The assay was performed according to manufacturer's protocol. After treatment, cells were washed with DPBS and trypsinized. Trypsinisation was stopped with serum containing culture medium. The suspended cells were transferred into a sample tube, centrifuged for five minutes at 1,400 x g at room temperature. The medium was carefully removed. The cells were then washed twice in DPBS followed by a centrifugation for five minutes at 1,000 x g. After the last washing step, DPBS was left in the tube and 100 µl of cell suspension was transferred into a new 1.5 ml sample tube, followed by adding 100 µl Muse™ Annexin V and Dead Cell Reagent to each tube. The tubes were mixed thoroughly and incubated in the dark for 20 minutes at room temperature. After incubation the samples were placed one by one in the Muse Cell Analyzer and the Annexin V and Dead Cell program was carried out.

2.16 *In silico* promoter analysis

In silico promoter analysis is an easy and low cost way to find transcription factor (TF) binding sites in a defined promoter region of a gene. TFs contain a DNA binding domain, which recognizes specific DNA sites, where they can bind. The matrices for the putative binding sites were determined experimentally, i.e. the binding sites for different TFs were proven experimentally with binding assays including mutations in the binding region. The promoter DNA sequence of interest can be obtained from genome browser. In this study, the PROMO[291,292] transcription factor binding site finder was used. In the first step, the species was selected. Then, the factors could be selected for which the software should search for, i.e. single transcription factors or groups. In this study all possible transcription factors were selected. In the last step, the DNA sequence was pasted into the software and then the analysis could be started. In this study the human Nox4 promoter from -3000 to + 300 was used to find transcription factor binding sites. The matrix dissimilarity was set to 10 %, this means, when the saved matrix for a transcription factor has more than 10 % dissimilarity, it is considered that there is no binding site for this TF in this region.

2.17 Statistics

Normality was tested via Shapiro-Wilkes test. Student's t test was used for comparison of two groups. Analysis of variance (ANOVA) followed by Fisher's protected least significant difference test was used to compare mean values between three or more groups. Data are expressed as the mean ± S.E.M (standard error of the mean). Values of $P < 0.05$ were considered significantly different. For statistical analysis GraphPad Prism (GraphPad Software, La Jolla, CA, USA) was used.

3 Results

3.1 Nox4 downregulation by HDAC inhibition

To find out if epigenetic mechanisms are involved in transcriptional regulation of Nox4, a pan-HDAC inhibitor scriptaid was used. Treatment of EA.hy926 cells with scriptaid led to a significant downregulation of Nox4 mRNA in a concentration-dependent manner, which could be shown by qPCR (Figure 27). 10 µM of scriptaid led to a marked downregulation of Nox4 mRNA. A significant downregulation of Nox4 mRNA to about 50 % compared to control cells was observed with 1 µM of scriptaid.

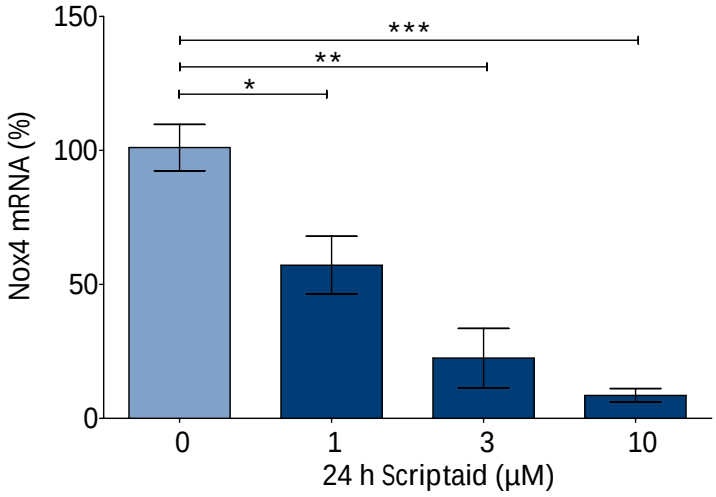

Figure 27: Downregulation of Nox4 mRNA by scriptaid in a concentration-dependent manner.
Human EA.hy926 endothelial cells were treated with the HDAC inhibitor scriptaid in different concentrations for 24 h. Relative mRNA expression was analyzed with quantitative real-time PCR. Columns represent mean ± SEM, n = 12 (* $p < 0.05$, ** $p < 0.01$, *** $p < 0.001$).

Treatment of HUVEC with 1 µM of scriptaid (Figure 28) had the same effect on Nox4 mRNA expression as seen in EA.hy926 cells. The experiments were repeated in HUVECs, which are primary cells, because EA.hy926 cells are hybridoma cells (see 2.1.1). To exclude any effects of the hybridoma character of the EA.hy926 cells also primary endothelial cells were used to confirm the specificity of the observed results.

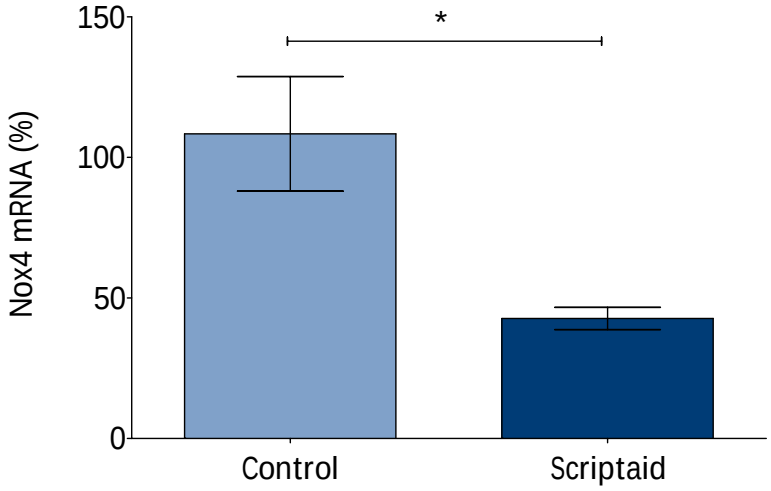

Figure 28: Downregulation of Nox4 mRNA by scriptaid in HUVEC.
Human umbilical vein endothelial cells (HUVEC) were treated with 1 µM of HDAC inhibitor scriptaid for 24 h. Relative mRNA expression was analyzed with quantitative real-time PCR. Columns represent mean ± SEM, n = 5-6 (* $p < 0.05$, ** $p < 0.01$, *** $p < 0.001$).

The downregulation of Nox4 mRNA in EA.hy926 cells was a time-dependent effect and occurred as early as 2 hours after treatment with 5 µM scriptaid (Figure 29). Downregulation of Nox4 could also be shown on protein level (Figure 30). Figure 31 shows the densitometric analysis of the Nox4 protein downregulation documented by Western blot (Figure 30).

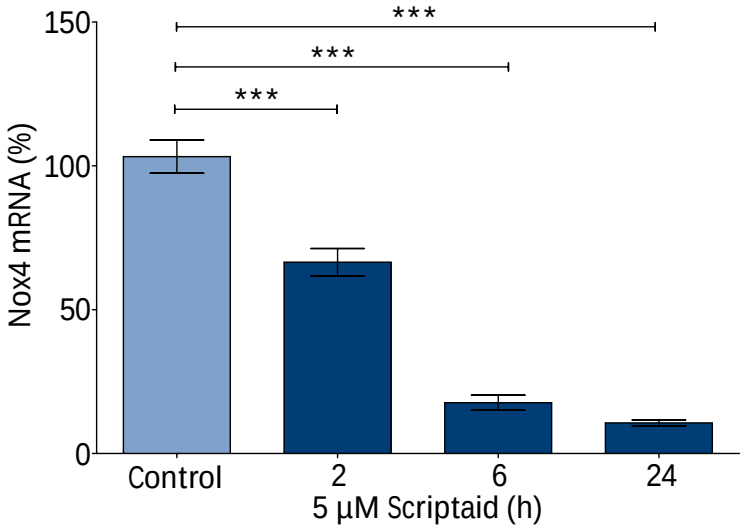

Figure 29: Time-dependent downregulation of Nox4 mRNA in EA.hy926 cells.
Human EA.hy926 endothelial cells were treated with 5 µM of the HDAC inhibitor scriptaid in different time-points. Relative mRNA expression was analyzed with quantitative real-time PCR. Columns represent mean ± SEM, n = 6 - 13 (* $p < 0.05$, ** $p < 0.01$, *** $p < 0.001$).

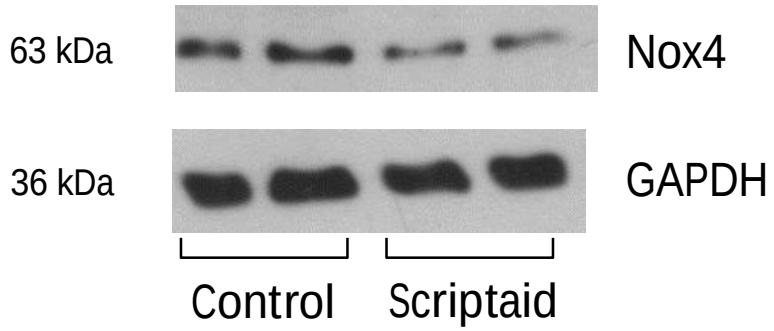

Figure 30: Downregulation of Nox4 protein after treatment with scriptaid.
Nox4 protein biosynthesis was analyzed in EA.hy926 cells treated with scriptaid (5 µM for 24 hours) by Western blot analysis using a polyclonal anti-Nox4 antibody. Glyceraldehyde-3-phosphate dehydrogenase (GAPDH) is shown as internal control.

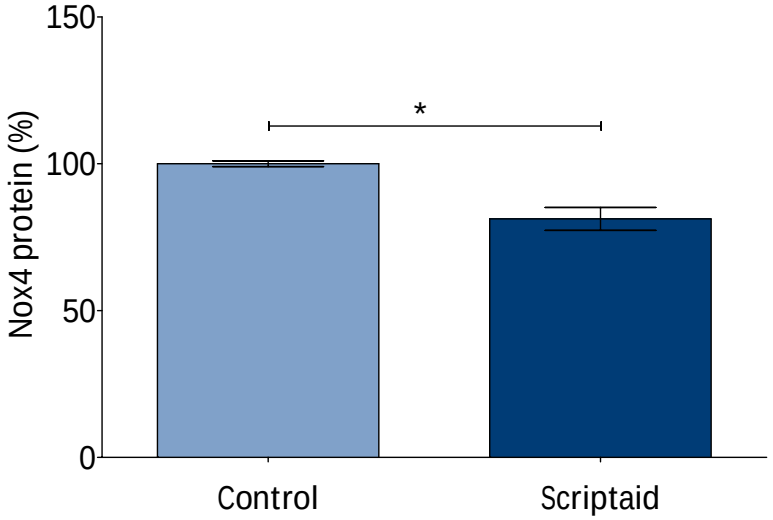

Figure 31: Densitometric analysis of Nox4 protein downregulation.
Western blot with samples from EA.hy926 cells treated with scriptaid (5 µM for 24 hours) using a polyclonal anti-Nox4 antibody was analyzed using Quantity One software from Bio-Rad. Columns represent mean ± SEM, n = 2 (* $p < 0.05$).

To verify whether the observed effects of scriptaid on Nox4 mRNA expression are a general effect induced by HDAC inhibitors and are not a scriptaid specific effect, other HDAC inhibitors were tested in this study. For this purpose, EA.hy926 cells were treated with suberoylanilide hydroxamic acid (SAHA, Vorinostat) or trichostatin A (TSA). Both HDAC inhibitors led to similar downregulation of Nox4 mRNA as that by scriptaid (Figure 32 and Figure 33).

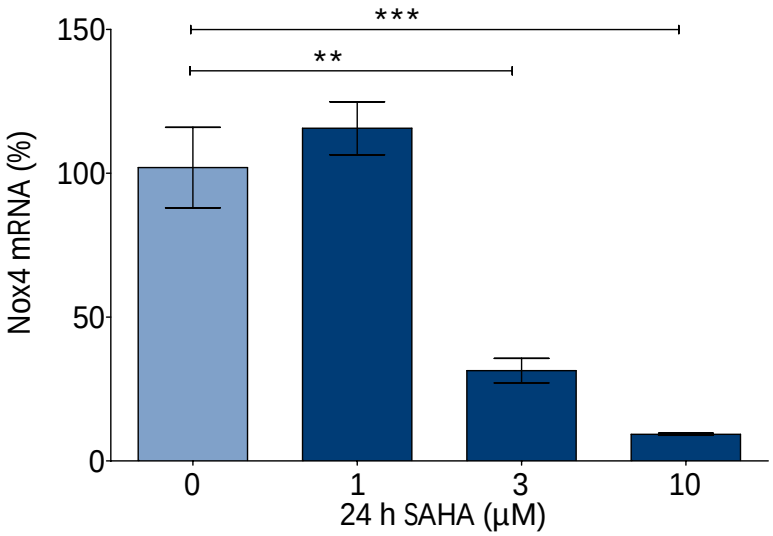

Figure 32: Downregulation of Nox4 mRNA by SAHA in a concentration-dependent manner.
Human EA.hy926 endothelial cells were treated with the HDAC inhibitor suberoylanilide hydroxamic acid (SAHA) at different concentrations for 24 h. Relative mRNA expression was analyzed with quantitative real-time PCR. Columns represent mean ± SEM, n = 6 (** $p < 0.01$, *** $p < 0.001$).

Among the three used HDAC inhibitors, TSA had the highest potency and a significant downregulation of Nox4 mRNA could be observed with as little as 0.3 µM of TSA (Figure 33).

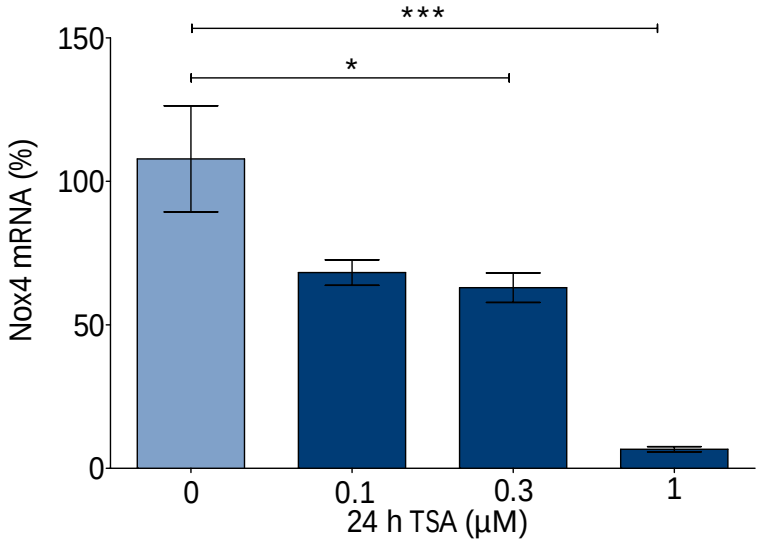

Figure 33: Downregulation of Nox4 mRNA by TSA in a concentration-dependent manner.
Human EA.hy926 endothelial cells were treated with HDAC inhibitor trichostatin A (TSA) in different concentrations for 24 h. Relative mRNA expression was analyzed with quantitative real-time PCR. Columns represent mean ± SEM, n = 6 (* $p < 0.05$, ** $p < 0.01$, *** $p < 0.001$).

3.2 Enhanced activity of an exogenous *Nox4* promoter by scriptaid

To test if promoter activity was involved in the regulation of Nox4 mRNA a promoter analyses was performed. Epigenetic changes include DNA methylation and histone modifications and both can have influence on the accessibility of the DNA. Therefore EA.hy926 cells were transiently transfected with either the promoter-less control (pGl3-basic) or a human *Nox4* promoter fragment of 672 bp cloned before the luciferase gene (pGl3-huNox4-672). The transiently transfected cells were treated with 3 µM scriptaid for 24 hours and luciferase activity was measured. Treatment with scriptaid led to an increase in *Nox4* promoter activity.

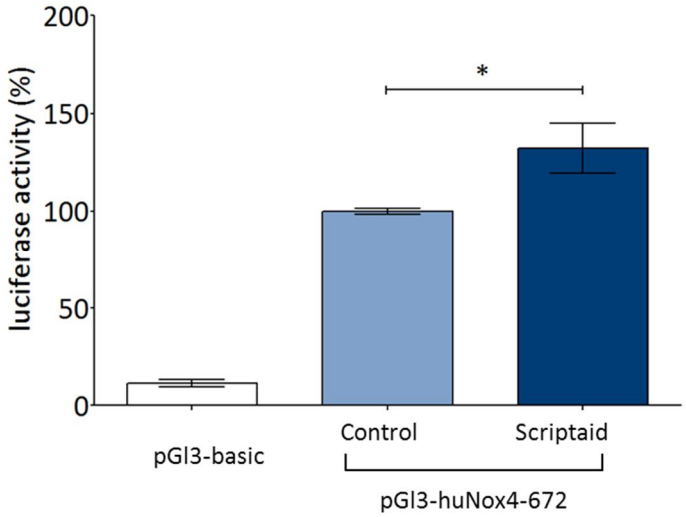

Figure 34: Activity of a human Nox4 promoter fragment after scriptaid treatment.
EA.hy926 cells were transiently transfected with either the promoter-less control (pGl3-basic) or a human *Nox4* promoter fragment of 672 bp cloned before the luciferase gene (pGl3-huNox4-672). 24 h after transfection, cells were treated with 3 µM scriptaid for 24 h and luciferase activity was measured as a determinant of *Nox4* promoter activity. Columns represent mean ± SEM, n = 8 (* $p < 0.05$).

3.3 HDAC expression in EA.hy926 cells

In EA.hy926 cells several HDAC isoforms could be detected (Figure 35). Among these isoforms, HDAC1, HDAC3 and HDAC7 were the most abundant ones. The isoforms of HDAC4, HDAC5, HDAC9 and HDAC11 could not be detected by qPCR. HDAC 2, 6, 8 and 10 had comparable mRNA levels as RNA polymerase IIA, which was used as housekeeping gene for normalization of the qPCR data. This was done to find out, which HDAC isoform might be important for the observed effect.

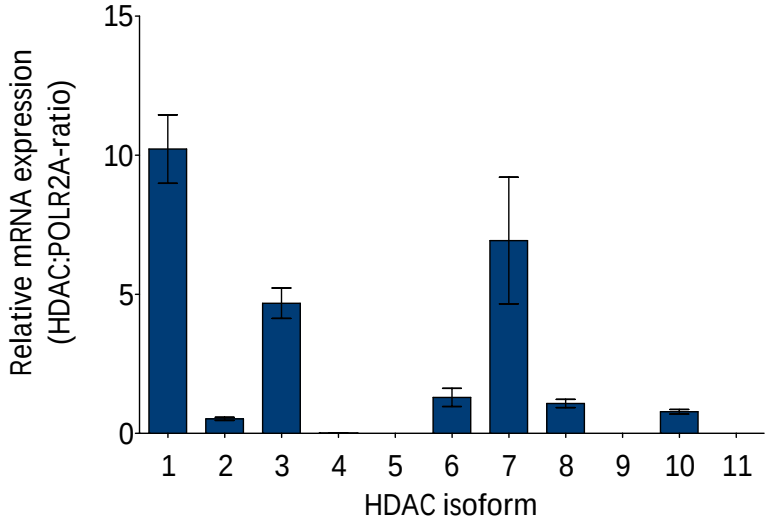

Figure 35: Relative expression of histone deacetylases in EA.hy926 cells.
Relative mRNA expression of HDAC isoforms in human EA.hy926 endothelial cells was analyzed with qPCR and expressed as HDAC:POL2RA-ratio. Columns represent mean ± SEM, n = 6.

Treatment of EA.hy926 cells with 5 µM scriptaid for 6 hours led to a change in the mRNA expression profile of the different HDAC isoforms (Figure 36). Whereas HDAC1 and HDAC3 were upregulated by scriptaid, HDAC7 was downregulated. HDAC2, HDAC6, HDAC8 and HDAC10 showed no changes in expression after scriptaid treatment.

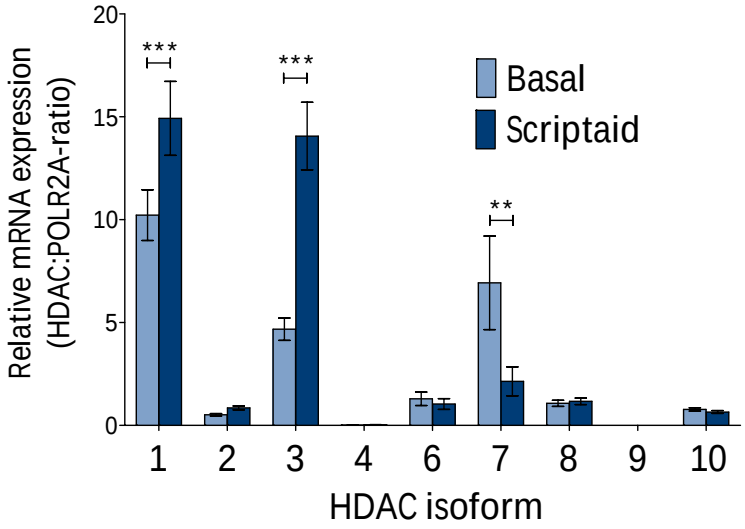

Figure 36: Changes in HDAC expression after treatment with scriptaid.
Relative mRNA expression of HDAC isoforms after treatment with HDAC inhibitor scriptaid 5 µM for 6 h in human EA.hy926 endothelial cells was analyzed with qPCR and expressed as HDAC:POL2RA-ratio. Columns represent mean ± SEM, n = 6 (** $p < 0.01$, *** $p < 0.001$).

3.4 Nox4 downregulation by HDAC3 knockdown

Based on the HDAC expression profile in EA.hy926 cells (Figure 35), HDAC1, HDAC3 and HDAC7 were selected for knockdown experiments. The siRNA-mediated knockdown of HDAC3 led to a significant downregulation of Nox4 mRNA in EA.hy926 (Figure 37) and HUVEC (Figure 38).

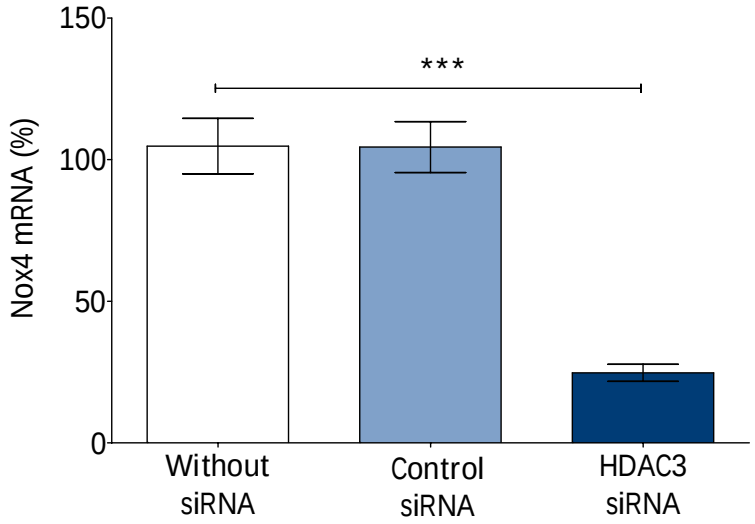

Figure 37: Effect of HDAC3 knockdown on Nox4 mRNA expression.
EA.hy926 endothelial cells were treated with siRNA (50 nM for 48 h) to knockdown HDAC3. Nox4 mRNA was analyzed with qPCR 48 h after siRNA transfection. Columns represent mean ± SEM, n = 8 - 12 (*** p < 0.001).

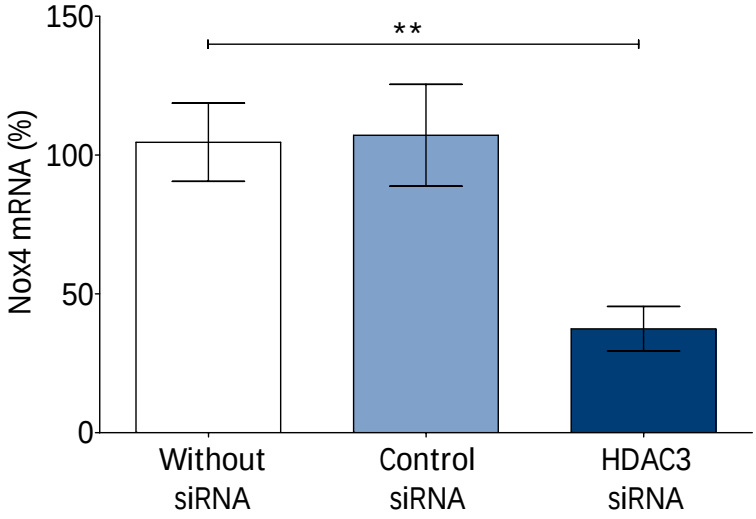

Figure 38: Effect of HDAC3 knockdown on Nox4 mRNA expression in HUVEC.
HUVEC were treated with siRNA (50 nM for 48 h) to knockdown HDAC3. Nox4 mRNA was analyzed with qPCR 48 h after siRNA transfection. Columns represent mean ± SEM, n = 6 - 7 (** p < 0.01).

The efficiency of the siRNA-mediated HDAC3 knockdown was examined by qPCR and Western blot (Figure 39). HDAC3 siRNA led to a significant downregulation of HDAC3 mRNA and protein levels.

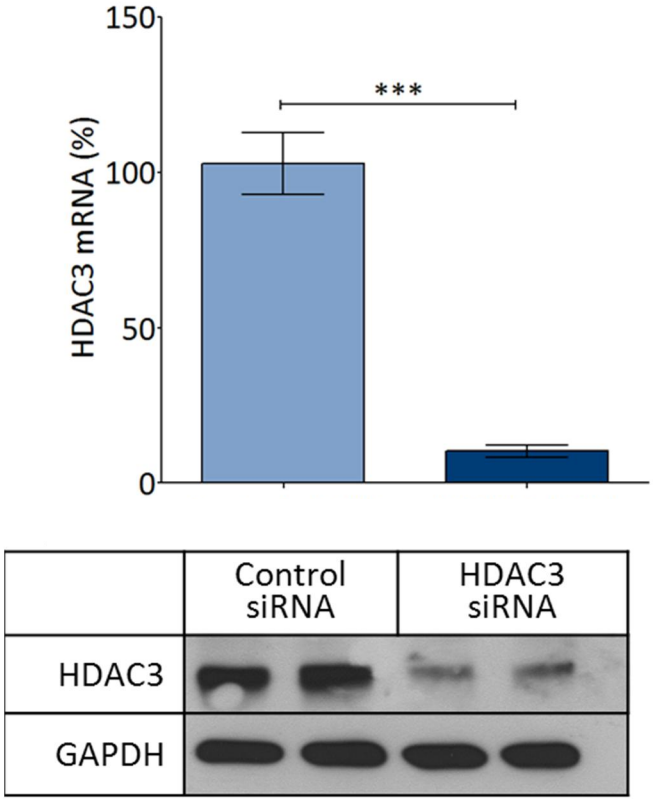

Figure 39: Effect of HDAC3 siRNA on HDAC3 mRNA and protein biosynthesis.
EA.hy926 endothelial cells were treated with siRNA (50 nM for 48 h) to knockdown HDAC3. The knockdown efficiency was verified with qPCR (upper part) and Western blot (lower part). HDAC3 mRNA was analyzed with qPCR 48 h after siRNA transfection. HDAC3 protein biosynthesis was analyzed by Western blot analysis 48 h after transfection using a polyclonal anti-HDAC3 antibody. Glyceraldehyde-3-phosphate dehydrogenase (GAPDH) was shown as internal control. Columns represent mean ± SEM, n = 7 - 8 (*** $p < 0.001$).

Knockdown of HDAC3 led to a decreased promoter activity of the human *Nox4* promoter (Figure 40). This was shown by transient transfection of EA.hy926 cells with the pGl3_huNox4 -672 plasmid containing a 672 bp long promoter construct. 24 hours prior to transfection with the plasmid, the cells were transfected with 50 nM HDAC3 siRNA and 24 h after plasmid transfection luciferase activity was measured.

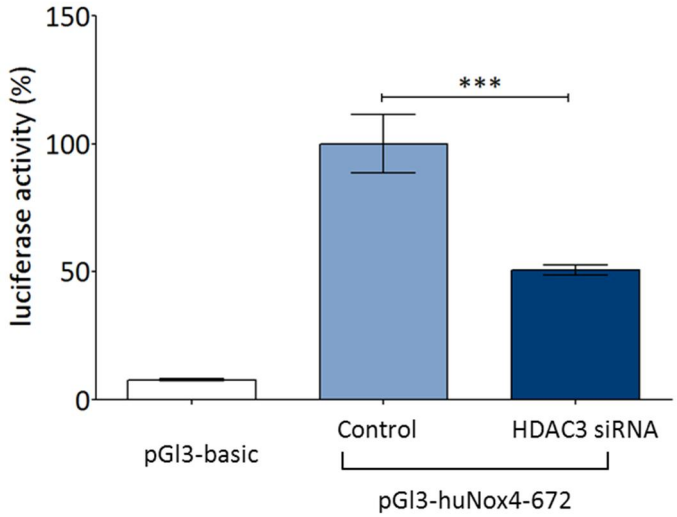

Figure 40: Human *Nox4* promoter activity after HDAC3 knockdown.
EA.hy926 cells were first treated with 50 nM HDAC3 siRNA for 24 h and then transfected with either the promoter-less control (pGl3-basic) or a human Nox4 promoter fragment of 672 bp cloned before the luciferase gene (pGl3-huNox4-672). 24 h after transfection, luciferase activity was measured as a determinant of Nox4 promoter activity. Columns represent mean ± SEM, n = 8 (*** $p < 0.001$).

siRNA-mediated knockdown of HDAC1 and HDAC7 had no significant effect on the expression of Nox4 mRNA (Figure 41). Cross-reactivity of HDAC3 siRNA against HDAC1 or HDAC7 mRNA was observed (Figure 42 and Figure 43), i.e. the siRNA against HDAC3 had not effect on HDAC1 or HDAC7 mRNA expression.

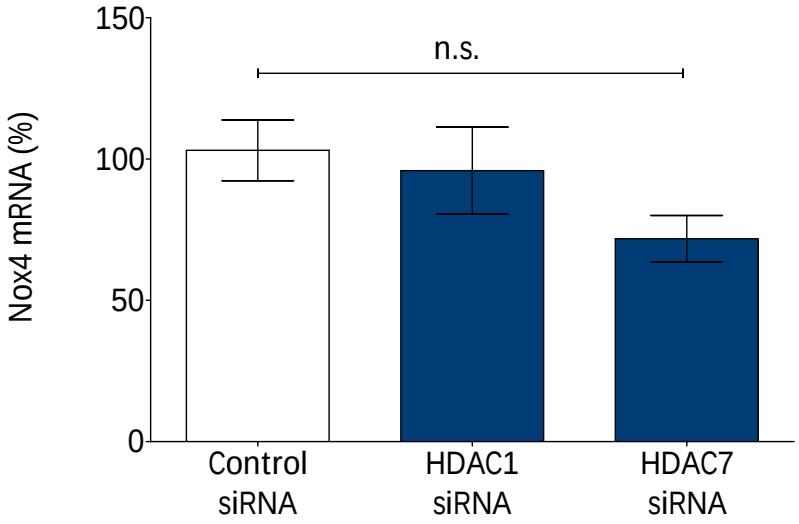

Figure 41: Effect of HDAC1 and HDAC7 knockdown on Nox4 mRNA expression.
Human EA.hy926 endothelial cells were treated with siRNA (50 nM for 48 h) to knockdown HDAC1 and HDAC7. mRNA expression of Nox4 was studied with qPCR. Columns represent mean ± SEM, n = 7 – 8 (n.s., not significant).

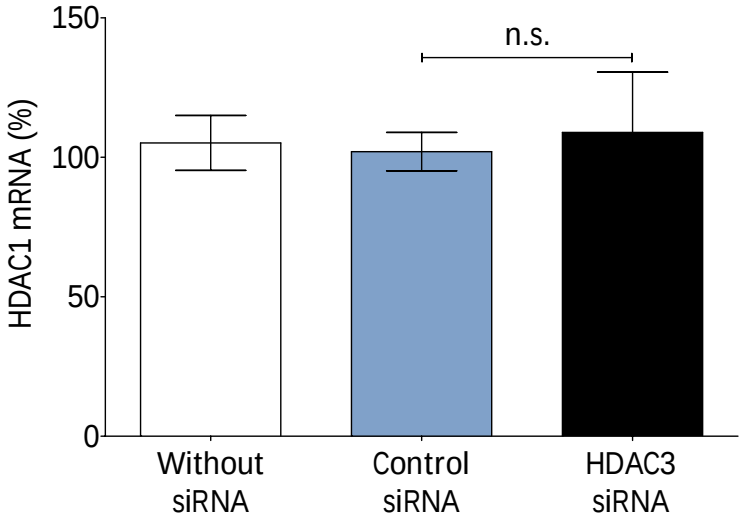

Figure 42: Effect of HDAC3 knockdown on HDAC1 expression.
Human EA.hy926 endothelial cells were treated with siRNA (50 nM for 48 h) to knockdown HDAC3. mRNA expression of HDAC1 was studied with qPCR. Columns represent mean ± SEM, n = 8 (n.s., not significant).

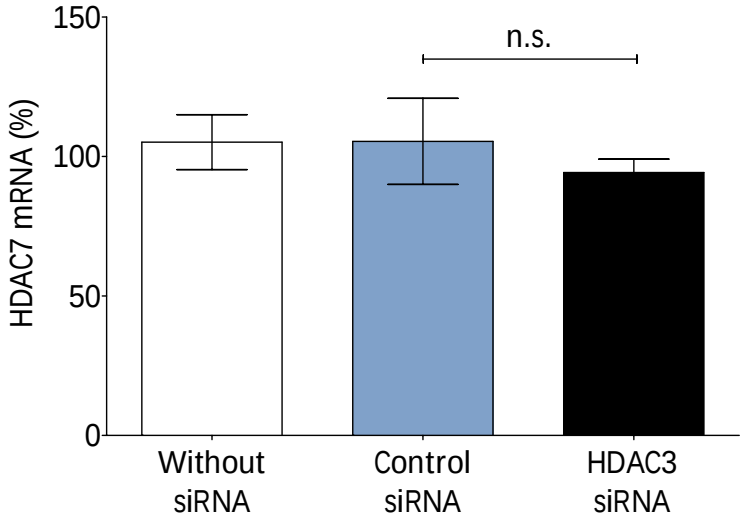

Figure 43: Effect of HDAC3 knockdown on HDAC7 expression.
Human EA.hy926 endothelial cells were treated with siRNA (50 nM for 48 h) to knockdown HDAC3. mRNA expression of HDAC7 was studied with qPCR. Columns represent mean ± SEM, n = 8 (n.s., not significant).

3.5 Histone modification, DNA methylation and chromatin accessibility

Treatment of EA.hy926 endothelial cells or HUVEC with scriptaid 3 µM for 4h led to an increase in acetylation of Histone H4 (H4ac) and of lysine 27 of Histone H3 (H3K27ac) in two examined *Nox4* promoter regions lying at -1287 to -1211 and +15 to +34, as shown in ChIP-qPCR experiments (Figure 44, Figure 45, Figure 46 and Figure 47).

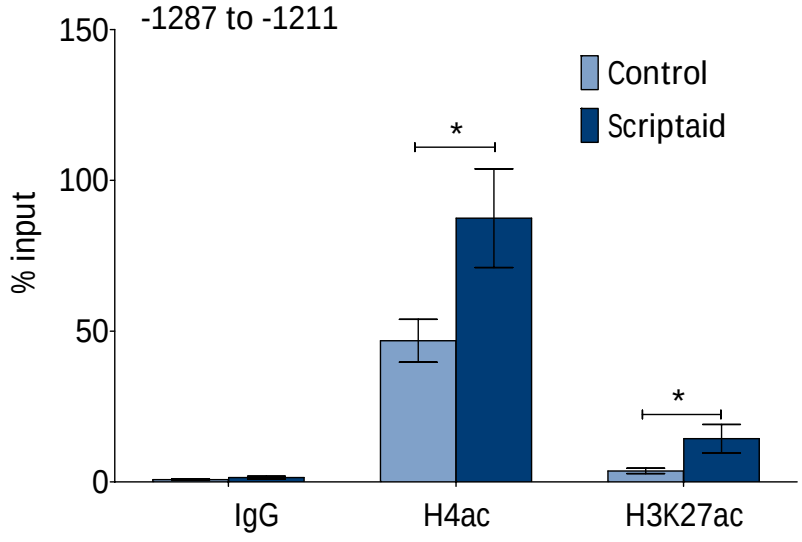

Figure 44: Increase in histone acetylation in *Nox4* promoter region -1287 to -1211 after scriptaid treatment.
Acetylation of Histone H4 (H4ac) and lysine 27 of Histone H3 (H3K27ac) in the Nox4 promoter region in EA.hy926 endothelial cells treated with scriptaid (5 µM for 4 h) was studied using Chromatin immunoprecipitation followed by qPCR. Columns represent mean ± SEM, n = 6 (* $p < 0.05$).

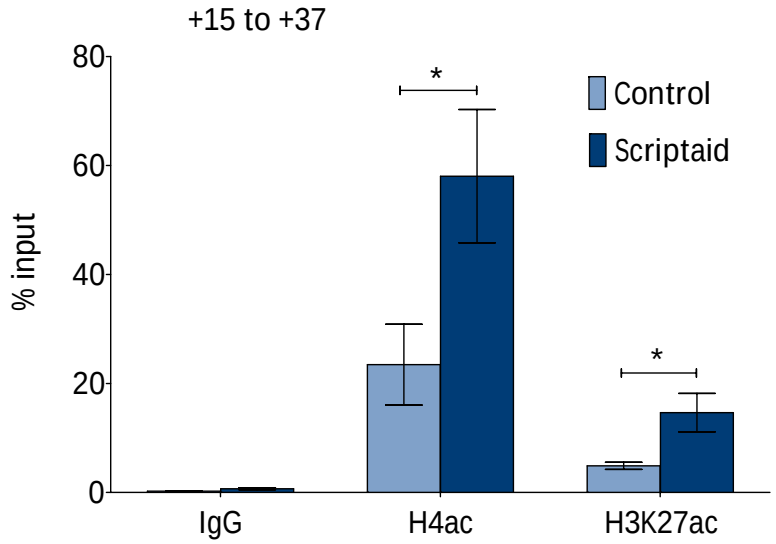

Figure 45: Increase in histone acetylation in *Nox4* promoter region +15 to +37 after scriptaid treatment.
Acetylation of Histone H4 (H4ac) and lysine 27 of Histone H3 (H3K27ac) in the Nox4 promoter region +15 to +34 in EA.hy926 endothelial cells treated with scriptaid (5 µM for 4 h) was studied using Chromatin immunoprecipitation followed by qPCR. Columns represent mean ± SEM, n = 6 (* $p < 0.05$).

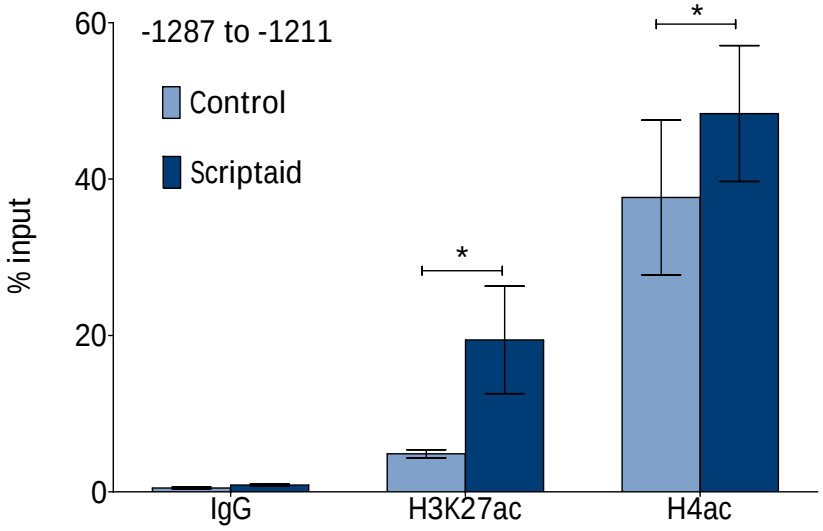

Figure 46: Increase in histone acetylation in *Nox4* promoter region -1287 to –1211 after scriptaid treatment in HUVEC.
Acetylation of lysine 27 of Histone H3 (H3K27ac) and Histone H4 (H4ac) in the Nox4 promoter region -1287 to -1211 in HUVEC treated with scriptaid (5 µM for 4 h) was studied using Chromatin immunoprecipitation followed by qPCR. Columns represent mean ± SEM, n = 6 (* $p < 0.05$).

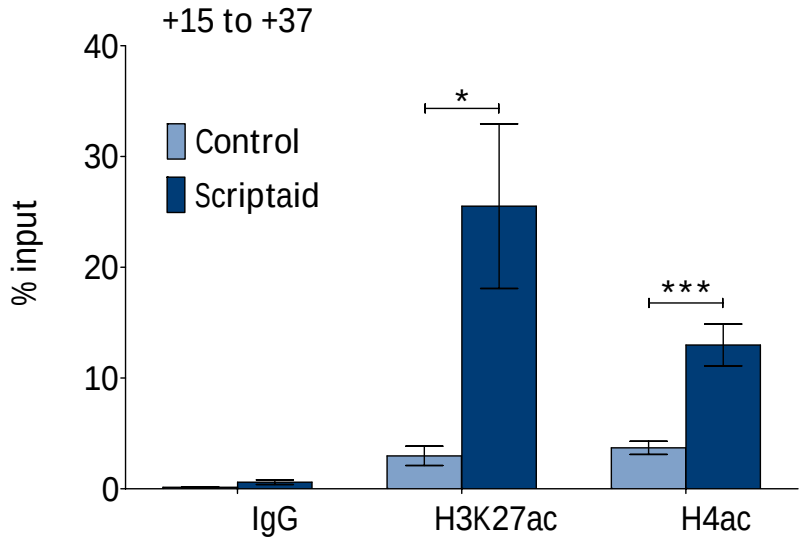

Figure 47: Increase in histone acetylation in *Nox4* promoter region +15 to +37 after scriptaid treatment in HUVEC.
Acetylation of lysine 27 of Histone H3 (H3K27ac) and Histone H4 (H4ac) in the Nox4 promoter region +15 to +34 in HUVEC treated with scriptaid (5 µM for 4 h) was studied using Chromatin immunoprecipitation followed by qPCR. Columns represent mean ± SEM, n = 6 (* $p < 0.05$, *** $p < 0.001$).

The human *Nox4* promoter contains a 302 bp long CpG island, which consists of 39 CpGs (1-39, Figure 48).

```
5′-GGCTGCGGGGGACGCCTCCAAGTTCCCACCCGGGACATC
       43      42                  41
  CTGAACAGCAGCAGCCACAACAACAGGCTCGCCCCTAGAC
                                  40
  AAAGGGGCCGGCGCGGCGGAGCAGACTGGTGCAGCCTGGG
          39  38 37  36
  CCGCGCGCTCAGAGCGCTGGGCGTCTGGGCAGCTGAGTGG
   35 34 33        32      31
  GCAGAGCTGACCCGGTGCGGGTGGGAGTCAGGGCGCCCGG
                30    29                28  27
  AAAACCCGGCTCTGGGTAGCAGACCCCGCCCGGGCTGGCT
         26                        25  24
  CGGCGCCGGGCCTTCGGGCTTCCACTCAGTCTTTGACCCT
  23  22  21       20
  CGGTCCTCGCTCAGCGGCCCGGCAGGCCGCACAACTGTAA
  19      18      17    16        15
  CCGCTGCCCCGGCGCCGCCCGCTCCTTCTCGGTCCGGCG
   14       13   12  11   10          9   8  7
  GGCACAGAGCGCAGCGCGGCGGGGCCGGCG-3′
            6    5 4   3     2  1
```

Figure 48: Human Nox4 CpG island sequence.
The human Nox4 promoter contains a 302 bp long CpG island. The CpG island consists of 39 CpGs (underlined and numbered). The CpGs 40 to 43 lie outside but close to the CpG island.

From the CpGs shown in Figure 48, the CpGs 20-25, 31-35 and 41-43 were examined by pyrosequencing to determine the methylation state of the different CpGs after treatment with 5 µM scriptaid for 24 hours. The CpGs 20-25 and 31-35 lie inside the CpG island and 41-43 lie proximal of the CpG island in 5' direction. The treatment with scriptaid didn't change the methylation pattern of the examined CpGs (Figure 49).

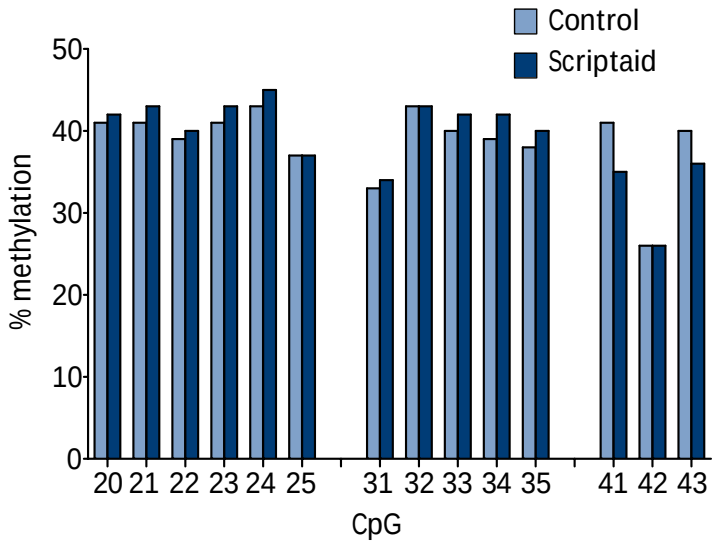

Figure 49: Methylation stat of different CpGs in the Nox4 promoter after scriptaid treatment.
Human EA.hy926 endothelial cells were treated with scriptaid (5 µM for 4 h) and DNA methylation of CpGs in the Nox4 promoter was determined by pyrosequencing.

Results from the EpiQ experiments showed that scriptaid (3 µM for 4 h) increased chromatin accessibility in the *Nox4* promoter region (-380 to +12). The ΔCt value of qPCR was higher using DNA from scriptaid-treated cells as template than from control cells, indicating that the chromatin in scriptaid-treated cells was more accessible to nuclease digestion (Table 36). In other words, scriptaid treatment was associated with more open chromatin structure in the *Nox4* promoter region.

Table 36: Chromatin accessibility of *Nox4* promoter after scriptaid treatment.
Chromatin accessibility in scriptaid (3 µM for 6 h)-treated EA.hy926 endothelial cells was analyzed with the EpiQ Chromatin Analysis Kit.

	Control	Scriptaid
C_T (no nuclease)	29.33	29.30
C_T (with nuclease)	30.52	31.73
ΔC_T	- 1.18	- 2.43

3.6 Regulation of Nox4 expression by AP-1

In silico analysis of the *Nox4* promoter revealed AP-1 binding sites. To test if AP-1 was involved in Nox4 mRNA expression regulation siRNA against c-Jun, an AP-1 subunit, was used. Treatment of EA.hy926 cells with c-Jun siRNA (50 nM for 48 h) resulted in marked reduction in c-Jun mRNA and protein (Figure 50).

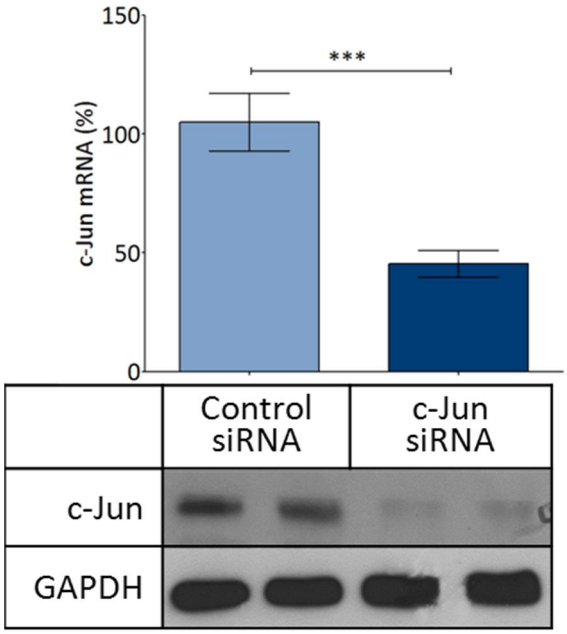

Figure 50: c-Jun mRNA and protein levels after siRNA treatment.
Human EA.hy926 cells endothelial cells were treated with siRNA (50 nM for 48 h) to knockdown c-Jun. The knockdown efficiency of the c-Jun siRNA was verified with qPCR and Western blot, respectively. Columns represent mean ± SEM, n = 8 (*** $p < 0.001$).

The knockdown of c-Jun or c-Fos, which together build the heterodimer AP-1, resulted in a significant decrease of Nox4 mRNA expression in EA.hy926 cells (Figure 51 and Figure 52). These data indicate that AP-1 may play an important role in the regulation of Nox4 expression.

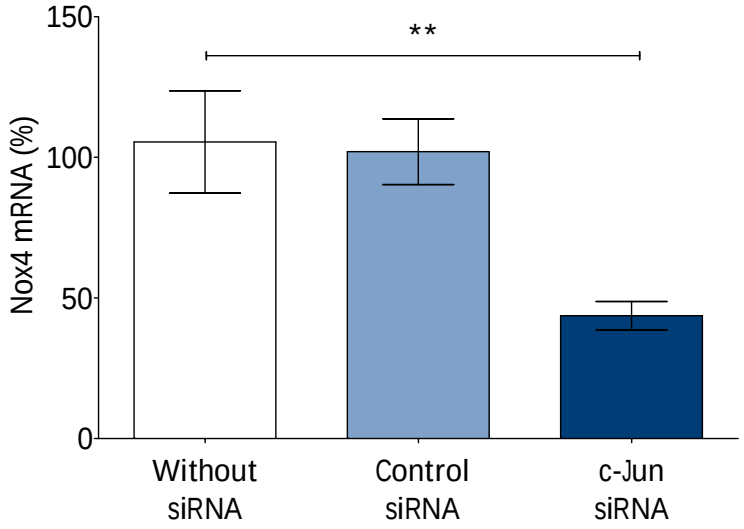

Figure 51: Nox4 mRNA expression after c-Jun siRNA treatment.
Human EA.hy926 cells endothelial cells were treated with siRNA (50 nM for 48 h) to knockdown c-Jun. Nox4 mRNA expression in the siRNA-treated cells was studied with qPCR. Columns represent mean ± SEM, n = 8 (** $p < 0.01$).

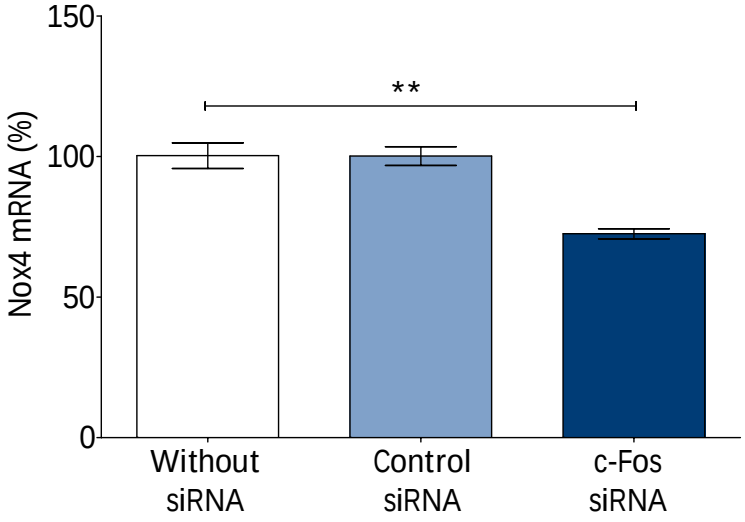

Figure 52: Nox4 mRNA expression after c-Fos siRNA treatment.
Human EA.hy926 cells endothelial cells were treated with siRNA (50 nM for 48 h) to knockdown c-Fos. Nox4 mRNA expression in the siRNA-treated cells was studied with qPCR. Columns represent mean ± SEM, n = 8 (** $p < 0.01$).

Treatment of EA.hy926 cells with scriptaid (3 µM for 24 h) led to an upregulation of c-Jun both at mRNA (Figure 53) and protein levels (Figure 54). In addition, c-Fos behaved in the same way on mRNA level as c-Jun did after scriptaid treatment (Figure 55).

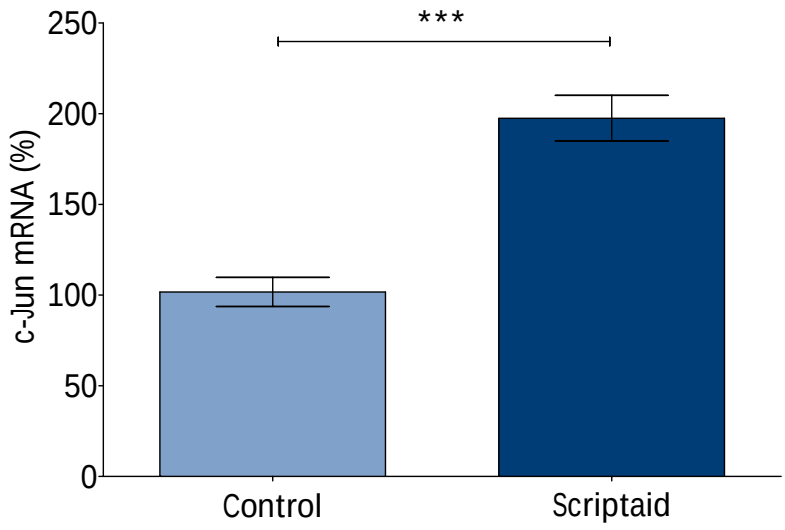

Figure 53: c-Jun mRNA expression after scriptaid treatment.
EA.hy926 endothelial cells were treated with scriptaid (5 µM for 24 h) and c-Jun mRNA expression was analyzed with qPCR. Columns represent mean ± SEM, n = 6 (*** $p < 0.001$).

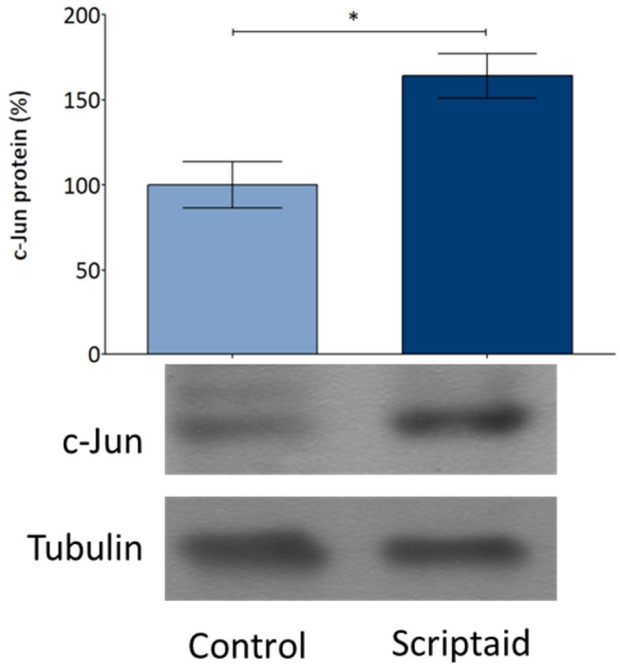

Figure 54: c-Jun protein level after scriptaid treatment.
EA.hy926 endothelial cells were treated with scriptaid (5 µM for 24 h) and c-Jun protein biosynthesis was studied with Western blot using polyclonal anti-c-Jun antibody. The Western blots were densitometrically analyzed using Quantity One software from Bio-Rad. Columns represent mean ± SEM, n = 3 (* $p < 0.05$).

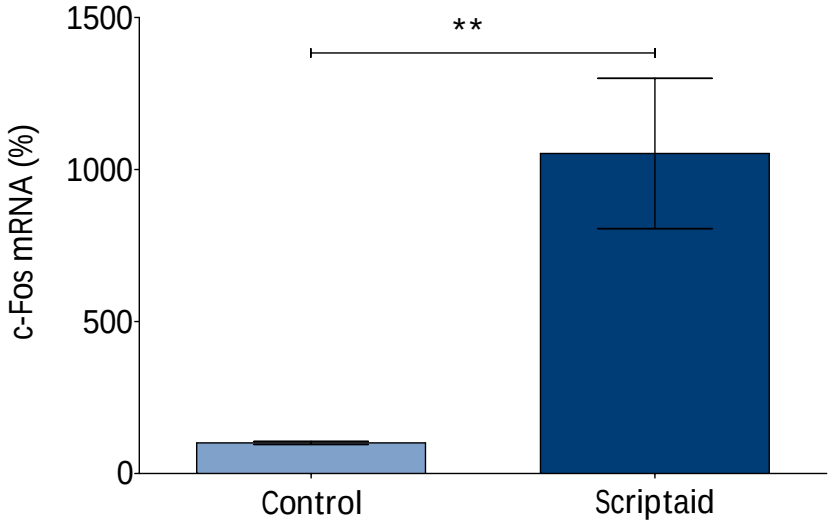

Figure 55: c-Fos mRNA expression after scriptaid treatment.
EA.hy926 endothelial cells were treated with scriptaid (5 µM for 24 h) and c-Fos mRNA expression was analyzed with qPCR. Columns represent mean ± SEM, n = 6 (** $p < 0.01$).

In EA.hy926 cells transiently transfected with the AP-1 reporter gene plasmid, the treatment of scriptaid increased the promoter activity showing an increase in AP-1 activity (Figure 56). These results were consistent with the upregulation of c-Jun and c-Fos after scriptaid treatment.

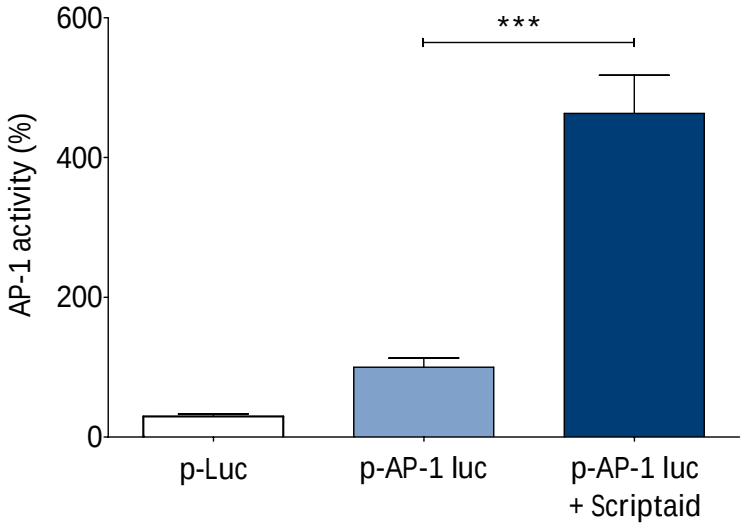

Figure 56: AP-1 activity after scriptaid treatment.
Human EA.hy926 endothelial cells were transiently transfected with the AP-1 reporter construct p-AP-1 luc. 24 h after transfection, cells were treated with scriptaid and luciferase activity was measured as a determinant of AP-1 activity. Columns represent mean ± SEM, n = 8 (*** p < 0.001).

3.7 Effects of HDAC3 knockdown on AP-1

Knockdown of HDAC3 led to an increase in the expression of c-Jun and c-Fos (Figure 57 and Figure 58). The mRNA expression was determined by qPCR.

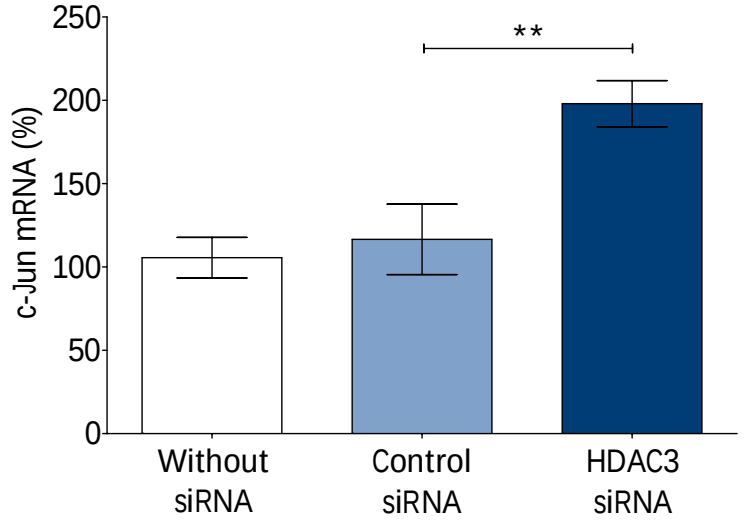

Figure 57: Effect of HDAC3 knockdown on c-Jun mRNA expression.
Human EA.hy926 cells endothelial cells were treated with siRNA (50 nM for 48 h) to knockdown HDAC3. c-Jun mRNA expression was studied with qPCR. Columns represent mean ± SEM, n = 8 (** p < 0.01).

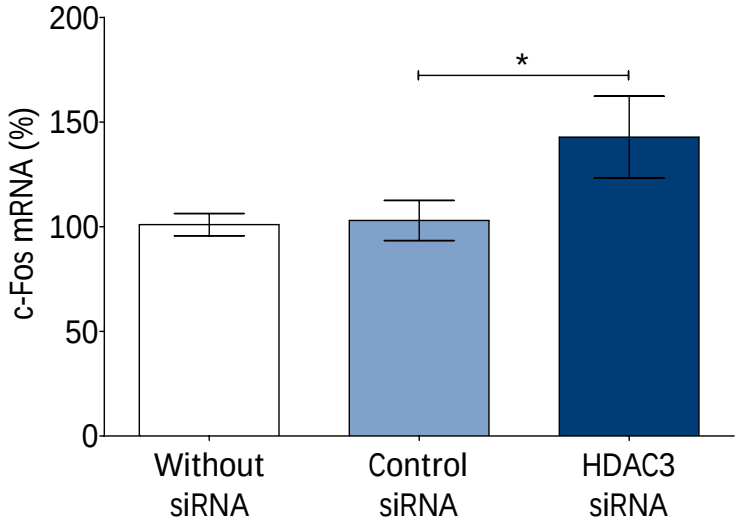

Figure 58: Effect of HDAC3 knockdown on c-Fos mRNA expression.
Human EA.hy926 cells endothelial cells were treated with siRNA (50 nM for 48 h) to knockdown HDAC3. c-Fos mRNA expression was studied with qPCR. Columns represent mean ± SEM, n = 8 (* $p < 0.05$).

After knockdown of HDAC3, both c-Jun and c-Fos are upregulated on mRNA level. Surprisingly, luciferase reporter assays with the AP-1 reporter gene showed a different result. The knockdown of HDAC3 resulted in a decreased luciferase activity (Figure 59), indicating that the knockdown of HDAC3 led to a decreased AP-1 activity.

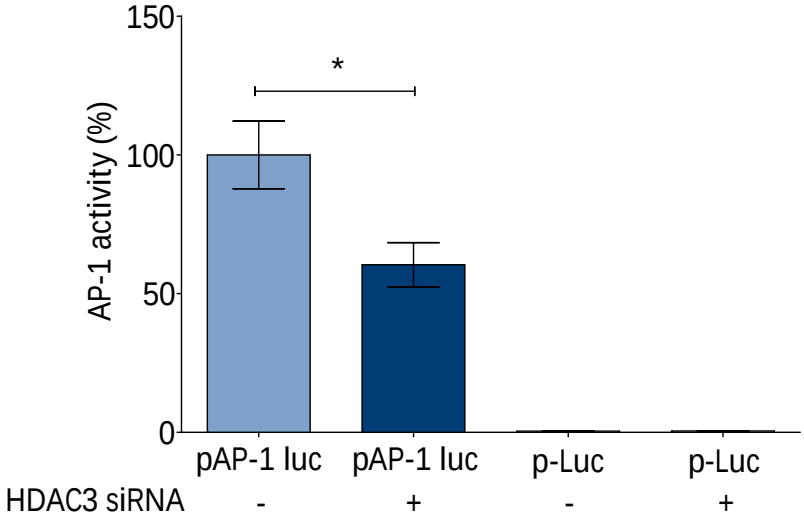

Figure 59: AP-1 activity after HDAC3 knockdown.
Human EA.hy926 cells endothelial cells were treated with 50 nM siRNA to knockdown HDAC3. 24 h after siRNA transfection, the cells were transfected with the AP-1 reporter construct pAP-1 luc or p-Luc (the control plasmid containing no AP-1 binding site). After another 24 h, luciferase activity was measured as a determinant of AP-1 activity. Columns represent mean ± SEM, n = 8 (* $p < 0.05$).

3.8 Reduced binding of c-Jun and polymerase II to the endogenous *Nox4* promoter

Treatment of EA.hy926 cells or HUVEC with scriptaid (5 µM for 24 h) reduced the binding of c-Jun to the endogenous *Nox4* promoter. As shown in ChIP-qPCR experiments, the binding of c-Jun to the AP-1 binding sites (-1287 to -1211 and +15 to +37) in the human *Nox4* promoter was significantly reduced by scriptaid treatment in EA.hy926 cells (Figure 60 and Figure 61) and in HUVEC (Figure 62 and Figure 63). In parallel, the binding of RNA polymerase IIA (POLR2A) to the region of transcription start site was reduced by scriptaid as well in both cell lines (Figure 63 and Figure 64).

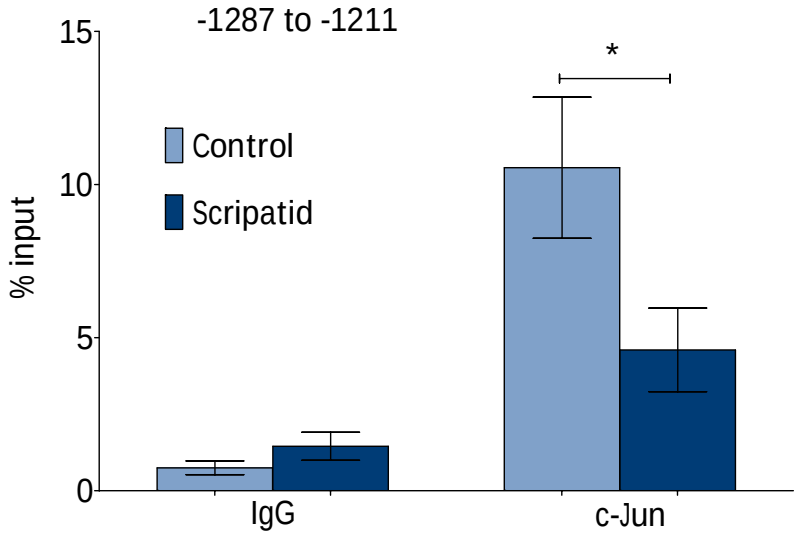

Figure 60: Binding of c-Jun to the *Nox4* promoter region -1287 to -1211 after scriptaid treatment.
Human EA.hy926 endothelial cells were treated with scriptaid (5 µM for 4 h). Binding of c-Jun to the Nox4 promoter region -1287 to -1211 was studied using ChIP followed by qPCR. Columns represent mean ± SEM, n = 6 (* p < 0.01).

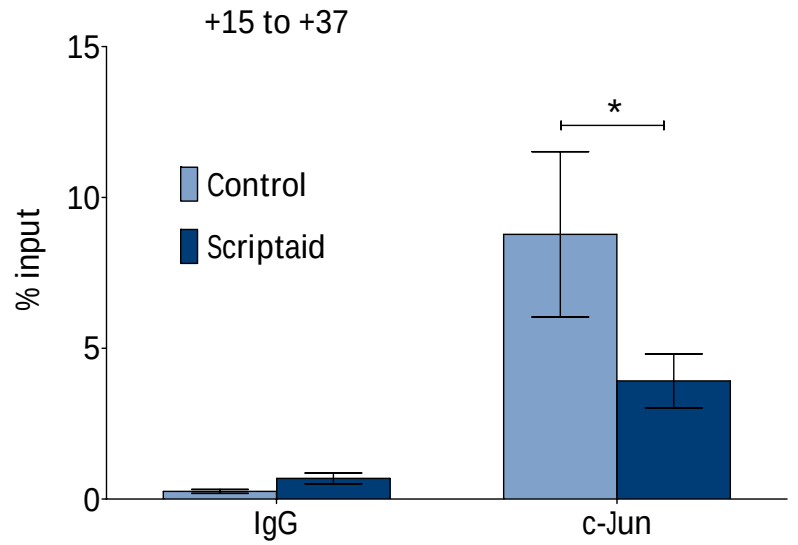

Figure 61: Binding of c-Jun to the *Nox4* promoter region +15 to +34 after scriptaid treatment.
Human EA.hy926 endothelial cells were treated with scriptaid (5 µM for 4 h). Binding of c-Jun to the Nox4 5'UTR region +15 to + 34 was studied using ChIP followed by qPCR. Columns represent mean ± SEM, n = 6 (* p < 0.01).

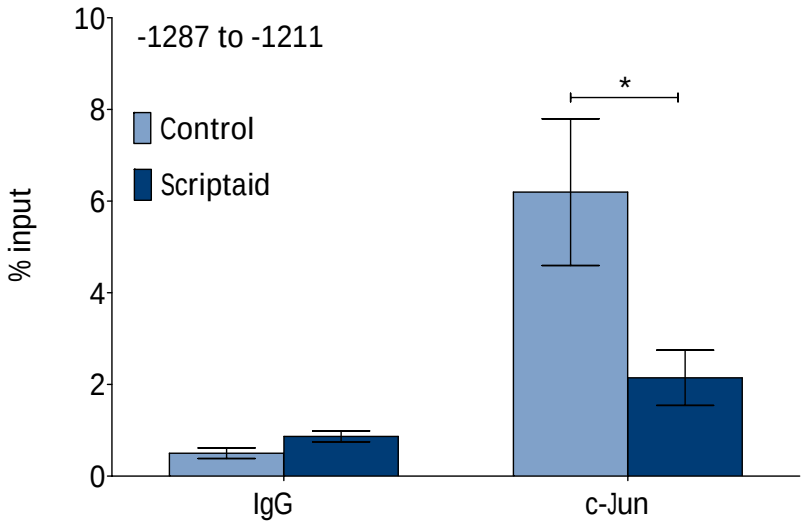

Figure 62: Binding of c-Jun to the *Nox4* promoter region -1287 to -1211 after scriptaid treatment in HUVEC.
HUVEC were treated with scriptaid (5 µM for 4 h). Binding of c-Jun to the Nox4 promoter region -1287 to -1211 was studied using ChIP followed by qPCR. Columns represent mean ± SEM, n = 3 (* $p < 0.01$).

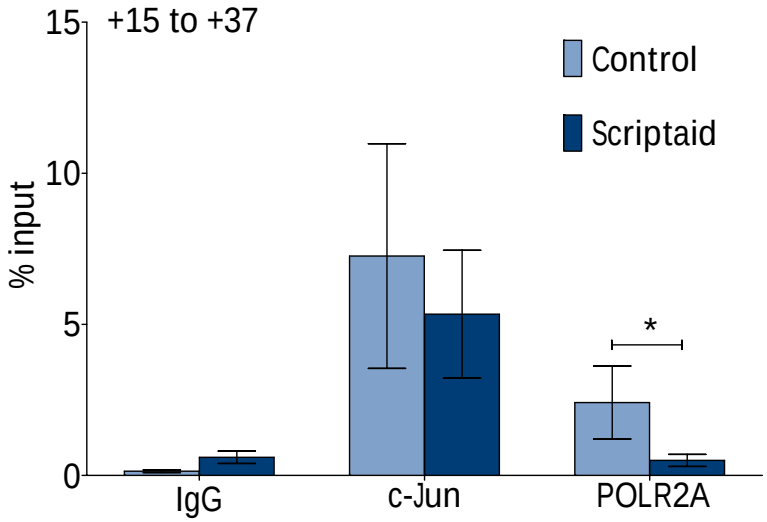

Figure 63: Binding of c-Jun and RNA polymerase II to the *Nox4* promoter region +15 to +34 after scriptaid treatment in HUVEC.
HUVEC were treated with scriptaid (5 µM for 4 h). Binding of c-Jun and polymerase II (POLR2A) to the Nox4 5'UTR region +15 to +34 was studied using ChIP followed by qPCR. Columns represent mean ± SEM, n = 3 (* $p < 0.01$).

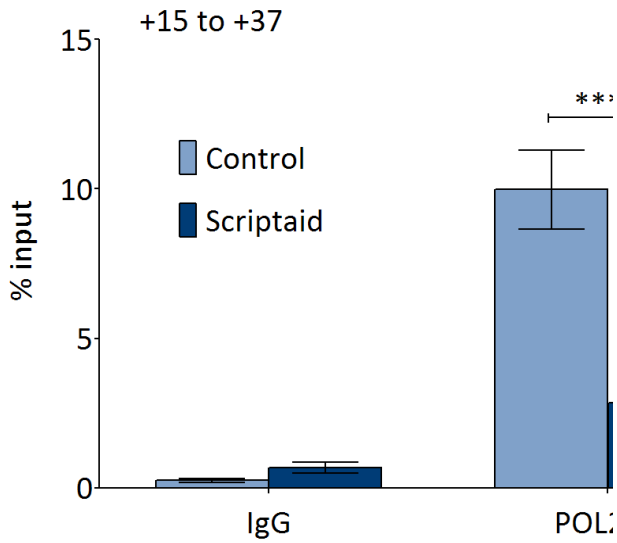

Figure 64: Binding of RNA polymerase II to the *Nox4* promoter region +15 to +34 after scriptaid treatment.
Human EA.hy926 endothelial cells were treated with scriptaid (5 µM for 4 h). Binding of RNA polymerase II (POL2RA) to the Nox4 5'UTR region +15 to + 34 was studied using ChIP followed by qPCR. Columns represent mean ± SEM, n = 6 (*** p < 0.001).

The specificity of the c-Jun antibody was verified by ChIP-qPCR (Figure 65). This was done by analyzing the binding of c-Jun to a region in which c-Jun was reported to bind (chr11:89340150-89340297)[286] and a region in which c-Jun should not bind (Igr5 intron 3)[287]

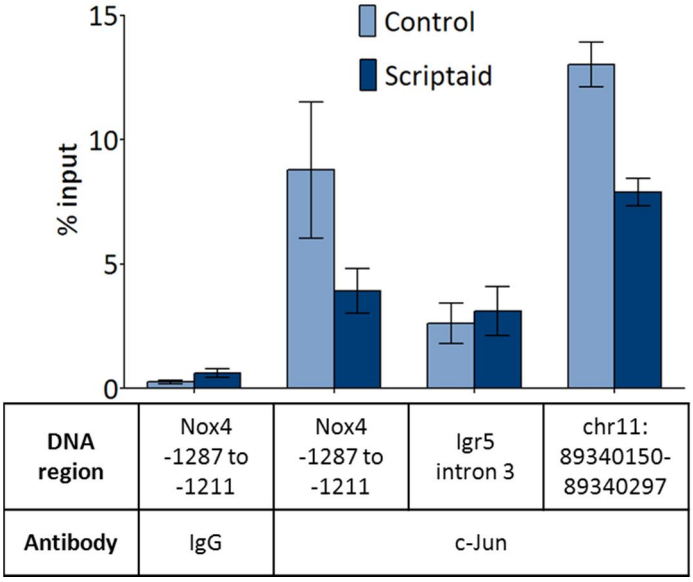

Figure 65: Validation of the specificity of the c-Jun antibody.
Human EA.hy926 endothelial cells were treated with scriptaid (5 µM for 24 h). Binding of c-Jun to the indicated DNA regions was studied by ChIP followed by qPCR. Columns represent mean ± SEM, n = 3. Igr5 intron 3 contains no c-Jun binding site and was used as a negative control[287]. Position 89340150-89340297 in chromosome 11 has a validated c-Jun site and was used as a positive control[286].

3.9 Determination of cytotoxicity

HUVEC or EA.hy926 cells were treated with 5 µM scriptaid for 24 h and cytotoxicity was measured with CytoTox-ONE™ Homogeneous Membrane Integrity Assay. Neither in HUVEC (Figure 66) nor EA.hy926 cells (Figure 67) a cytotoxic effect of 5 µM scriptaid after 24 h was observed.

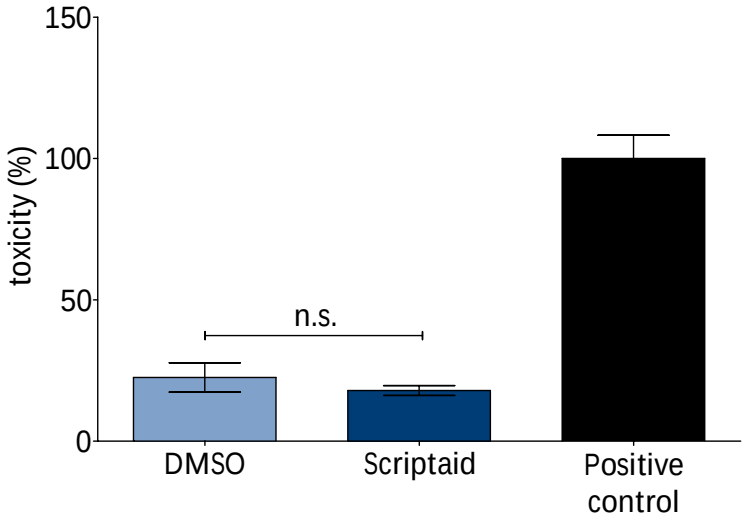

Figure 66: No cytotoxic effect of scriptaid in HUVEC.
Human umbilical vein endothelial cells (HUVEC) were treated with 5 µM scriptaid for 24 h. Cytotoxicity was measured using CytoTox-ONE™ Homogeneous Membrane Integrity Assay Kit. Columns represent mean ± SEM, n = 6. n.s., not significant.

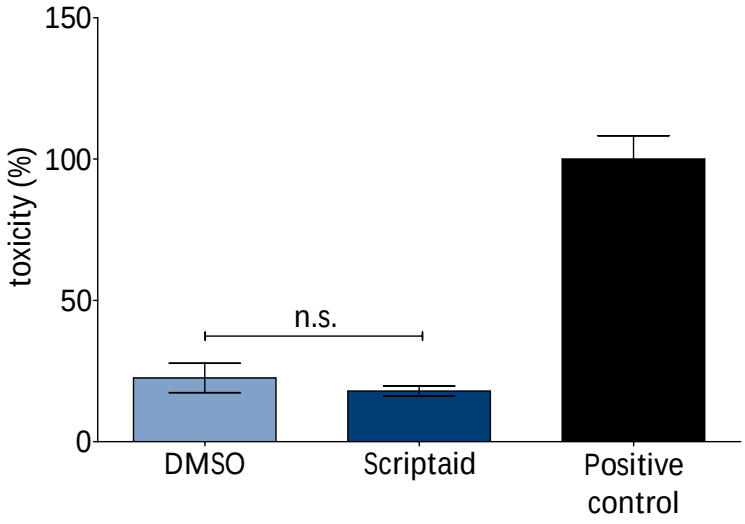

Figure 67: No cytotoxic effect of scriptaid in EA.hy926 endothelial cells.
Human EA.hy926 endothelial cells were treated with 5 µM scriptaid for 24 h. Cytotoxicity was measured using CytoTox-ONE™ Homogeneous Membrane Integrity Assay Kit. Columns represent mean ± SEM, n = 6. n.s., not significant.

The Membrane Integrity Assay results show that scriptaid had no cytotoxic effects. These results were confirmed using the Muse Annexin V and Dead Cell Kit. EA.hy926 cells were either left untreated (A), treated with the solvent control (dimethyl sulfoxide, DMSO, B), with 5 µM scriptaid for 24 h (C) or with 1 µM staurosporine (Staur., D, as a positive control). Again no cytotoxicity of scriptaid was (Figure 68).

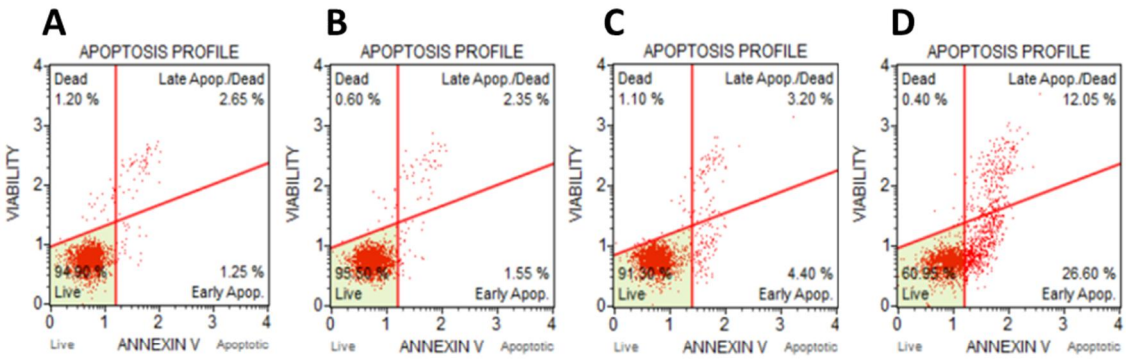

	Untreated (A)	DMSO (B)	Scriptaid (C)	Staur. (D)
Live cells (LL)	94.90	95.50	91.3	60.95
Early apoptotic cells (LR)	1.25	1.55	4.40	26.60
Late apoptotic/dead cells (UR)	2.65	2.35	3.20	12.05
Debris (UL)	1.20	0.60	1.10	0.40

Figure 68: No cytotoxic effect of scriptaid in EA.hy926 cells determined using MUSE Cell Analyzer.
EA.hy926 endothelial cells were treated with 5 µM scriptaid for 24 h. Cytotoxicity was measured with the Muse Annexin V and Dead Cell Kit on the Muse™ Cell Analyzer.

3.10 Nox4 mRNA stability after scriptaid treatment

EA.hy926 cells were treated for 2 h with 3 µM scriptaid followed by a treatment with 60 µM 5,6-Dichloro-1-β-D-ribofuranosylbenzimidazole (DRB) for 3 h and 6 h, respectively. The quantity of Nox4 mRNA was then determined by qPCR. Figure 69 shows that treatment of scriptaid leads to a faster decay of Nox4 mRNA.

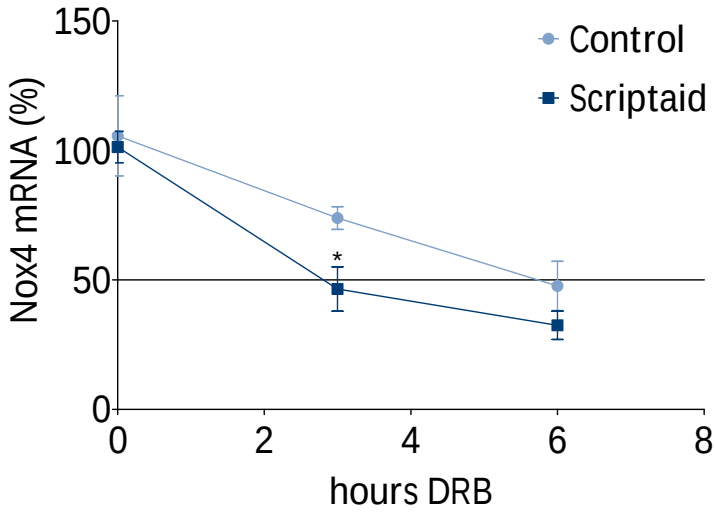

Figure 69: Nox4 mRNA stability after scriptaid treatment.
EA.hy926 endothelial cells were treated with scriptaid (3 µM for 2h), followed by DRB (60 µM) treatment for 3 h and 6 h, respectively. Nox4 mRNA was analyzed by qPCR. Symbols show mean ± SEM, n = 8 (* $p < 0.05$, compared with control).

3.11 Involvement of RNA interference on Nox4 regulation

Treatment with Dicer1 siRNA (50 nM for 48 h) had little effect on Nox4 mRNA expression (Figure 70), indicating that RNA interference alone plays only a minor role in basal Nox4 mRNA regulation. Treatment of EA.hy926 endothelial cells with 3 µM scriptaid for 24 h led to a downregulation of Nox4 mRNA. This downregulation was attenuated by Dicer1 knockdown (Figure 70). The efficiency of the Dicer1 siRNA was verified by qPCR (Figure 71).

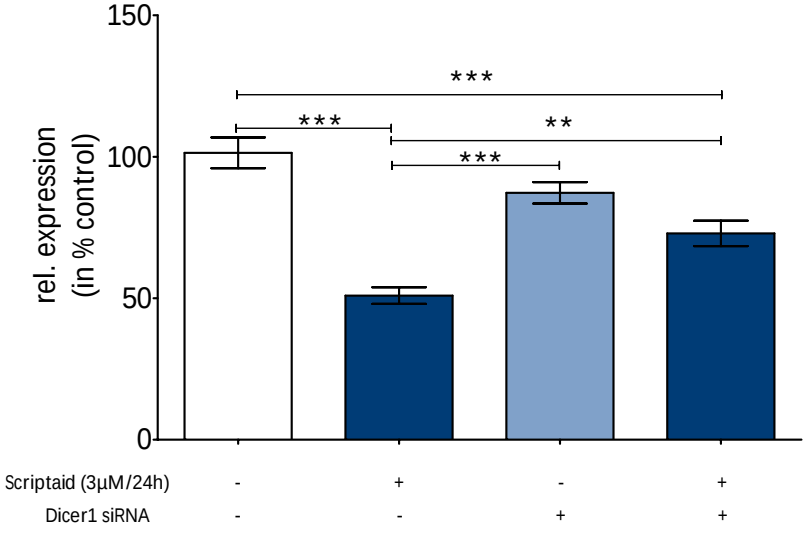

Figure 70: Effect of scriptaid on Nox4 mRNA expression after Dicer1 knockdown.
Human EA.hy926 endothelial cells were transfected with siRNA (50 nM for 48 h) to knockdown Dicer1. 24 h after transfection, cells were treated with scriptaid (3 µM for 24 h) and Nox4 mRNA expression was analyzed by qPCR. Columns show mean ± SEM, n = 11 – 12 (** p < 0.01, *** p < 0.001).

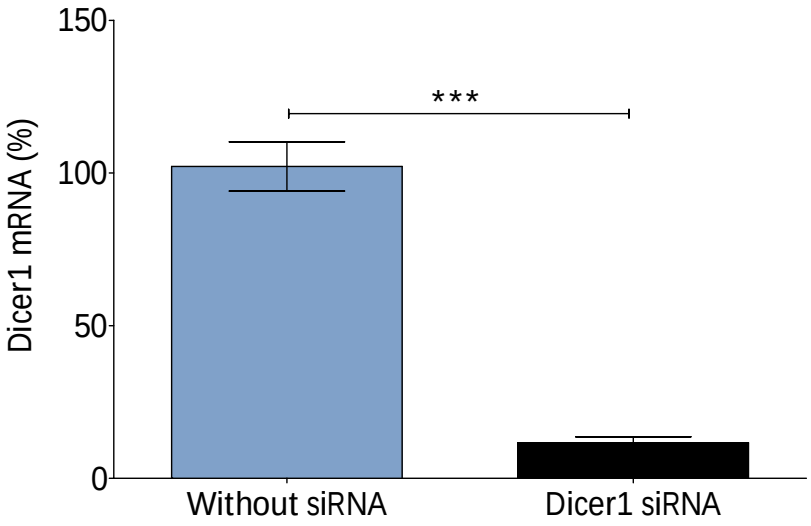

Figure 71: siRNA-mediated Dicer1 knockdown.
EA.hy926 endothelial cells were transfected with siRNA (50 nM for 48 h) to knockdown Dicer1. The knockdown efficiency was verified with qPCR. Columns show mean ± SEM, n = 7 – 8 (*** p < 0.001).

In another experiment, EA.hy926 cells were treated with 60 µM DRB for 30 minutes to block transcription. Then, cells were additionally treated with 3 µM scriptaid for 4 h. Treatment of scriptaid alone led to a significant downregulation of Nox4 mRNA. This downregulation was significantly reduced but not completely blocked by DRB (Figure 72).

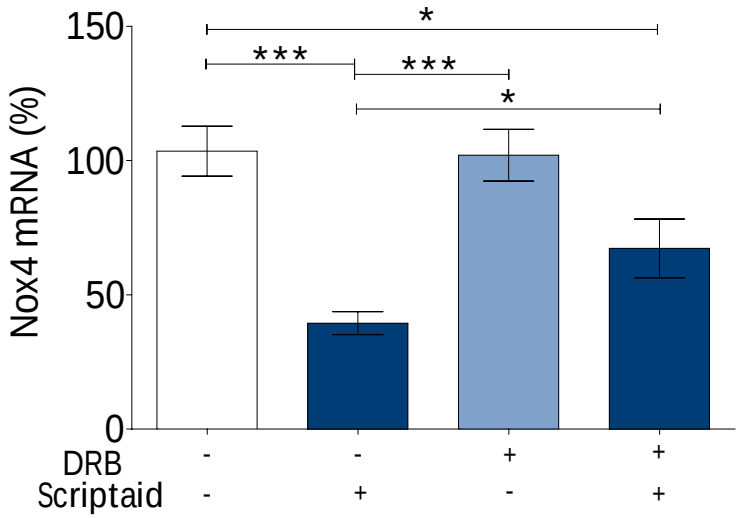

Figure 72: Effect of scriptaid on Nox4 mRNA expression after transcription inhibition.
Human EA.hy926 endothelial cells were treated with DRB (60 µM for 30 minutes) to block inhibition. Then, scriptaid (3 µM for 4 h) was added and Nox4 mRNA was measured with qPCR. Columns show mean ± SEM, n = 9 (* $p < 0.05$, *** $p < 0.001$).

4 Discussion

Until now, several factors have been identified that regulate Nox4 transcription.[293] In human aortic smooth muscle cells (SMC), the enhanced expression of Nox4 (and Nox1) in response to treatment with tumor necrosis factor-α (TNF-α) has been shown to be mediated by an activation of NF-κB.[294] Nox4 upregulation induced by interferon-γ (IFN-γ) in human SMC involves the JAK/STAT pathway.[295] Hypoxia enhances Nox4 mRNA and protein levels in pulmonary artery smooth-muscle cells. This response is dependent on the hypoxia-inducible transcription factor HIF-1α[296] and NF-E2-related factor 2 (Nrf2).[297] Transforming growth factor-β1 (TGF-β1) induces the expression of Nox4 in human pulmonary artery smooth muscle cells through a signaling pathway involving Smad2/3.[243] Whereas Nox4 expression is reduced by peroxisome proliferator-activated receptor-γ ligands[298], E2F factor(s) have been shown to be positive regulators of Nox4 transcription in SMC.[299] An ARE-like/Oct-1 binding site has been shown to be essential for shear stress-dependent downregulation of Nox4.[300] In addition to regulation at the transcriptional level, Nox4 expression has also been found to be regulated by the microRNAs miR-25[301], miR-23b[302] and miR-146a[303] via posttranscriptional mechanisms.

In this study, I found a new transcription factor positively regulating Nox4 expression: c-Jun. Computational analysis with PROMO[304,305] revealed that the 5'-flanking region of human *Nox4* gene contains putative binding elements for AP-1 (5'-TGA CTT Cct tcc agt gga gag acc cct tgg gtt ttt cgt gtg ctc ttt ccc tga tcc ttt aGG TGT CAc ATG GTC A-3'; -1287 to -1211); and (5'-TGA CCC Ggt gcg ggt gGG AGT CA-3'; +15 to +37) (putative AP-1 binding sites in capital letters). I therefore studied the relevance of AP-1 in the regulation of Nox4 expression. Knockdown of c-Jun by siRNA (Figure 50) led to a downregulation of Nox4 (Figure 51), indicating that c-Jun was a positive regulator of Nox4 transcription. Then, I wanted to find out whether the reduction of Nox4 by scriptaid was due to a downregulation/inhibition of c-Jun. Unexpectedly, the mRNA and protein levels of c-Jun were increased by scriptaid treatment (Figure 53 and Figure 54). In transient transfection experiments using luciferase as reporter gene, the activity of the artificial promoter (containing binding sites for AP-1) was increased by scriptaid treatment (Figure 56). These results indicated that the expression and activity of c-Jun was enhanced rather than reduced by scriptaid. The activity of a Nox4 promoter construct was found increased in transient transfection experiments (see Figure 34), which could be a consequence of the enhanced c-Jun activity.

A discrepancy between the promoter activity of transiently transfected luciferase constructs and endogenous transcription has been reported previously for eNOS.[306] HDAC inhibition reduces eNOS mRNA and protein biosynthesis.[306] The eNOS promoter activity in transient transfection experiments, however, was found paradoxically enhanced. The activity of transiently transfected promoter constructs does not necessarily reflect the activity of the endogenous promoter. Indeed, the endogenous eNOS promoter was not activated by HDAC inhibitors.[306] Whereas the transiently transfected plasmids (e.g. the pAP-1-Luc) are "naked" DNA and not packed into chromatin in the same way as genomic DNA, the endogenous Nox4 promoter lies under the control of epigenetic mechanisms. Although the activity of c-Jun was increased by scriptaid as shown in the transient transfection experiments, this did not necessarily lead to an activation of the endogenous Nox4 promoter. Actually, the binding of c-Jun to the endogenous Nox4 promoter was reduced in scriptaid treated cells (Figure 60 to Figure 63). Both cell lines used in this study (EA.hy926 and HUVEC) showed

the same response, i.e. decreased binding of c-Jun to the putative binding sites after scriptaid treatment. EA.hy926 cells are a hybridome cell line as mentioned in 2.1.1. To find out whether the mechanisms discovered EA.hy926 cells also apply to native endothelial cells, some key experiments were repeated in HUVECs. The specificity of the c-Jun antibody was verified with a known binding site of c-Jun (chr11:89340150-89340297)[286] and a region in which c-Jun does not bind (Igr5 intron 3)[287] (see Figure 65).

The AP-1 transcription factor is a dimeric complex that comprises members of the Jun, Fos, ATF and MAF protein families.[307] In addition to c-Jun, I also studied the role of c-Fos in Nox4 expression. Similar to c-Jun, c-Fos expression was enhanced by scriptaid treatment in EA.hy926 cells (Figure 55). Knockdown of c-Fos by siRNA reduced the expression of Nox4 mRNA (Figure 52); further supporting the concept that AP-1 is an important regulator of Nox4 expression.

As mentioned HDACs might play an important role in the regulation of Nox4 transcription. Scriptaid, TSA and SAHA are hydroxamic acid derivatives and specific inhibitors of HDAC classes I and II.[218] In the present study, all three HDAC inhibitors downregulated Nox4 expression in a concentration-dependent manner in human EA.hy926 endothelial cells (Figure 27, Figure 32 and Figure 33). It has been previously reported that genes are differentially regulated by histone deacetylase inhibitors including scriptaid and SAHA.[202,308] Such a differential regulation is also evident in EA.hy926 cells. Scriptaid enhanced the expression of c-Jun and c-Fos, decreased the expression of Nox4, eNOS and sirtuin 1, and left β-tubulin expression unchanged (data not shown). Therefore, the Nox4 downregulation by scriptaid is likely to be a gene-specific effect. In addition, no cytotoxic effects were found for scriptaid under the present experimental conditions (Figure 67 and Figure 68).

HDACs, by definition, are enzymes that remove acetyl groups from histones and HDAC inhibition with scriptaid should thus enhance histone acetylation. To address this subject the acetylation status of histone H4 and histone H3K27 was examined by ChIP. Indeed, the acetylation of H4 and H3K27 in the Nox4 promoter regions was increased by scriptaid treatment (Figure 44 and Figure 45). Generally, lysine acetylation can neutralize the basic charge of lysine residues and prevent the higher-order compaction of chromatin, resulting in a more open (or accessible) chromatin configuration. The chromatin structure of the Nox4 promoter region was studied using EpiQ kit. As shown in Table 36, scriptaid treatment was indeed associated with more accessible chromatin structure. Therefore, the downregulation of Nox4 by scriptaid was not due to a change in chromatin accessibility.

Generally, histone acetylation is a mark broadly associated with transcriptional activation. However, histone acetylation may also play a negative role in transcription at specific promoters.[129] This can be explained by the model of “steric inhibition”.[129] In this model, a transcriptional coactivator with a bromodomain binds to a promoter via interactions with both transcription factors and acetylated lysine residues on the histone tail. The geometry of the transcription complex allows for interaction of the factor with particular acetylated lysines. An HDAC at the promoter keeps the histone tail deacetylated to allow for optimal interaction with the coactivator. HDAC inhibition leads to hyperacetylation. Acetylation of an additional nearby lysine residues may sterically hinder that interaction and destabilize the association of the coactivator with the promoter.[129] This is likely to be the situation at the human Nox4 promoter in scriptaid-treated cells. Although the chromatin is more

accessible and the transcription factor c-Jun is activated, its binding to the DNA is prevented due to hyperacetylation-mediated steric inhibition. The result is a reduced transcription rate. The reduced binding to RNA polymerase POLR2A to the transcription start site of Nox4 (see Figure 64) supported this concept. Also in HUVECs, an increase of acetylation of the histone tails as well as a decreased binding of POL2R was observed (see Figure 46, Figure 47 and Figure 63).

All used HDAC inhibitors are pan-HDAC inhibitors, this means they inhibit all class I, II and IV HDACs with different IC_{50}.[218] Nearly all HDACs could be found in EA.hy926 cells, with relatively high levels of HDAC1, HDAC3 and HDAC7 (Figure 35). Treatment with scriptaid increased the expression of HDAC1 and HDAC3, whereas mRNA expression of HDAC7 was decreased after scriptaid treatment (Figure 36). Neither the knockdown of HDAC1 nor of HDAC7 had a significant effect on Nox4 expression (Figure 41). According to the expression profile of different HDACs in EA.hy926 obtained by qPCR, HDAC3 might be one of the HDAC enzymes responsible for the effect of HDAC inhibitors on Nox4 expression because (i) the expression level of HDAC3 in EA.hy926 cells was relatively high; (ii) previous studies showed that HDAC3 plays an important role in endothelial cells[211,309,310]; and (iii) all 3 compounds I used had high inhibition potency on HDAC3.[218] Indeed, siRNA-mediated knockdown of HDAC3, in EA.hy926 and HUVEC, had a similar downregulating effect on Nox4 expression as the HDAC inhibitors (Figure 37 and Figure 38). Because of the sequence similarity between the different HDACs, a cross-reaction of HDAC3 siRNA on HDAC1 or HDAC7 must be ruled out. Knockdown of HDAC3 had no effect on the expression of HDAC1 or HDAC7 (Figure 42 and Figure 43). These results indicate that HDAC3 is a candidate molecule regulating Nox4 expression in human endothelial cells and native human umbilical vein endothelial cells. Nevertheless, possible contribution of other HDAC isoforms could not be excluded.

There is increasing evidence supporting the concept of direct crosstalk between histone modifications, DNA methylation[311,312] and RNAi.[313] Direct interaction between DNA methyltransferases and HDACs has also been reported.[314] Genome research revealed a CpG island in the promoter region of the *Nox4* gene. CpG islands are under evolutionary pressure because methylated cytosines tend to turn into thymines due to spontaneous deamination.[315]

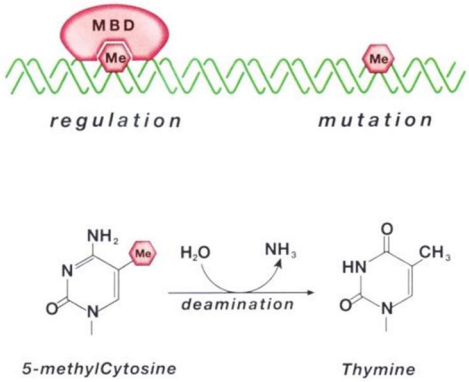

Figure 73: Spontaneous deamination of 5-methyl cytosine.
(From Allis at al. 2007)[2]

Therefore, it was investigated in the present study whether the downregulation of Nox4 expression was the result of enhanced DNA methylation followed by histone acetylation. However,

pyrosequencing experiments could not find any changes in DNA methylation in response to scriptaid in the promoter region of Nox4 (see Figure 49).
Genome Browser[316], Transterm[317] and UTRScan[318] revealed miRNA binding sites in the 3'UTR of the Nox4 mRNA and others have shown that Nox4 is regulated by miRNAs.[301–303] RNAi is an epigenetic mechanism. The involvement of RNAi in Nox4 regulation was examined with Dicer1 siRNA (see Figure 71). Knockdown of Dicer1 caused only a slight decrease in basal Nox4 expression, but it significantly diminished the effect of scriptaid on Nox4 mRNA expression (see Figure 70). These results indicate that miRNAs play a role in the regulation of Nox4 expression and are involved in the scriptaid-induced Nox4 downregulation.

The downregulation of Nox4 expression by scriptaid is a concentration- but also time-dependent event, with a significant Nox4 mRNA reduction within two hours (see Figure 29). This fast downregulation indicates either a low half-life of Nox4 mRNA or the involvement of direct degrading mechanisms. Consistently, treatment with scriptaid decreased the stability of Nox4 mRNA (Figure 69). The blockade of RNA synthesis with DRB decreased the effect of scriptaid on Nox4 mRNA expression, indicating the involvement of RNA synthesis in the scriptaid-induced Nox4 mRNA degradation (see Figure 72). This is in agreement with the finding that Dicer1 knockdown reduced the effect of scriptaid (Figure 70). However, Dicer1 knockdown did not completely block the effect of scriptaid; because part of the scriptaid effects is mediated by inhibition of transcription (mRNA synthesis).
To test the effect of miRNA on Nox4 mRNA expression, a luciferase construct containing the part of the Nox4 3'UTR (in which the miRNA binding sites were predicted) was generated. The reporter construct should be more suitable to test the effect of miRNA on Nox4 mRNA than Dicer1 knockdown or RNA synthesis inhibition, because this is a gene-specific approach. EA.hy926 cells were transfected with the plasmid and 24 hours later treated with scriptaid for another 24 h. Unexpectedly, the scriptaid treatment resulted in increased luciferase activity (data not shown). However, this was not due to specific effects on the Nox4 3'UTR on the luciferase reporter mRNA, but due to an promoter activation. HDAC inhibitors are known to enhance viral promoters like simian virus 40 (SV40)[319] or cytomegalovirus (CMV).[320–322] Therefore, studies with the luciferase plasmids containing the Nox4 3'UTR didn't help to clarify the function of Nox4 3'UTR, unfortunately.

In conclusion, Nox4 expression is regulated by HDAC in human endothelial cells. HDAC inhibition reduces Nox4 transcription despite an open chromatin structure. This is likely to be attributable to an inhibition of the binding of transcription factor(s) and polymerase(s) to the Nox4 promoter. Figure 74 shows a model of the described mechanism. If the balance of acetylation and deactylation is disturbed by inhibition of HDACs, coactivators of transcription or transcription factors (in this case c-Jun) can no longer bind properly to the promoter due to steric inhibition. In addition, HDAC inhibition-induced Nox4 downregulation may also involves miRNA-mediated mRNA degradation.

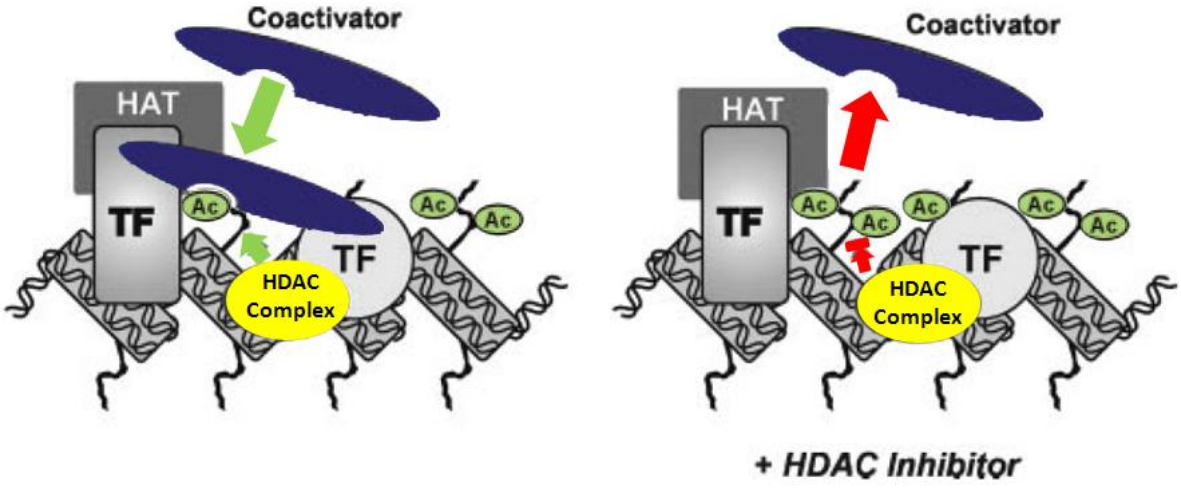

Figure 74: Model steric inhibition.
HDAC complexes (yellow) are important regulators of transcription. Coordinated histone acetylation (green Ac) by HATs and deacetylation by HDACs allow the binding of coactivators and transcription factors (TF) to the DNA. If HDACs are blocked by HDAC inhibitors (right panel) the balance between acetylation and deacetylation is disturbed, which may cause the dissociation of coactivators and/or transcription factors due to steric inhibition. (Modified from Smith et al. 2008)[129]

5 References

1. Waddington, C.H. The epigenotype. *Endeavour* 1, 18-20 (1942).

2. Allis, C.D., Jenuwein, T. & Reinberg, D. *Epigenetics*. 23-62 (Cold Spring Harbor Laboratory Press: New York, 2007).

3. Matouk, C.C. & Marsden, P.A. Epigenetic regulation of vascular endothelial gene expression. *Circulation research* 102, 873-87 (2008).

4. Chambon, P. Summary: the molecular biology of the eukaryotic genome is coming of age. *Cold Spring Harbor symposia on quantitative biology* 42 Pt 2, 1209-34 (1978).

5. Holliday, R. & Pugh, J.E. DNA modification mechanisms and gene activity during development. *Science (New York, N.Y.)* 187, 226-32 (1975).

6. Jaenisch, R. & Bird, A. Epigenetic regulation of gene expression: how the genome integrates intrinsic and environmental signals. *Nature genetics* 33 Suppl, 245-54 (2003).

7. Borrelli, E., Nestler, E.J., Allis, C.D. & Sassone-Corsi, P. Decoding the epigenetic language of neuronal plasticity. *Neuron* 60, 961-74 (2008).

8. Kawasaki, H. & Taira, K. Induction of DNA methylation and gene silencing by short interfering RNAs in human cells. *Nature* 431, 211-7 (2004).

9. Zilberman, D., Cao, X. & Jacobsen, S.E. ARGONAUTE4 control of locus-specific siRNA accumulation and DNA and histone methylation. *Science (New York, N.Y.)* 299, 716-9 (2003).

10. Aufsatz, W., Mette, M.F., van der Winden, J., Matzke, A.J.M. & Matzke, M. RNA-directed DNA methylation in Arabidopsis. *Proceedings of the National Academy of Sciences of the United States of America* 99 Suppl 4, 16499-506 (2002).

11. Viré, E. *et al.* The Polycomb group protein EZH2 directly controls DNA methylation. *Nature* 439, 871-4 (2006).

12. Jackson, J.P., Lindroth, A.M., Cao, X. & Jacobsen, S.E. Control of CpNpG DNA methylation by the KRYPTONITE histone H3 methyltransferase. *Nature* 416, 556-60 (2002).

13. Tamaru, H. & Selker, E.U. A histone H3 methyltransferase controls DNA methylation in Neurospora crassa. *Nature* 414, 277-83 (2001).

14. Razin, A. & Riggs, A.D. DNA methylation and gene function. *Science (New York, N.Y.)* 210, 604-10 (1980).

15. Huang, Y.-W., Kuo, C.-T., Stoner, K., Huang, T.H.-Y. & Wang, L.-S. An overview of epigenetics and chemoprevention. *FEBS letters* 585, 2129-36 (2011).

16. Arber, W. & Linn, S. DNA modification and restriction. *Annual review of biochemistry* 38, 467-500 (1969).

17. Gorovsky, M.A., Hattman, S. & Pleger, G.L. (6 N)methyl adenine in the nuclear DNA of a eucaryote, Tetrahymena pyriformis. *The Journal of cell biology* 56, 697-701 (1973).

18. Cummings, D.J., Tait, A. & Goddard, J.M. Methylated bases in DNA from Paramecium aurelia. *Biochimica et biophysica acta* 374, 1-11 (1974).

19. Hattman, S., Kenny, C., Berger, L. & Pratt, K. Comparative study of DNA methylation in three unicellular eucaryotes. *Journal of bacteriology* 135, 1156-7 (1978).

20. Doerfler, W. DNA methylation and gene activity. *Annual review of biochemistry* 52, 93-124 (1983).

21. Tweedie, S., Charlton, J., Clark, V. & Bird, A. Methylation of genomes and genes at the invertebrate-vertebrate boundary. *Molecular and cellular biology* 17, 1469-75 (1997).

22. Kriaucionis, S. & Bird, A. DNA methylation and Rett syndrome. *Human molecular genetics* 12 Spec No, R221-7 (2003).

23. Selker, E.U. Epigenetic phenomena in filamentous fungi: useful paradigms or repeat-induced confusion? *Trends in Genetics* 13, 296-301 (1997).

24. Tariq, M. & Paszkowski, J. DNA and histone methylation in plants. *Trends in genetics : TIG* 20, 244-51 (2004).

25. Bird, A.P. CpG-rich islands and the function of DNA methylation. *Nature* 321, 209-13 (1986).

26. Cross, S.H. & Bird, A.P. CpG islands and genes. *Current Opinion in Genetics & Development* 5, 309-314 (1995).

27. Ehrlich, M. *et al.* Amount and distribution of 5-methylcytosine in human DNA from different types of tissues of cells. *Nucleic acids research* 10, 2709-21 (1982).

28. Ohlsson, R. & Kanduri, C. New twists on the epigenetics of CpG islands. *Genome research* 12, 525-6 (2002).

29. Park, J.G. & Chapman, V.M. CpG island promoter region methylation patterns of the inactive-X-chromosome hypoxanthine phosphoribosyltransferase (Hprt) gene. *Mol. Cell. Biol.* 14, 7975-7983 (1994).

30. Razin, A. & Cedar, H. DNA methylation and genomic imprinting. *Cell* 77, 473-476 (1994).

31. Strichman-Almashanu, L.Z. *et al.* A genome-wide screen for normally methylated human CpG islands that can identify novel imprinted genes. *Genome research* 12, 543-54 (2002).

32. Fatemi, M. *et al.* Footprinting of mammalian promoters: use of a CpG DNA methyltransferase revealing nucleosome positions at a single molecule level. *Nucleic acids research* 33, e176 (2005).

33. Gardiner-Garden, M. & Frommer, M. CpG islands in vertebrate genomes. *Journal of molecular biology* 196, 261-82 (1987).

34. Kumar, S. *et al.* The DNA (cytosine-5) methyltransferases. *Nucleic acids research* 22, 1-10 (1994).

35. Bestor, T.H. The DNA methyltransferases of mammals. *Human molecular genetics* 9, 2395-402 (2000).

36. Riggs, A.D. X inactivation, differentiation, and DNA methylation. *Cytogenetics and cell genetics* 14, 9-25 (1975).

37. Li, E., Bestor, T.H. & Jaenisch, R. Targeted mutation of the DNA methyltransferase gene results in embryonic lethality. *Cell* 69, 915-926 (1992).

38. Okano, M., Bell, D.W., Haber, D.A. & Li, E. DNA methyltransferases Dnmt3a and Dnmt3b are essential for de novo methylation and mammalian development. *Cell* 99, 247-57 (1999).

39. Chen, C.-C., Wang, K.-Y. & Shen, C.-K.J. The Mammalian de novo DNA Methyltransferases Dnmt3a and Dnmt3b Are Also DNA 5-Hydroxymethyl Cytosine Dehydroxymethylases. *Journal of Biological Chemistry* C112.406975- (2012).at <http://www.jbc.org/cgi/content/abstract/C112.406975v1>

40. Okano, M., Xie, S. & Li, E. Cloning and characterization of a family of novel mammalian DNA (cytosine-5) methyltransferases. *Nature genetics* 19, 219-20 (1998).

41. Hata, K., Okano, M., Lei, H. & Li, E. Dnmt3L cooperates with the Dnmt3 family of de novo DNA methyltransferases to establish maternal imprints in mice. *Development (Cambridge, England)* 129, 1983-93 (2002).

42. Kaneda, M. *et al.* Role of de novo DNA methyltransferases in initiation of genomic imprinting and X-chromosome inactivation. *Cold Spring Harbor symposia on quantitative biology* 69, 125-9 (2004).

43. Suetake, I., Shinozaki, F., Miyagawa, J., Takeshima, H. & Tajima, S. DNMT3L stimulates the DNA methylation activity of Dnmt3a and Dnmt3b through a direct interaction. *The Journal of biological chemistry* 279, 27816-23 (2004).

44. Goll, M.G. *et al.* Methylation of tRNAAsp by the DNA methyltransferase homolog Dnmt2. *Science (New York, N.Y.)* 311, 395-8 (2006).

45. Yoder, J.A. & Bestor, T.H. A candidate mammalian DNA methyltransferase related to pmt1p of fission yeast. *Human molecular genetics* 7, 279-84 (1998).

46. Stein, R., Razin, A. & Cedar, H. In vitro methylation of the hamster adenine phosphoribosyltransferase gene inhibits its expression in mouse L cells. *Proceedings of the National Academy of Sciences of the United States of America* 79, 3418-22 (1982).

47. Vardimon, L., Günthert, U. & Doerfler, W. In vitro methylation of the BsuRI (5'-GGCC-3') sites in the E2a region of adenovirus type 2 DNA does not affect expression in Xenopus laevis oocytes. *Molecular and cellular biology* 2, 1574-80 (1982).

48. Watt, F. & Molloy, P.L. Cytosine methylation prevents binding to DNA of a HeLa cell transcription factor required for optimal expression of the adenovirus major late promoter. *Genes & development* 2, 1136-43 (1988).

49. Fatemi, M. & Wade, P.A. MBD family proteins: reading the epigenetic code. *Journal of cell science* 119, 3033-7 (2006).

50. Sarraf, S.A. & Stancheva, I. Methyl-CpG binding protein MBD1 couples histone H3 methylation at lysine 9 by SETDB1 to DNA replication and chromatin assembly. *Molecular cell* 15, 595-605 (2004).

51. Kornberg, R.D. Chromatin structure: a repeating unit of histones and DNA. *Science (New York, N.Y.)* 184, 868-71 (1974).

52. Luger, K., Mäder, A.W., Richmond, R.K., Sargent, D.F. & Richmond, T.J. Crystal structure of the nucleosome core particle at 2.8 A resolution. *Nature* 389, 251-60 (1997).

53. Richmond, T.J. & Davey, C.A. The structure of DNA in the nucleosome core. *Nature* 423, 145-50 (2003).

54. Schalch, T., Duda, S., Sargent, D.F. & Richmond, T.J. X-ray structure of a tetranucleosome and its implications for the chromatin fibre. *Nature* 436, 138-41 (2005).

55. Khorasanizadeh, S. The nucleosome: from genomic organization to genomic regulation. *Cell* 116, 259-72 (2004).

56. Lee, J.Y. & Lee, T.-H. Effects of histone acetylation and CpG methylation on the structure of nucleosomes. *Biochimica et biophysica acta* 1824, 974-82 (2012).

57. Wei, Y., Yu, L., Bowen, J., Gorovsky, M.A. & Allis, C.D. Phosphorylation of histone H3 is required for proper chromosome condensation and segregation. *Cell* 97, 99-109 (1999).

58. Nowak, S.J. & Corces, V.G. Phosphorylation of histone H3: a balancing act between chromosome condensation and transcriptional activation. *Trends in genetics : TIG* 20, 214-20 (2004).

59. Dou, Y. & Gorovsky, M.A. Phosphorylation of linker histone H1 regulates gene expression in vivo by creating a charge patch. *Molecular cell* 6, 225-31 (2000).

60. Misteli, T. Spatial positioning; a new dimension in genome function. *Cell* 119, 153-6 (2004).

61. Fisher, A.G. & Merkenschlager, M. Gene silencing, cell fate and nuclear organisation. *Current opinion in genetics & development* 12, 193-7 (2002).

62. Felsenfeld, G. & Groudine, M. Controlling the double helix. *Nature* 421, 448-53 (2003).

63. Tost, J. *Epigenetics*. (Caister Academic Press: Norfolk, UK, 2008).

64. Sarma, K. & Reinberg, D. Histone variants meet their match. *Nature reviews. Molecular cell biology* 6, 139-49 (2005).

65. Henikoff, S. & Ahmad, K. Assembly of variant histones into chromatin. *Annual review of cell and developmental biology* 21, 133-53 (2005).

66. Bernstein, E. & Hake, S.B. The nucleosome: a little variation goes a long way. *Biochemistry and cell biology = Biochimie et biologie cellulaire* 84, 505-17 (2006).

67. Cairns, B.R. Chromatin remodeling complexes: strength in diversity, precision through specialization. *Current opinion in genetics & development* 15, 185-90 (2005).

68. Tagami, H., Ray-Gallet, D., Almouzni, G. & Nakatani, Y. Histone H3.1 and H3.3 complexes mediate nucleosome assembly pathways dependent or independent of DNA synthesis. *Cell* 116, 51-61 (2004).

69. Mizuguchi, G. *et al.* ATP-driven exchange of histone H2AZ variant catalyzed by SWR1 chromatin remodeling complex. *Science (New York, N.Y.)* 303, 343-8 (2004).

70. Johnson, L. *et al.* Mass spectrometry analysis of Arabidopsis histone H3 reveals distinct combinations of post-translational modifications. *Nucleic acids research* 32, 6511-8 (2004).

71. Ahmad, K. & Henikoff, S. The histone variant H3.3 marks active chromatin by replication-independent nucleosome assembly. *Molecular cell* 9, 1191-200 (2002).

72. Vos, L.J., Famulski, J.K. & Chan, G.K.T. How to build a centromere: from centromeric and pericentromeric chromatin to kinetochore assembly. *Biochemistry and cell biology = Biochimie et biologie cellulaire* 84, 619-39 (2006).

73. Fukagawa, T. Formation of a centromere-specific chromatin structure. *Epigenetics : official journal of the DNA Methylation Society* 7, 672-5 (2012).

74. Witt, O., Albig, W. & Doenecke, D. Testis-specific expression of a novel human H3 histone gene. *Experimental cell research* 229, 301-6 (1996).

75. Workman, J.L. Nucleosome displacement in transcription. *Genes & development* 20, 2009-17 (2006).

76. Guillemette, B. & Gaudreau, L. Reuniting the contrasting functions of H2A.Z. *Biochemistry and cell biology = Biochimie et biologie cellulaire* 84, 528-35 (2006).

77. Jin, J. *et al.* In and out: histone variant exchange in chromatin. *Trends in biochemical sciences* 30, 680-7 (2005).

78. Fillingham, J., Keogh, M.-C. & Krogan, N.J. GammaH2AX and its role in DNA double-strand break repair. *Biochemistry and cell biology = Biochimie et biologie cellulaire* 84, 568-77 (2006).

79. van Attikum, H. & Gasser, S.M. ATP-dependent chromatin remodeling and DNA double-strand break repair. *Cell cycle (Georgetown, Tex.)* 4, 1011-4 (2005).

80. Rogakou, E.P., Pilch, D.R., Orr, A.H., Ivanova, V.S. & Bonner, W.M. DNA double-stranded breaks induce histone H2AX phosphorylation on serine 139. *The Journal of biological chemistry* 273, 5858-68 (1998).

81. Unal, E. *et al.* DNA damage response pathway uses histone modification to assemble a double-strand break-specific cohesin domain. *Molecular cell* 16, 991-1002 (2004).

82. Shroff, R. *et al.* Distribution and dynamics of chromatin modification induced by a defined DNA double-strand break. *Current biology : CB* 14, 1703-11 (2004).

83. Rogakou, E.P., Boon, C., Redon, C. & Bonner, W.M. Megabase chromatin domains involved in DNA double-strand breaks in vivo. *The Journal of cell biology* 146, 905-16 (1999).

84. Stucki, M. *et al.* MDC1 directly binds phosphorylated histone H2AX to regulate cellular responses to DNA double-strand breaks. *Cell* 123, 1213-26 (2005).

85. Ward, I.M., Minn, K., Jorda, K.G. & Chen, J. Accumulation of checkpoint protein 53BP1 at DNA breaks involves its binding to phosphorylated histone H2AX. *The Journal of biological chemistry* 278, 19579-82 (2003).

86. Chow, J.C., Yen, Z., Ziesche, S.M. & Brown, C.J. Silencing of the mammalian X chromosome. *Annual review of genomics and human genetics* 6, 69-92 (2005).

87. Chow, J.C. & Brown, C.J. Forming facultative heterochromatin: silencing of an X chromosome in mammalian females. *Cellular and molecular life sciences : CMLS* 60, 2586-603 (2003).

88. Rasmussen, T.P., Mastrangelo, M.A., Eden, A., Pehrson, J.R. & Jaenisch, R. Dynamic relocalization of histone MacroH2A1 from centrosomes to inactive X chromosomes during X inactivation. *The Journal of cell biology* 150, 1189-98 (2000).

89. Mermoud, J.E., Costanzi, C., Pehrson, J.R. & Brockdorff, N. Histone macroH2A1.2 relocates to the inactive X chromosome after initiation and propagation of X-inactivation. *The Journal of cell biology* 147, 1399-408 (1999).

90. Angelov, D. *et al.* The histone variant macroH2A interferes with transcription factor binding and SWI/SNF nucleosome remodeling. *Molecular cell* 11, 1033-41 (2003).

91. Doyen, C.-M. *et al.* Mechanism of polymerase II transcription repression by the histone variant macroH2A. *Molecular and cellular biology* 26, 1156-64 (2006).

92. Chadwick, B.P. & Willard, H.F. A novel chromatin protein, distantly related to histone H2A, is largely excluded from the inactive X chromosome. *The Journal of cell biology* 152, 375-84 (2001).

93. Bao, Y. *et al.* Nucleosomes containing the histone variant H2A.Bbd organize only 118 base pairs of DNA. *The EMBO journal* 23, 3314-24 (2004).

94. Angelov, D. *et al.* SWI/SNF remodeling and p300-dependent transcription of histone variant H2ABbd nucleosomal arrays. *The EMBO journal* 23, 3815-24 (2004).

95. McBryant, S.J., Adams, V.H. & Hansen, J.C. Chromatin architectural proteins. *Chromosome research : an international journal on the molecular, supramolecular and evolutionary aspects of chromosome biology* 14, 39-51 (2006).

96. Wolffe, A.P. *Chromatin: Structure and function*. (Academic Press, San Diego: 1994).

97. Khochbin, S. Histone H1 diversity: bridging regulatory signals to linker histone function. *Gene* 271, 1-12 (2001).

98. Govin, J., Caron, C., Lestrat, C., Rousseaux, S. & Khochbin, S. The role of histones in chromatin remodelling during mammalian spermiogenesis. *European journal of biochemistry / FEBS* 271, 3459-69 (2004).

99. Khadake, J.R. & Rao, M.R. DNA- and chromatin-condensing properties of rat testes H1a and H1t compared to those of rat liver H1bdec; H1t is a poor condenser of chromatin. *Biochemistry* 34, 15792-801 (1995).

100. De Lucia, F. *et al.* Histone-induced condensation of rat testis chromatin: testis-specific H1t versus somatic H1 variants. *Biochemical and biophysical research communications* 198, 32-9 (1994).

101. Kingston, R.E. & Narlikar, G.J. ATP-dependent remodeling and acetylation as regulators of chromatin fluidity. *Genes & development* 13, 2339-52 (1999).

102. Narlikar, G.J., Fan, H.-Y. & Kingston, R.E. Cooperation between complexes that regulate chromatin structure and transcription. *Cell* 108, 475-87 (2002).

103. Becker, P.B. & Hörz, W. ATP-dependent nucleosome remodeling. *Annual review of biochemistry* 71, 247-73 (2002).

104. Wang, H.B. & Zhang, Y. Mi2, an auto-antigen for dermatomyositis, is an ATP-dependent nucleosome remodeling factor. *Nucleic acids research* 29, 2517-21 (2001).

105. Brehm, A. *et al.* dMi-2 and ISWI chromatin remodelling factors have distinct nucleosome binding and mobilization properties. *The EMBO journal* 19, 4332-41 (2000).

106. Längst, G. & Becker, P.B. Nucleosome mobilization and positioning by ISWI-containing chromatin-remodeling factors. *Journal of cell science* 114, 2561-8 (2001).

107. Sudarsanam, P. & Winston, F. The Swi/Snf family nucleosome-remodeling complexes and transcriptional control. *Trends in genetics : TIG* 16, 345-51 (2000).

108. Muchardt, C. & Yaniv, M. When the SWI/SNF complex remodels...the cell cycle. *Oncogene* 20, 3067-75 (2001).

109. Müller, C. & Leutz, A. Chromatin remodeling in development and differentiation. *Current opinion in genetics & development* 11, 167-74 (2001).

110. Meersseman, G., Pennings, S. & Bradbury, E.M. Mobile nucleosomes--a general behavior. *The EMBO journal* 11, 2951-9 (1992).

111. Whitehouse, I. *et al.* Nucleosome mobilization catalysed by the yeast SWI/SNF complex. *Nature* 400, 784-7 (1999).

112. Jaskelioff, M., Gavin, I.M., Peterson, C.L. & Logie, C. SWI-SNF-mediated nucleosome remodeling: role of histone octamer mobility in the persistence of the remodeled state. *Molecular and cellular biology* 20, 3058-68 (2000).

113. Studitsky, V.M., Clark, D.J. & Felsenfeld, G. A histone octamer can step around a transcribing polymerase without leaving the template. *Cell* 76, 371-82 (1994).

114. Lorch, Y., Zhang, M. & Kornberg, R.D. Histone octamer transfer by a chromatin-remodeling complex. *Cell* 96, 389-92 (1999).

115. Lee, D.Y., Hayes, J.J., Pruss, D. & Wolffe, A.P. A positive role for histone acetylation in transcription factor access to nucleosomal DNA. *Cell* 72, 73-84 (1993).

116. Hamiche, A., Sandaltzopoulos, R., Gdula, D.A. & Wu, C. ATP-dependent histone octamer sliding mediated by the chromatin remodeling complex NURF. *Cell* 97, 833-42 (1999).

117. Aalfs, J.D., Narlikar, G.J. & Kingston, R.E. Functional differences between the human ATP-dependent nucleosome remodeling proteins BRG1 and SNF2H. *The Journal of biological chemistry* 276, 34270-8 (2001).

118. Ringrose, L. & Paro, R. Epigenetic regulation of cellular memory by the Polycomb and Trithorax group proteins. *Annual review of genetics* 38, 413-43 (2004).

119. Jeon, K.W. & Berezney, R. Structural and functional organization of the nuclear matrix. (1995).

120. Murray, K. The occurrence of epsilon-N-methyl lysine in histones. *Biochemistry* 3, 10-5 (1964).

121. Allfrey, V.G., Faulkner, R., M & Irsky, A.E. Acetylation and methylation of histones and their possible role in the regulation of RNA Synthesis. *Proceedings of the National Academy of Sciences of the United States of America* 51, 786-94 (1964).

122. Vaquero, A., Loyola, A. & Reinberg, D. The constantly changing face of chromatin. *Science of aging knowledge environment : SAGE KE* 2003, RE4 (2003).

123. Roth, S.Y., Denu, J.M. & Allis, C.D. Histone acetyltransferases. *Annual review of biochemistry* 70, 81-120 (2001).

124. Grozinger, C.M. & Schreiber, S.L. Deacetylase enzymes: biological functions and the use of small-molecule inhibitors. *Chemistry & biology* 9, 3-16 (2002).

125. Hebbes, T.R., Thorne, A.W. & Crane-Robinson, C. A direct link between core histone acetylation and transcriptionally active chromatin. *The EMBO journal* 7, 1395-402 (1988).

126. Bannister, A.J. & Kouzarides, T. The CBP co-activator is a histone acetyltransferase. *Nature* 384, 641-3

127. Dhalluin, C. *et al.* Structure and ligand of a histone acetyltransferase bromodomain. *Nature* 399, 491-6 (1999).

128. Winston, F. & Allis, C.D. The bromodomain: a chromatin-targeting module? *Nature structural biology* 6, 601-4 (1999).

129. Smith, C.L. A shifting paradigm: histone deacetylases and transcriptional activation. *Bioessays* 30, 15-24 (2008).

130. Siuda, D. *et al.* Transcriptional regulation of Nox4 by histone deacetylases in human endothelial cells. *Basic research in cardiology* 107, 283 (2012).

131. Allis, C.D. & Strahl, B.D. The language of covalent histone modifications. *Nature* 403, 41-45 (2000).

132. Besant, P.G. & Attwood, P.V. Histone H4 histidine phosphorylation: kinases, phosphatases, liver regeneration and cancer. *Biochemical Society transactions* 40, 290-3 (2012).

133. Clayton, A.L., Rose, S., Barratt, M.J. & Mahadevan, L.C. Phosphoacetylation of histone H3 on c-fos- and c-jun-associated nucleosomes upon gene activation. *The EMBO journal* 19, 3714-26 (2000).

134. Sassone-Corsi, P. *et al.* Requirement of Rsk-2 for epidermal growth factor-activated phosphorylation of histone H3. *Science (New York, N.Y.)* 285, 886-91 (1999).

135. Hendzel, M.J. *et al.* Mitosis-specific phosphorylation of histone H3 initiates primarily within pericentromeric heterochromatin during G2 and spreads in an ordered fashion coincident with mitotic chromosome condensation. *Chromosoma* 106, 348-60 (1997).

136. Berger, S.L. Histone modifications in transcriptional regulation. *Current opinion in genetics & development* 12, 142-8 (2002).

137. Fischle, W., Wang, Y. & Allis, C.D. Histone and chromatin cross-talk. *Current opinion in cell biology* 15, 172-83 (2003).

138. Zhang, Y., LeRoy, G., Seelig, H.P., Lane, W.S. & Reinberg, D. The dermatomyositis-specific autoantigen Mi2 is a component of a complex containing histone deacetylase and nucleosome remodeling activities. *Cell* 95, 279-89 (1998).

139. Rice, J.C. & Allis, C.D. Histone methylation versus histone acetylation: new insights into epigenetic regulation. *Current opinion in cell biology* 13, 263-73 (2001).

140. Byvoet, P., Shepherd, G.R., Hardin, J.M. & Noland, B.J. The distribution and turnover of labeled methyl groups in histone fractions of cultured mammalian cells. *Archives of Biochemistry and Biophysics* 148, 558-567 (1972).

141. Baxter, C.S. & Byvoet, P. Intercalating agents as probes of the spatial relationship between chromatin components. *Biochemical and biophysical research communications* 63, 286-91 (1975).

142. Lachner, M., Sengupta, R., Schotta, G. & Jenuwein, T. Trilogies of histone lysine methylation as epigenetic landmarks of the eukaryotic genome. *Cold Spring Harbor symposia on quantitative biology* 69, 209-18 (2004).

143. Lee, D.Y., Teyssier, C., Strahl, B.D. & Stallcup, M.R. Role of protein methylation in regulation of transcription. *Endocrine reviews* 26, 147-70 (2005).

144. Lachner, M., O'Sullivan, R.J. & Jenuwein, T. An epigenetic road map for histone lysine methylation. *Journal of cell science* 116, 2117-24 (2003).

145. Bannister, A.J. & Kouzarides, T. Reversing histone methylation. *Nature* 436, 1103-6 (2005).

146. Shi, Y. *et al.* Histone demethylation mediated by the nuclear amine oxidase homolog LSD1. *Cell* 119, 941-53 (2004).

147. Tsukada, Y.-ichi *et al.* Histone demethylation by a family of JmjC domain-containing proteins. *Nature* 439, 811-6 (2006).

148. Whetstine, J.R. *et al.* Reversal of histone lysine trimethylation by the JMJD2 family of histone demethylases. *Cell* 125, 467-81 (2006).

149. Fodor, B.D. *et al.* Jmjd2b antagonizes H3K9 trimethylation at pericentric heterochromatin in mammalian cells. *Genes & development* 20, 1557-62 (2006).

150. Jenuwein, T. Re-SET-ting heterochromatin by histone methyltransferases. *Trends in cell biology* 11, 266-73 (2001).

151. Jacobson, M.K. & Jacobson, E.L. Discovering new ADP-ribose polymer cycles: protecting the genome and more. *Trends in biochemical sciences* 24, 415-7 (1999).

152. Kappus, S., Apweiler, R., White, C.J. & Whish, W.J. In vitro poly-(ADP-ribosyl)ation of chromatin proteins in the rat tapeworm, Hymenolepis diminuta. *Comparative biochemistry and physiology. B, Comparative biochemistry* 104, 711-6 (1993).

153. Tanny, J.C., Dowd, G.J., Huang, J., Hilz, H. & Moazed, D. An enzymatic activity in the yeast Sir2 protein that is essential for gene silencing. *Cell* 99, 735-45 (1999).

154. Chiarugi, A. Poly(ADP-ribose) polymerase: killer or conspirator? The "suicide hypothesis" revisited. *Trends in pharmacological sciences* 23, 122-9 (2002).

155. Golderer, G. & Gröbner, P. ADP-ribosylation of core histones and their acetylated subspecies. *The Biochemical journal* 277 (Pt 3, 607-10 (1991).

156. Pieper, A.A., Verma, A., Zhang, J. & Snyder, S.H. Poly (ADP-ribose) polymerase, nitric oxide and cell death. *Trends in pharmacological sciences* 20, 171-81 (1999).

157. Pickart, C.M. Mechanisms underlying ubiquitination. *Annual review of biochemistry* 70, 503-33 (2001).

158. Jason, L.J.M., Moore, S.C., Lewis, J.D., Lindsey, G. & Ausió, J. Histone ubiquitination: a tagging tail unfolds? *BioEssays : news and reviews in molecular, cellular and developmental biology* 24, 166-74 (2002).

159. Hicke, L. Protein regulation by monoubiquitin. *Nature reviews. Molecular cell biology* 2, 195-201 (2001).

160. Sun, Z.-W. & Allis, C.D. Ubiquitination of histone H2B regulates H3 methylation and gene silencing in yeast. *Nature* 418, 104-8 (2002).

161. Shiio, Y. & Eisenman, R.N. Histone sumoylation is associated with transcriptional repression. *Proceedings of the National Academy of Sciences of the United States of America* 100, 13225-30 (2003).

162. Kuroishi, T., Rios-Avila, L., Pestinger, V., Wijeratne, S.S.K. & Zempleni, J. Biotinylation is a natural, albeit rare, modification of human histones. *Molecular genetics and metabolism* 104, 537-45 (2011).

163. Nelson, C.J., Santos-Rosa, H. & Kouzarides, T. Proline isomerization of histone H3 regulates lysine methylation and gene expression. *Cell* 126, 905-16 (2006).

164. Latham, J.A. & Dent, S.Y.R. Cross-regulation of histone modifications. *Nature structural & molecular biology* 14, 1017-24 (2007).

165. Cai, X., Hagedorn, C.H. & Cullen, B.R. Human microRNAs are processed from capped, polyadenylated transcripts that can also function as mRNAs. *RNA (New York, N.Y.)* 10, 1957-66 (2004).

166. Borchert, G.M., Lanier, W. & Davidson, B.L. RNA polymerase III transcribes human microRNAs. *Nature structural & molecular biology* 13, 1097-101 (2006).

167. Wang, Y., Medvid, R., Melton, C., Jaenisch, R. & Blelloch, R. DGCR8 is essential for microRNA biogenesis and silencing of embryonic stem cell self-renewal. *Nature genetics* 39, 380-5 (2007).

168. Esquela-Kerscher, A. & Slack, F.J. Oncomirs - microRNAs with a role in cancer. *Nature reviews. Cancer* 6, 259-69 (2006).

169. Kim, V.N. MicroRNA biogenesis: coordinated cropping and dicing. *Nature reviews. Molecular cell biology* 6, 376-85 (2005).

170. Wassenegger, M. The role of the RNAi machinery in heterochromatin formation. *Cell* 122, 13-6 (2005).

171. Volpe, T.A. *et al.* Regulation of heterochromatic silencing and histone H3 lysine-9 methylation by RNAi. *Science (New York, N.Y.)* 297, 1833-7 (2002).

172. Reinhart, B.J. & Bartel, D.P. Small RNAs correspond to centromere heterochromatic repeats. *Science (New York, N.Y.)* 297, 1831 (2002).

173. Hall, I.M. *et al.* Establishment and maintenance of a heterochromatin domain. *Science (New York, N.Y.)* 297, 2232-7 (2002).

174. Verdel, A. *et al.* RNAi-mediated targeting of heterochromatin by the RITS complex. *Science (New York, N.Y.)* 303, 672-6 (2004).

175. Motamedi, M.R. *et al.* Two RNAi complexes, RITS and RDRC, physically interact and localize to noncoding centromeric RNAs. *Cell* 119, 789-802 (2004).

176. Maison, C. *et al.* Higher-order structure in pericentric heterochromatin involves a distinct pattern of histone modification and an RNA component. *Nature genetics* 30, 329-34 (2002).

177. Fukagawa, T. *et al.* Dicer is essential for formation of the heterochromatin structure in vertebrate cells. *Nature cell biology* 6, 784-91 (2004).

178. Morris, K.V., Chan, S.W.-L., Jacobsen, S.E. & Looney, D.J. Small interfering RNA-induced transcriptional gene silencing in human cells. *Science (New York, N.Y.)* 305, 1289-92 (2004).

179. Royo, H., Bortolin, M.-L., Seitz, H. & Cavaillé, J. Small non-coding RNAs and genomic imprinting. *Cytogenetic and genome research* 113, 99-108 (2006).

180. Heard, E., Chaumeil, J., Masui, O. & Okamoto, I. Mammalian X-chromosome inactivation: an epigenetics paradigm. *Cold Spring Harbor symposia on quantitative biology* 69, 89-102 (2004).

181. Matzke, M.A. & Matzke, A.J.M. Planting the seeds of a new paradigm. *PLoS biology* 2, E133 (2004).

182. Yang, X.-J. & Seto, E. Collaborative spirit of histone deacetylases in regulating chromatin structure and gene expression. *Current opinion in genetics & development* 13, 143-53 (2003).

183. Glozak, M. a, Sengupta, N., Zhang, X. & Seto, E. Acetylation and deacetylation of non-histone proteins. *Gene* 363, 15-23 (2005).

184. Heinzel, T., Spange, S., Wagner, T. & Kramer, O.H. Acetylation of non-histone proteins modulates cellular signalling at multiple levels. *International Journal of Biochemistry & Cell Biology* 41, 185-198 (2009).

185. Gregoretti, I.V., Lee, Y.-M. & Goodson, H.V. Molecular evolution of the histone deacetylase family: functional implications of phylogenetic analysis. *Journal of molecular biology* 338, 17-31 (2004).

186. de Ruijter, A.J.M., van Gennip, A.H., Caron, H.N., Kemp, S. & van Kuilenburg, A.B.P. Histone deacetylases (HDACs): characterization of the classical HDAC family. *The Biochemical journal* 370, 737-49 (2003).

187. Longworth, M.S. & Laimins, L.A. Histone deacetylase 3 localizes to the plasma membrane and is a substrate of Src. *Oncogene* 25, 4495-500 (2006).

188. Guardiola, A.R. & Yao, T.-P. Molecular cloning and characterization of a novel histone deacetylase HDAC10. *The Journal of biological chemistry* 277, 3350-6 (2002).

189. Yang, X.-J. & Seto, E. The Rpd3/Hda1 family of lysine deacetylases: from bacteria and yeast to mice and men. *Nature reviews. Molecular cell biology* 9, 206-18 (2008).

190. Fischle, W. *et al.* Enzymatic activity associated with class II HDACs is dependent on a multiprotein complex containing HDAC3 and SMRT/N-CoR. *Molecular cell* 9, 45-57 (2002).

191. Yang, X.-J. & Seto, E. HATs and HDACs: from structure, function and regulation to novel strategies for therapy and prevention. *Oncogene* 26, 5310-8 (2007).

192. Buglio, D. *et al.* HDAC11 plays an essential role in regulating OX40 ligand expression in Hodgkin lymphoma. *Blood* 117, 2910-7 (2011).

193. Sippl, W. & Jung, M. *Epigenetic targets in drug discovery*. (WILEY-VCH Verlag GmbH & Co. KGaA, Weinheim: 2009).

194. Vanommeslaeghe, K., De Proft, F., Loverix, S., Tourwé, D. & Geerlings, P. Theoretical study revealing the functioning of a novel combination of catalytic motifs in histone deacetylase. *Bioorganic & medicinal chemistry* 13, 3987-92 (2005).

195. Vannini, A. *et al.* Substrate binding to histone deacetylases as shown by the crystal structure of the HDAC8-substrate complex. *EMBO reports* 8, 879-84 (2007).

196. Luo, Y. *et al.* Trans-regulation of histone deacetylase activities through acetylation. *The Journal of biological chemistry* 284, 34901-10 (2009).

197. Zhang, Y. *et al.* Analysis of the NuRD subunits reveals a histone deacetylase core complex and a connection with DNA methylation. *Genes & development* 13, 1924-35 (1999).

198. Lagger, G. *et al.* Essential function of histone deacetylase 1 in proliferation control and CDK inhibitor repression. *The EMBO journal* 21, 2672-81 (2002).

199. Montgomery, R.L. *et al.* Histone deacetylases 1 and 2 redundantly regulate cardiac morphogenesis, growth, and contractility. *Genes & development* 21, 1790-802 (2007).

200. Haberland, M., Montgomery, R.L. & Olson, E.N. The many roles of histone deacetylases in development and physiology: implications for disease and therapy. *Nature reviews. Genetics* 10, 32-42 (2009).

201. Zupkovitz, G. *et al.* Negative and positive regulation of gene expression by mouse histone deacetylase 1. *Molecular and cellular biology* 26, 7913-28 (2006).

202. LaBonte, M.J. *et al.* DNA microarray profiling of genes differentially regulated by the histone deacetylase inhibitors vorinostat and LBH589 in colon cancer cell lines. *BMC medical genomics* 2, 67 (2009).

203. Granger, A. *et al.* Histone deacetylase inhibition reduces myocardial ischemia-reperfusion injury in mice. *FASEB journal : official publication of the Federation of American Societies for Experimental Biology* 22, 3549-60 (2008).

204. Trivedi, C.M. *et al.* Hdac2 regulates the cardiac hypertrophic response by modulating Gsk3 beta activity. *Nature medicine* 13, 324-31 (2007).

205. Yang, W.-M., Tsai, S.-C., Wen, Y.-D., Fejer, G. & Seto, E. Functional domains of histone deacetylase-3. *The Journal of biological chemistry* 277, 9447-54 (2002).

206. Guenther, M.G., Barak, O. & Lazar, M.A. The SMRT and N-CoR co-repressors are activating cofactors for histone deacetylase 3. *Molecular and cellular biology* 21, 6091-101 (2001).

207. Knutson, S.K. *et al.* Liver-specific deletion of histone deacetylase 3 disrupts metabolic transcriptional networks. *The EMBO journal* 27, 1017-28 (2008).

208. Bhaskara, S. *et al.* Deletion of histone deacetylase 3 reveals critical roles in S phase progression and DNA damage control. *Molecular cell* 30, 61-72 (2008).

209. Montgomery, R.L. *et al.* Maintenance of cardiac energy metabolism by histone deacetylase 3 in mice. *The Journal of clinical investigation* 118, 3588-97 (2008).

210. Zeng, L. *et al.* HDAC3 is crucial in shear- and VEGF-induced stem cell differentiation toward endothelial cells. *The Journal of cell biology* 174, 1059-69 (2006).

211. Zampetaki, A. *et al.* Histone deacetylase 3 is critical in endothelial survival and atherosclerosis development in response to disturbed flow. *Circulation* 121, 132-42 (2010).

212. Fischle, W. *et al.* Human HDAC7 histone deacetylase activity is associated with HDAC3 in vivo. *The Journal of biological chemistry* 276, 35826-35 (2001).

213. Kao, H.Y., Downes, M., Ordentlich, P. & Evans, R.M. Isolation of a novel histone deacetylase reveals that class I and class II deacetylases promote SMRT-mediated repression. *Genes & development* 14, 55-66 (2000).

214. McKinsey, T.A., Zhang, C.L. & Olson, E.N. Control of muscle development by dueling HATs and HDACs. *Current opinion in genetics & development* 11, 497-504 (2001).

215. Chang, S. *et al.* Histone deacetylase 7 maintains vascular integrity by repressing matrix metalloproteinase 10. *Cell* 126, 321-34 (2006).

216. Kim, H.-J. & Bae, S.-C. Histone deacetylase inhibitors: molecular mechanisms of action and clinical trials as anti-cancer drugs. *American journal of translational research* 3, 166-79 (2011).

217. Drummond, D.C. *et al.* Clinical development of histone deacetylase inhibitors as anticancer agents. *Annual Review of Pharmacology and Toxicology* 45, 495-528 (2005).

218. Blackwell, L., Norris, J., Suto, C.M. & Janzen, W.P. The use of diversity profiling to characterize chemical modulators of the histone deacetylases. *Life sciences* 82, 1050-8 (2008).

219. Vannini, A. *et al.* Crystal structure of a eukaryotic zinc-dependent histone deacetylase, human HDAC8, complexed with a hydroxamic acid inhibitor. *Proceedings of the National Academy of Sciences of the United States of America* 101, 15064-9 (2004).

220. Somoza, J.R. *et al.* Structural snapshots of human HDAC8 provide insights into the class I histone deacetylases. *Structure (London, England : 1993)* 12, 1325-34 (2004).

221. Arrowsmith, C.H., Bountra, C., Fish, P.V., Lee, K. & Schapira, M. Epigenetic protein families: a new frontier for drug discovery. *Nature Reviews Drug Discovery* 11, 384-400 (2012).

222. Schapira, M. Structural biology of human metal-dependent histone deacetylases. *Handbook of experimental pharmacology* 206, 225-40 (2011).

223. Bradner, J.E. *et al.* Chemical phylogenetics of histone deacetylases. *Nature chemical biology* 6, 238-243 (2010).

224. Butler, L.M. *et al.* Suberoylanilide hydroxamic acid, an inhibitor of histone deacetylase, suppresses the growth of prostate cancer cells in vitro and in vivo. *Cancer research* 60, 5165-70 (2000).

225. Marks, P.A. The clinical development of histone deacetylase inhibitors as targeted anticancer drugs. *Expert opinion on investigational drugs* 19, 1049-66 (2010).

226. Marks, P. *et al.* Histone deacetylases and cancer: causes and therapies. *Nature reviews. Cancer* 1, 194-202 (2001).

227. Richon, V.M. Cancer biology: mechanism of antitumour action of vorinostat (suberoylanilide hydroxamic acid), a novel histone deacetylase inhibitor. *British Journal of Cancer* 95, S2-S6 (2006).

228. Drummond, G.R., Selemidis, S., Griendling, K.K. & Sobey, C.G. Combating oxidative stress in vascular disease: NADPH oxidases as therapeutic targets. *Nature reviews. Drug discovery* 10, 453-71 (2011).

229. Bedard, K. & Krause, K.-H. The NOX family of ROS-generating NADPH oxidases: physiology and pathophysiology. *Physiological reviews* 87, 245-313 (2007).

230. Förstermann, U. Oxidative stress in vascular disease: causes, defense mechanisms and potential therapies. *Nature clinical practice. Cardiovascular medicine* 5, 338-49 (2008).

231. Brandes, R.P. & Kreuzer, J. Vascular NADPH oxidases: molecular mechanisms of activation. *Cardiovascular research* 65, 16-27 (2005).

232. Griendling, K.K. Novel NAD(P)H oxidases in the cardiovascular system. *Heart (British Cardiac Society)* 90, 491-3 (2004).

233. Leto, T.L. & Geiszt, M. Role of Nox family NADPH oxidases in host defense. *Antioxidants & redox signaling* 8, 1549-61

234. Ushio-Fukai, M. & Nakamura, Y. Reactive oxygen species and angiogenesis: NADPH oxidase as target for cancer therapy. *Cancer letters* 266, 37-52 (2008).

235. Huo, Y. *et al.* Reactive oxygen species (ROS) are essential mediators in epidermal growth factor (EGF)-stimulated corneal epithelial cell proliferation, adhesion, migration, and wound healing. *Experimental eye research* 89, 876-86 (2009).

236. Beckman, K.B. & Ames, B.N. The free radical theory of aging matures. *Physiological reviews* 78, 547-81 (1998).

237. Harman, D. Aging: a theory based on free radical and radiation chemistry. *Journal of gerontology* 11, 298-300 (1956).

238. Simon, H.U., Haj-Yehia, A. & Levi-Schaffer, F. Role of reactive oxygen species (ROS) in apoptosis induction. *Apoptosis : an international journal on programmed cell death* 5, 415-8 (2000).

239. Harrison, D., Griendling, K.K., Landmesser, U., Hornig, B. & Drexler, H. Role of oxidative stress in atherosclerosis. *The American journal of cardiology* 91, 7A-11A (2003).

240. Guzik, T.J. *et al.* Coronary artery superoxide production and nox isoform expression in human coronary artery disease. *Arteriosclerosis, thrombosis, and vascular biology* 26, 333-9 (2006).

241. Miyano, K., Ueno, N., Takeya, R. & Sumimoto, H. Direct involvement of the small GTPase Rac in activation of the superoxide-producing NADPH oxidase Nox1. *The Journal of biological chemistry* 281, 21857-68 (2006).

242. Lassègue, B. & Clempus, R.E. Vascular NAD(P)H oxidases: specific features, expression, and regulation. *American journal of physiology. Regulatory, integrative and comparative physiology* 285, R277-97 (2003).

243. Sturrock, A. *et al.* Transforming growth factor-beta1 induces Nox4 NAD(P)H oxidase and reactive oxygen species-dependent proliferation in human pulmonary artery smooth muscle cells. *American journal of physiology. Lung cellular and molecular physiology* 290, L661-L673 (2006).

244. Ago, T. *et al.* Nox4 as the major catalytic component of an endothelial NAD(P)H oxidase. *Circulation* 109, 227-33 (2004).

245. Ellmark, S.H.M., Dusting, G.J., Fui, M.N.T., Guzzo-Pernell, N. & Drummond, G.R. The contribution of Nox4 to NADPH oxidase activity in mouse vascular smooth muscle. *Cardiovascular research* 65, 495-504 (2005).

246. Bánfi, B. *et al.* NOX3, a superoxide-generating NADPH oxidase of the inner ear. *The Journal of biological chemistry* 279, 46065-72 (2004).

247. De Deken, X. *et al.* Cloning of two human thyroid cDNAs encoding new members of the NADPH oxidase family. *The Journal of biological chemistry* 275, 23227-33 (2000).

248. Takac, I. *et al.* The E-loop is involved in hydrogen peroxide formation by the NADPH oxidase Nox4. *The Journal of biological chemistry* 286, 13304-13 (2011).

249. Martyn, K.D., Frederick, L.M., von Loehneysen, K., Dinauer, M.C. & Knaus, U.G. Functional analysis of Nox4 reveals unique characteristics compared to other NADPH oxidases. *Cellular signalling* 18, 69-82 (2006).

250. Brandes, R.P., Takac, I. & Schröder, K. No superoxide--no stress?: Nox4, the good NADPH oxidase! *Arteriosclerosis, thrombosis, and vascular biology* 31, 1255-7 (2011).

251. Dikalova, A.E. *et al.* Upregulation of Nox1 in vascular smooth muscle leads to impaired endothelium-dependent relaxation via eNOS uncoupling. *American journal of physiology. Heart and circulatory physiology* 299, H673-9 (2010).

252. Bendall, J.K. *et al.* Endothelial Nox2 overexpression potentiates vascular oxidative stress and hemodynamic response to angiotensin II: studies in endothelial-targeted Nox2 transgenic mice. *Circulation research* 100, 1016-25 (2007).

253. Ray, R. *et al.* Endothelial Nox4 NADPH oxidase enhances vasodilatation and reduces blood pressure in vivo. *Arteriosclerosis, thrombosis, and vascular biology* 31, 1368-76 (2011).

254. Edgell, C.J., McDonald, C.C. & Graham, J.B. Permanent cell line expressing human factor VIII-related antigen established by hybridization. *Proceedings of the National Academy of Sciences of the United States of America* 80, 3734-7 (1983).

255. Giard, D.J. *et al.* In vitro cultivation of human tumors: establishment of cell lines derived from a series of solid tumors. *Journal of the National Cancer Institute* 51, 1417-23 (1973).

256. Edgell, C.J. *et al.* Endothelium specific Weibel-Palade bodies in a continuous human cell line, EA.hy926. *In vitro cellular & developmental biology : journal of the Tissue Culture Association* 26, 1167-72 (1990).

257. Marko, M.A., Chipperfield, R. & Birnboim, H.C. A procedure for the large-scale isolation of highly purified plasmid DNA using alkaline extraction and binding to glass powder. *Analytical biochemistry* 121, 382-7 (1982).

258. Boom, R. *et al.* Rapid and simple method for purification of nucleic acids. *Journal of clinical microbiology* 28, 495-503 (1990).

259. Chomcyznski, P. & Sacchi, N. Single-step method of RNA isolation by acid guanidinium thiocyanate-phenol-chloroform extraction. *Analytical Biochemistry* 162, 156-159 (1987).

260. Chomczynski, P. & Sacchi, N. The single-step method of RNA isolation by acid guanidinium thiocyanate-phenol-chloroform extraction: twenty-something years on. *Nature protocols* 1, 581-5 (2006).

261. Chien, A., Edgar, D.B. & Trela, J.M. Deoxyribonucleic acid polymerase from the extreme thermophile Thermus aquaticus. *Journal of bacteriology* 127, 1550-7 (1976).

262. Saiki, R.K. *et al.* Primer-directed enzymatic amplification of DNA with a thermostable DNA polymerase. *Science (New York, N.Y.)* 239, 487-91 (1988).

263. Wong, M.L. & Medrano, J.F. Real-time PCR for mRNA quantitation. *BioTechniques* 39, 75-85 (2005).

264. Battaglia, M. *et al.* Epithelial tumour cell detection and the unsolved problems of nested RT-PCR: a new sensitive one step method without false positive results. *Bone marrow transplantation* 22, 693-8 (1998).

265. Vandesompele, J., De Paepe, A. & Speleman, F. Elimination of primer-dimer artifacts and genomic coamplification using a two-step SYBR green I real-time RT-PCR. *Analytical biochemistry* 303, 95-8 (2002).

266. Temin, H.M. & Mizutani, S. RNA-dependent DNA polymerase in virions of Rous sarcoma virus. *Nature* 226, 1211-3 (1970).

267. Baltimore, D. RNA-dependent DNA polymerase in virions of RNA tumour viruses. *Nature* 226, 1209-11 (1970).

268. Crick, F. Central dogma of molecular biology. *Nature* 227, 561-3 (1970).

269. Central dogma reversed. *Nature* 226, 1198-9 (1970).

270. Higuchi, R., Fockler, C., Dollinger, G. & Watson, R. Kinetic PCR analysis: real-time monitoring of DNA amplification reactions. *Bio/technology (Nature Publishing Company)* 11, 1026-30 (1993).

271. Mackay, I.M., Arden, K.E. & Nitsche, A. Real-time PCR in virology. *Nucleic acids research* 30, 1292-305 (2002).

272. Holland, P.M., Abramson, R.D., Watson, R. & Gelfand, D.H. Detection of specific polymerase chain reaction product by utilizing the 5'----3' exonuclease activity of Thermus aquaticus DNA polymerase. *Proceedings of the National Academy of Sciences of the United States of America* 88, 7276-80 (1991).

273. Smith, P.K. *et al.* Measurement of protein using bicinchoninic acid. *Analytical biochemistry* 150, 76-85 (1985).

274. Olson, B.J.S.C. & Markwell, J. Assays for determination of protein concentration. *Current protocols in protein science / editorial board, John E. Coligan ... [et al.]* Chapter 3, Unit 3.4 (2007).

275. Laemmli, U.K. Cleavage of Structural Proteins during the Assembly of the Head of Bacteriophage T4. *Nature* 227, 680-685 (1970).

276. Hanahan, D. Studies on transformation of Escherichia coli with plasmids. *Journal of Molecular Biology* 166, 557-580 (1983).

277. Nicholls, R.D., Hill, A.V., Clegg, J.B. & Higgs, D.R. Direct cloning of specific genomic DNA sequences in plasmid libraries following fragment enrichment. *Nucleic acids research* 13, 7569-78 (1985).

278. Casadaban, M.J. & Cohen, S.N. Analysis of gene control signals by DNA fusion and cloning in Escherichia coli. *Journal of molecular biology* 138, 179-207 (1980).

279. Steinkamp-Fenske, K. Identifikation protektiver Naturstoffe aus kardiovaskulär wirksamen chinesischen Heilpflanzen. 149 (2007).

280. Ronaghi, M., Karamohamed, S., Pettersson, B., Uhlén, M. & Nyrén, P. Real-time DNA sequencing using detection of pyrophosphate release. *Analytical biochemistry* 242, 84-9 (1996).

281. Fuller, C.W. *et al.* The challenges of sequencing by synthesis. *Nature biotechnology* 27, 1013-23 (2009).

282. Sanger, F., Nicklen, S. & Coulson, A.R. DNA sequencing with chain-terminating inhibitors. *Proceedings of the National Academy of Sciences of the United States of America* 74, 5463-7 (1977).

283. Orlando, V. Mapping chromosomal proteins in vivo by formaldehyde-crosslinked-chromatin immunoprecipitation. *Trends in biochemical sciences* 25, 99-104 (2000).

284. Kuo, M.H. & Allis, C.D. In vivo cross-linking and immunoprecipitation for studying dynamic Protein:DNA associations in a chromatin environment. *Methods (San Diego, Calif.)* 19, 425-33 (1999).

285. Gilmour, D.S. & Lis, J.T. In vivo interactions of RNA polymerase II with genes of Drosophila melanogaster. *Mol. Cell. Biol.* 5, 2009-2018 (1985).

286. Myers, R.M. *et al.* A user's guide to the encyclopedia of DNA elements (ENCODE). *PLoS biology* 9, e1001046 (2011).

287. Aguilera, C. *et al.* c-Jun N-terminal phosphorylation antagonises recruitment of the Mbd3/NuRD repressor complex. *Nature* 469, 231-5 (2011).

288. Geer, L.Y. *et al.* The NCBI BioSystems database. *Nucleic acids research* 38, D492-6 (2010).

289. Rozen, S. & Skaletzky, H.J. Primer3 on the WWW for general users and for biologist programmers. *Methods in Molecular Biology* 132, 365-386 (2000).

290. Kent, W.J. *et al.* The human genome browser at UCSC. *Genome Research* 12, 996-1006 (2002).

291. Messeguer, X. *et al.* PROMO: detection of known transcription regulatory elements using species-tailored searches. *Bioinformatics* 18, 333-334 (2002).

292. Messeguer, X. *et al.* Identification of patterns in biological sequences at the ALGGEN server: PROMO and MALGEN. *Nucleic Acids Research* 31, 3651-3653 (2003).

293. Katsuyama, M. *et al.* Sp3 transcription factor is crucial for transcriptional activation of the human NOX4 gene. *The FEBS journal* 278, 964-72 (2011).

294. Manea, A., Tanase, L.I., Raicu, M. & Simionescu, M. Transcriptional regulation of NADPH oxidase isoforms, Nox1 and Nox4, by nuclear factor-kappaB in human aortic smooth muscle cells. *Biochemical and biophysical research communications* 396, 901-7 (2010).

295. Manea, A., Tanase, L.I., Raicu, M. & Simionescu, M. Jak/STAT signaling pathway regulates nox1 and nox4-based NADPH oxidase in human aortic smooth muscle cells. *Arteriosclerosis, thrombosis, and vascular biology* 30, 105-12 (2010).

296. Diebold, I., Petry, A., Hess, J. & Görlach, A. The NADPH oxidase subunit NOX4 is a new target gene of the hypoxia-inducible factor-1. *Molecular biology of the cell* 21, 2087-96 (2010).

297. Pendyala, S. *et al.* Nrf2 regulates hyperoxia-induced Nox4 expression in human lung endothelium: identification of functional antioxidant response elements on the Nox4 promoter. *Free radical biology & medicine* 50, 1749-59 (2011).

298. Hwang, J. *et al.* Peroxisome proliferator-activated receptor-gamma ligands regulate endothelial membrane superoxide production. *American journal of physiology. Cell physiology* 288, C899-905 (2005).

299. Zhang, L., Sheppard, O.R., Shah, A.M. & Brewer, A.C. Positive regulation of the NADPH oxidase NOX4 promoter in vascular smooth muscle cells by E2F. *Free radical biology & medicine* 45, 679-85 (2008).

300. Goettsch, C. *et al.* Arterial flow reduces oxidative stress via an antioxidant response element and Oct-1 binding site within the NADPH oxidase 4 promoter in endothelial cells. *Basic research in cardiology* 106, 551-61 (2011).

301. Fu, Y. *et al.* Regulation of NADPH oxidase activity is associated with miRNA-25-mediated NOX4 expression in experimental diabetic nephropathy. *American journal of nephrology* 32, 581-9 (2010).

302. Im, Y.B. *et al.* miR23b ameliorates neuropathic pain in spinal cord by silencing NADPH oxidase 4. *Antioxidants & redox signaling* 16, 1046-60 (2012).

303. Vasa-Nicotera, M. *et al.* miR-146a is modulated in human endothelial cell with aging. *Atherosclerosis* 217, 326-30 (2011).

304. Farré, D. *et al.* Identification of patterns in biological sequences at the ALGGEN server: PROMO and MALGEN. *Nucleic acids research* 31, 3651-3 (2003).

305. Messeguer, X. *et al.* PROMO: detection of known transcription regulatory elements using species-tailored searches. *Bioinformatics (Oxford, England)* 18, 333-4 (2002).

306. Rössig, L. *et al.* Inhibitors of histone deacetylation downregulate the expression of endothelial nitric oxide synthase and compromise endothelial cell function in vasorelaxation and angiogenesis. *Circulation research* 91, 837-44 (2002).

307. Eferl, R. & Wagner, E.F. AP-1: a double-edged sword in tumorigenesis. *Nature reviews. Cancer* 3, 859-68 (2003).

308. Granger, A. *et al.* Histone deacetylase inhibition reduces myocardial ischemia-reperfusion injury in mice. *FASEB journal : official publication of the Federation of American Societies for Experimental Biology* 22, 3549-60 (2008).

309. Jung, S.-B. *et al.* Histone deacetylase 3 antagonizes aspirin-stimulated endothelial nitric oxide production by reversing aspirin-induced lysine acetylation of endothelial nitric oxide synthase. *Circulation research* 107, 877-87 (2010).

310. Alam, S. *et al.* Galectin-9 protein expression in endothelial cells is positively regulated by histone deacetylase 3. *The Journal of biological chemistry* 286, 44211-7 (2011).

311. Klose, R.J. & Bird, A.P. Genomic DNA methylation: the mark and its mediators. *Trends in biochemical sciences* 31, 89-97 (2006).

312. Kondo, Y. Epigenetic cross-talk between DNA methylation and histone modifications in human cancers. *Yonsei medical journal* 50, 455-63 (2009).

313. Suganuma, T. & Workman, J.L. Signals and combinatorial functions of histone modifications. *Annual review of biochemistry* 80, 473-99 (2011).

314. Fuks, F., Burgers, W.A., Godin, N., Kasai, M. & Kouzarides, T. Dnmt3a binds deacetylases and is recruited by a sequence-specific repressor to silence transcription. *The EMBO journal* 20, 2536-44 (2001).

315. Cohen, N.M., Kenigsberg, E. & Tanay, A. Primate CpG islands are maintained by heterogeneous evolutionary regimes involving minimal selection. *Cell* 145, 773-86 (2011).

316. Kuhn, R.M., Haussler, D. & Kent, W.J. The UCSC genome browser and associated tools. *Briefings in bioinformatics* (2012).doi:10.1093/bib/bbs038

317. Jacobs, G.H. *et al.* Transterm: a database to aid the analysis of regulatory sequences in mRNAs. *Nucleic acids research* 37, D72-6 (2009).

318. Grillo, G. *et al.* UTRdb and UTRsite (RELEASE 2010): a collection of sequences and regulatory motifs of the untranslated regions of eukaryotic mRNAs. *Nucleic acids research* 38, D75-80 (2010).

319. Balakrishnan, L. & Milavetz, B. HDAC inhibitors stimulate viral transcription by multiple mechanisms. *Virology journal* 5, 43 (2008).

320. Grassi, G. *et al.* Inhibitors of DNA methylation and histone deacetylation activate cytomegalovirus promoter-controlled reporter gene expression in human glioblastoma cell line U87. *Carcinogenesis* 24, 1625-35 (2003).

321. Lai, M.-D. *et al.* An HDAC inhibitor enhances the antitumor activity of a CMV promoter-driven DNA vaccine. *Cancer gene therapy* 17, 203-11 (2010).

322. Goldsmith, M.E. *et al.* The Histone Deacetylase Inhibitor FK228 Preferentially Enhances Adenovirus Transgene Expression in Malignant Cells. *Clin. Cancer Res.* 9, 5394-5401 (2003).

Publications

Articles

Siuda, D., Zechner, U., El Hajj, N., Prawitt, D., Langen, D., Xia, N., Horke, S., Pautz, A., Kleinert, H., Förstermann, U., and Li, H. (2012) „Transcriptional regulation of Nox4 by histone deacetylases in human endothelial cells." Basic Research in Cardiology, Sep 2012; 107(5): 283.

Xia, N., Strand, S., Schlufter, F., Siuda, D., Reifenberg, G., Kleinert, H., Förstermann, U., and Li, H. "Role of SIRT1 and FOXO factors in eNOS transcriptional activation by resveratrol 2013." Nitric Oxide, Apr 2013; doi: 10.1016/j.niox.2013.04.001. [Epub ahead of print]

Art, J., Henke, J., Bollmann, F., Besche, V.,Bros, M., Li, H., Siuda, D., Handler, N., Bauer, F., Erker,T., Behnke, F., Mönch, B., Förstermann, U., Dirsch, V., Werz, O., Kleinert, H., and Pautz, A. (2013) „Resveratrol post-transcriptionally regulates pro-inflammatory gene expression via activation of KSRP" (submitted)

Siuda, D., Wu, Z., Chen, Y., Guo, L., Xia, N., Reifenberg, G., Kleinert, H., Förtsermann, U., and Li, H. (2013) „Social isolation-induced epigenetic changes in midbrain of adult mice." (submitted)

Siuda, D., Tobias, S., Daiber, A., Schmidt, H., Förstermann, U., and Li, H. (2013) „Effect of dexamethasone on vascular Nox1 expression" (in preparation)

Meeting Abstracts

Siuda, D., Wu, Z. Chen, Y., Guo, L., Xia, N., Reifenberg, G., Kleinert, H., Förstermann, U., and Li, H. (2013) "Social isolation-induced epigenetic changes in midbrain of adult mice." (3. Clinical Epigenetics International Meeting, Solingen, Germany)

Siuda, D., Wu, Z., and Li, H. (2013) "Transgenerational blood pressure regulation in spontaneously hypertensive rats." (Keystone Symposia Nutrition, Epigenetics and Human Disease, Santa Fe, New Mexico, USA)

Bollmann, F., Wu, Z., Oelze, M., Siuda, D., Daiber, A., Kleinert, H., Li, H., and Pautz, A. (2012) „Is chronic inflammation the main trigger for cardiovascular diseases?" (78. Jahrestagung der Deutschen Gesellschaft für Experimentelle und Klinische Pharmakologie und Toxikologie, Dresden, Germany)

Siuda, D., Zechner, U., Prawitt, D., Xia, N., Kleinert, H., Förstermann, U., and Li, H. (2012) „ Transcriptional regulation of Nox4 by histone deacetylases" (78. Jahrestagung der Deutschen Gesellschaft für Experimentelle und Klinische Pharmakologie und Toxikologie, Dresden, Germany)

Siuda, D., Xia, N., Tobias, S., Förstermann, U., and Li, H. (2012) „Regulation of Nox1 expression by histone deacetylases in vascular smooth muscle cells." (77. Jahrestagung der Deutschen Gesellschaft für Experimentelle und Klinische Pharmakologie und Toxikologie, Frankfurt a.M., Germany)